

# THE BELL SYSTEM TECHNICAL JOURNAL

---

VOLUME XXXIX

JULY 1960

NUMBER 4

---

*Copyright 1960, American Telephone and Telegraph Company*

## The Theory and Design of Chirp Radars

By J. R. KLAUDER, A. C. PRICE,  
S. DARLINGTON and W. J. ALBERSHEIM

(Manuscript received April 5, 1960)

*A new radar technique has been developed that provides a solution for the conflicting requirements of simultaneous long-range and high-resolution performance in radar systems. This technique, called Chirp at Bell Telephone Laboratories, recognizes that resolution depends on the transmitted pulse bandwidth. A long high-duty-factor transmitted pulse, with suitable modulation (linear frequency modulation in the case of Chirp), which covers a frequency interval many times the inherent bandwidth of the envelope, is employed. The receiver is designed to make optimum use of the additional signal bandwidth. This paper contains many of the important analytical methods required for the design of a Chirp radar system. The details of two signal generation methods are considered and the resulting signal waveforms and power spectra are calculated. The required receiver characteristics are derived and the receiver output waveforms are presented. The time-bandwidth product is introduced and related to the effective increase in the performance of Chirp systems. The concept of a matched filter is presented and used as a reference standard in receiver design. The effect of amplitude and phase distortion is analyzed by the method of paired echoes. One consequence of the signal design is the presence of time side lobes on the receiver output pulse analogous to the spatial side lobes in antenna theory. A method to reduce the time side lobes by weighting the pulse energy spectrum is explained in terms of paired echoes. The weighting process is described, and calculated pulse envelopes, weighting network characteristics and dele-*

terious effects are presented. The effects of quadratic phase distortion are analyzed and the resultant pulse envelopes are presented. The receiver response characteristics in the presence of Doppler-shifted signals from moving targets are examined. Schematic ambiguity diagrams are presented for current signal designs.

#### FOREWORD

A recent declassification makes it possible to publish information concerning an important advance in military electronics that has been pursued in classified work at Bell Telephone Laboratories since 1951.

Traditionally, warfare has been a continuing competition between armament and firepower. This competition has carried over to the electronics of warfare. In particular, radar has been hard put to keep pace with the requirements determined by faster and higher-flying aircraft and missiles and the various radar countermeasures that they require. Therefore, anything that enhances the capability of radar, either in range, range resolution or rate of acquisition has always been most welcome.

Simple pulsed radar is limited in range by the average power radiated, in resolution by the pulse length and in acquisition time by the beam width. The design of any radar involves a compromise among these three factors—range, resolution and speed. Anything that eases this compromise is of great interest.

During most of the war, the principal emphasis in development of radar techniques and components was centered on increasing range and range resolution performance by increasing transmitter peak power and reducing pulse length. Thus, shortly after the end of the war, transmitting tubes were in existence with average power capabilities in excess of 100 times that which could be used in straightforward short-pulse operation. At about this time a number of investigators realized that targets separated in range by a distance  $\Delta R$  could be resolved by using an appropriately modulated pulse provided that  $c/2\Delta f \geq \Delta R$ , where  $c$  is the velocity of propagation and  $\Delta f$  is the width of the frequency spectrum of the transmitted pulse. The familiar case of short-pulse transmission where the free-space wave train is of the order of twice the distance between targets to be resolved satisfies this condition. The important point is that this criterion can also be satisfied with a variety of other signal waveforms. Thus, a linearly frequency-modulated pulse with frequency span set by the resolution required and with duration set by the energy required in the pulse for range performance is at once suggested. By transmitting a modulated pulse, it is possible to obtain range resolutions

that are smaller than the transmitted pulse length by very large factors. The range resolution is inherently limited to approximately the reciprocal of the signal bandwidth, and one can (in retrospect) imagine many methods of pulse modulation that utilize a given bandwidth as efficiently as does a short pulse, but that do not involve the high peak powers of a very short pulse.

Such considerations led to early theoretical and experimental work on various types of radar signals. Some of this work was concerned primarily with frequency-modulated pulses. At Bell Telephone Laboratories this followed ideas that were first proposed in 1947 by Darlington in connection with waveguide transmission, and were later covered by a patent.<sup>1</sup> This approach is also to be found in the work of Hüttman,<sup>2</sup> Sproule and Hughes,<sup>3</sup> Cauer,<sup>4</sup> and Dicke.<sup>5</sup> \* The early experimental work at Bell Telephone Laboratories by A. F. Dietrich and O. E. De Lange and by W. J. Albersheim in 1951 utilized a reflex klystron to obtain the frequency-modulated or "Chirped" † transmitted signal. The receiver was modified to obtain the resolution compatible with the transmitted bandwidth.

Other work by C. C. Cutler envisaged more elaborate signals which included frequency-modulated pulses as a special case. Analytical work by A. W. Schelling clarified the ideas involved and clearly pointed up the problems of "side lobes in range" which arise from pulse and spectrum shaping.

The fact that the pulse compression idea, so valuable to radar, grew out of the work of a mathematician on a problem in waveguide communication is an illustration of how each branch of our complex technology supports the other.

Fundamental work in this field has been supported since the Spring of 1955 by the Weapons Guidance Laboratory of Wright Air Development Division in Dayton, Ohio.

Today, the pulse compression technique is in use in a variety of very important radar applications. Through its use, these radars transmit a pulse with about 100 times the energy of a short pulse with equivalent resolution and peak power. The paper that follows covers in detail the design and analysis necessary in applying this technique, and a second paper by Klauder<sup>7</sup> covers an aspect of this technique that is still evolving: the synthesis of a signal function to provide a specified ambiguity diagram. It is interesting to note that here, too, the technique has been

\* An investigation based on this patent is reported by Cook.<sup>6</sup>

† The appellation "Chirp" was first used by B. M. Oliver in an internal Bell Laboratories Memorandum, "Not with a Bang, but a Chirp", in 1951.

advanced because Klauder recognized the similarity between the processes of synthesis of a signal function to get a specified ambiguity diagram and a method for the generation of quantum-mechanical wave functions developed by E. Wigner.

### I. INTRODUCTION

The specifications of modern, highly complex communication and defense systems continually require more powerful and more sophisticated radar or radar-like systems. Such radars must be capable of detecting very small targets at greater ranges and with greater range and angular resolution than ever before. To satisfy these demands, unusual innovations in radar techniques have been required. This paper is devoted to some of the theoretical and design considerations of one such innovation, the so-called "Chirp" system, which has proved highly successful.

A familiar and intuitive figure of merit on the performance of a radar is provided by the average transmitted power: the higher the transmitted power, the greater the range of detectable targets, other things being equal. Suppose one regards the pulse repetition frequency (PRF) as being essentially fixed and seeks ways to profitably increase the transmitted power in each pulse. Clearly, an amplification of each transmitted signal constitutes the natural way to increase this power. However, the usefulness of this approach is fixed by fundamental *equipment limitations*, which frequently take the form of component breakdown. Furthermore, this presents such a serious limitation that it is necessary to seek additional means of raising the transmitted power to satisfy the requirements of modern systems.

To accomplish this it is necessary to use the only "dimension" remaining available: the time. One can surely increase the average power if the duration of each pulse is increased. Again, this technique has its limitations. First, there will be a maximum obtainable pulse width limited typically by *duty factor* considerations, i.e., the fraction of time the transmitting tubes will actually be in operation. However, there is a second limitation dictated by the desired *range resolution* of the over-all system, which determines the ability to separate multiple targets clustered closely together. In numerous present and projected systems it is an important fact that the pulse-width limitation imposed by the desired range resolution may be *several orders of magnitude less* than the limitation imposed by the present "state-of-the-art" in high duty-factor tubes. Thus, high-power, high-resolution radars are, in principle, *not* limited in a fundamental way by equipment breakdown. Rather, they are affected by poor "signal design". What is required is a transmitted

signal that combines the large amplitude and long pulse width available with existing apparatus, but retains the range resolution capabilities inherent in a pulse of much shorter duration.

One solution to this problem was recognized by Darlington.<sup>1</sup> Although his precise technique will not be pursued in detail, it does provide an intuitive picture of the operation of an actual Chirp system. The following section presents Darlington's model and a survey of the remaining sections of the present paper.

## II. DISCUSSION OF A SIMPLE CHIRP MODEL; SURVEY AND SUMMARY OF REMAINING SECTIONS

It is the large-frequency content, or bandwidth, of a short radar pulse that accounts for its high resolution capabilities. It follows, as a consequence of Fourier analysis, that a long pulse of constant carrier frequency contains a narrow bandwidth and, therefore, possesses poor resolution properties. However, the spectrum of this long signal can be significantly broadened by introducing modulation. To utilize the transmitting tubes efficiently, this modulation must take the form of *frequency modulation* (FM). By this method one can introduce the frequency-spread characteristic of a short pulse within the envelope of a long-duration signal. The linearity of a radar system permits one to realize the potential of this shorter pulse by a suitable phase equalization in the radar receiver. Darlington's model for such a system is illustrated in Fig. 1. The transmitted signal consists of a sequence of adjacent pulses each possessing a unique carrier frequency,  $f_n$  [see Fig. 1(a)]. To realize the short pulse potential, one imagines that the received signal is passed

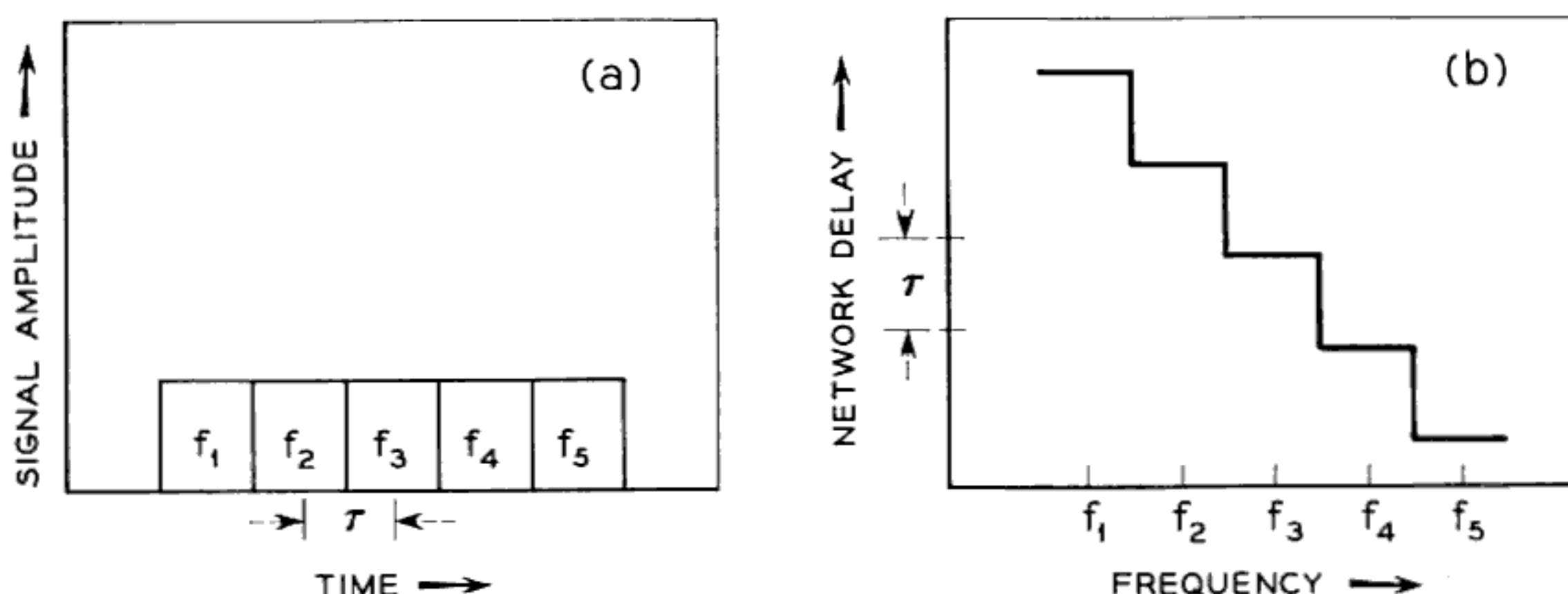


Fig. 1 — (a) Model Chirp radar signal composed of five adjacent pulses each possessing a unique frequency. (b) Suitable delay equalizer for the signal in (a). The output of this network is qualitatively a pulse of increased amplitude with a pulse width of  $\tau$  seconds. The network is illustrated for the particular case where  $f_n < f_{n+1}$ .

through a network possessing a delay versus frequency character, as illustrated in Fig. 1(b). Although the frequency  $f_1$  is the first to be received, it is just this frequency that is delayed the longest amount by the network. In this manner each pulse of distinct carrier frequency is made to "wait" until the highest-frequency component arrives, whereupon all the short pulses emerge simultaneously. Thus, following the delay equalization, the original signal of Fig. 1(a) will be compressed in time, and, by energy conservation, the collapsed signal will be necessarily increased in amplitude.

For several practical as well as theoretical reasons the signal chosen for the Chirp system is characterized by a *linear* FM illustrated, for example, by Fig. 2. This important case consists of a rectangular envelope of  $T$  seconds duration [see Fig. 2(a)]. Within this envelope the

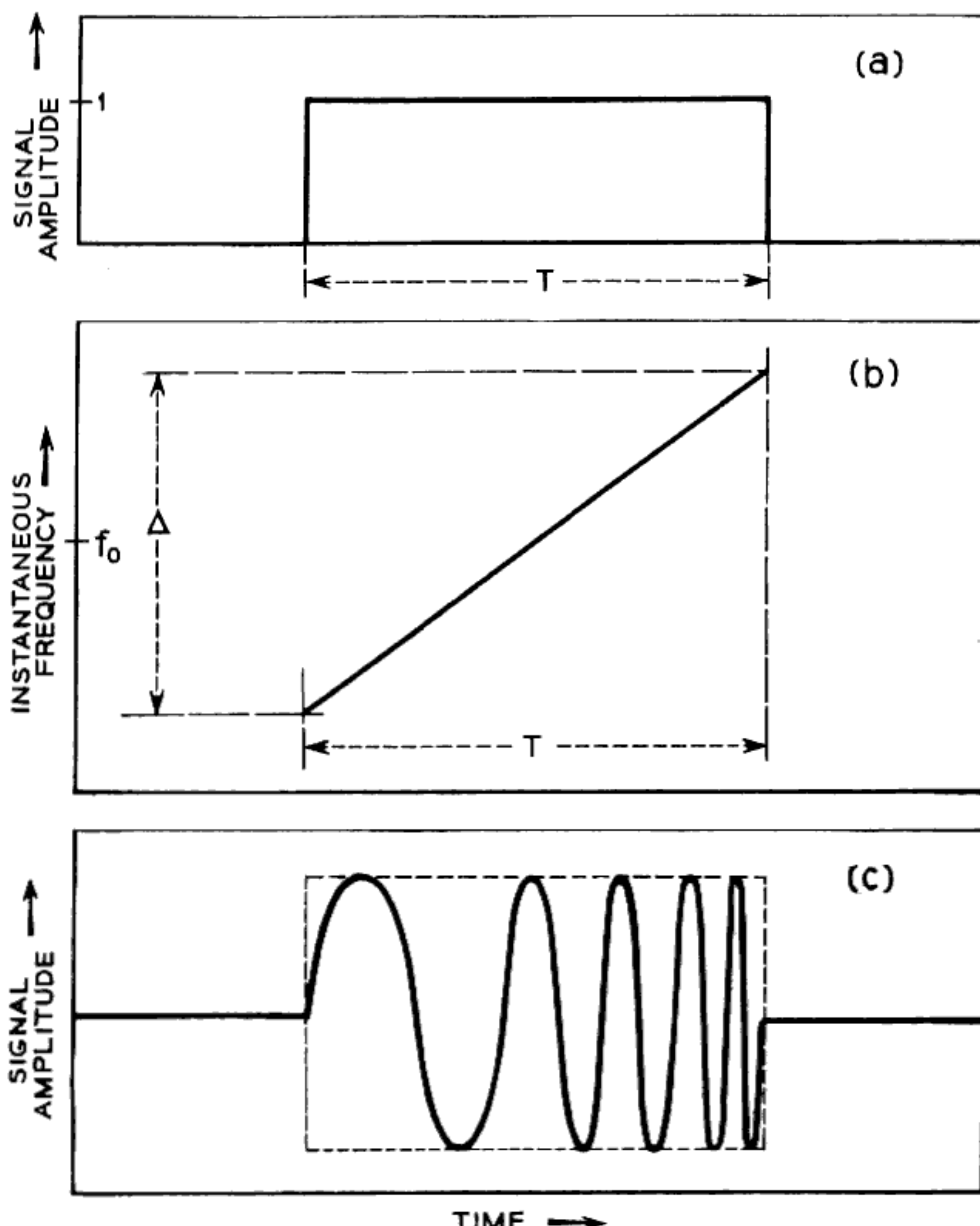


Fig. 2 — (a) Ideal envelope of actual Chirp signal, of  $T$  seconds duration and chosen to be of unit amplitude. (b) Instantaneous frequency vs. time characteristic of Chirp signal; a band of frequencies,  $\Delta$ , centered at  $f_0$  is linearly swept during the pulse duration. (c) Schematic diagram of a signal having the properties indicated in (a) and (b).

instantaneous frequency is modulated in a linear manner covering a band of frequencies  $\Delta$ , centered at a frequency  $f_0$  [see Fig. 2(b)]. Fig. 2(c) schematically illustrates a signal possessing a linear FM. It is clear that this signal is a limiting form of the one illustrated in Fig. 1(a). A suitable delay-equalizing network for the signal with linear FM is given, therefore, by a limiting form of the equalizer in Fig. 1(b). The delay characteristic of this limiting network is shown in Fig. 3(a). The response of the delay network to the rectangular pulse with linear FM is discussed in Section 3.1 of this paper. This response envelope is given analytically by the absolute value of  $\sqrt{D}[(\sin \pi \Delta t)/(\pi \Delta t)]$  and is

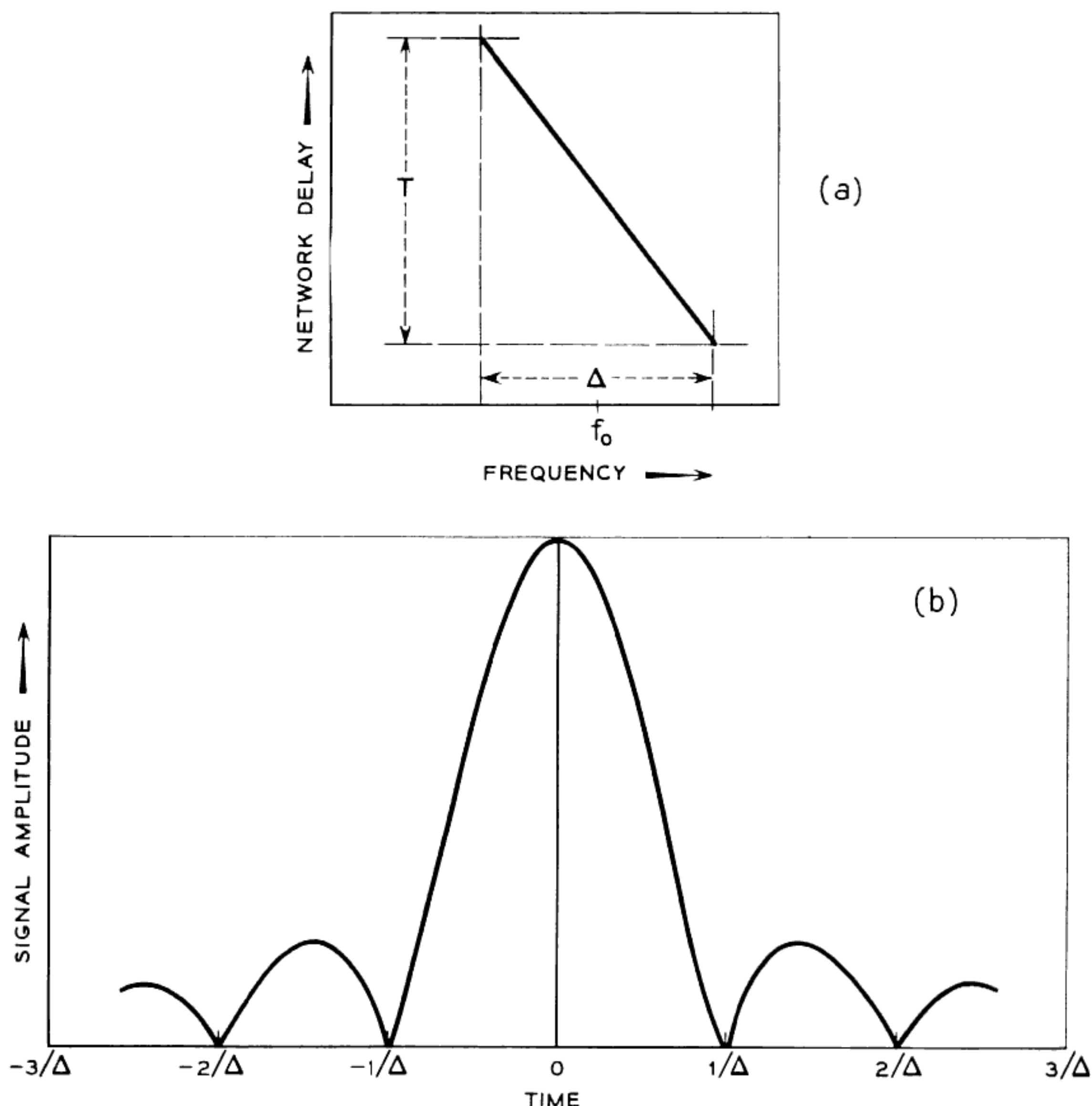


Fig. 3 — (a) Network delay vs. frequency characteristic suitable for phase equalization of the Chirp signal in Fig. 2; ideally, this network is chosen to have a flat loss characteristic. (b) Envelope of output response from the network in (a); this pulse now has a pulse width about  $1/\Delta$  and an amplitude increase given by  $\sqrt{D}$ , where  $D = T\Delta$  is called the dispersion factor.

illustrated in Fig. 3(b). In this expression,  $D$ , called the *dispersion factor*, is defined by the product  $T\Delta$  and represents a parameter of fundamental significance. The collapsed pulse width,  $\tau$ , is of the order of  $1/\Delta$ . Consequently, there has been a pulse width reduction given by the ratio

$$T/\tau \simeq T\Delta = D,$$

and a signal amplification given by  $\sqrt{D}$ . Useful systems already proposed will possess dispersion factors of 100, and even greater! Experimental measurements already made exhibit output signals such as Fig. 3(b) for  $D = 120$ .

Along with the problem of constructing delay networks having the characteristics shown in Fig. 3(a) there is also the problem of actually generating a signal having the properties illustrated in Fig. 2. Two techniques have been devised that are basically equivalent. First, an "active" generation scheme may be used; for example, such a signal may be obtained by suitable modulation of a voltage-tunable device. It was an active generation technique that was used in early demonstrations of the Chirp principle by A. F. Dietrich and O. E. DeLange and by W. J. Albersheim in 1951. The second generation scheme, which will be called "passive" generation, relies on using another network that will perform the inverse operation of the network in Fig. 3(a). That is, the additional network should generate a long FM output pulse from a very short input pulse. Of course, the long pulse achieved in this manner may then be amplified to achieve the desired transmission level. Both of these important generation schemes will be considered from an analytical point of view in this paper.

In Section 3.3 a brief review of "matched filter" theory is presented. This theory provides a linear filtering scheme which yields the largest obtainable signal-to-noise ratio (S/N), and serves principally as a standard of comparison. Fortunately, there is a rather broad maximum in the S/N, and filters based on the one illustrated in Fig. 3(a) provide an excellent approximation to the "optimum" filter. Such approximate filters or receivers are eminently more desirable from a practical point of view.

In compressing the rectangular Chirp pulse, one unfortunately introduces an undesirable feature, which is illustrated in Fig. 3(b): the spurious signals on both sides of the central pulse generally present unwanted ambiguities. Curves of this shape occur as antenna patterns in the theory of antenna design. By analogy, these spurious signals shall be referred to as *side lobes*. Techniques for reducing the relative side-lobe level have been extensively studied in antenna design. The analysis presented in Sections 3.3 and 3.4 to reduce the side lobes of the Chirp signal

will draw heavily on these antenna analogs. In particular, considerable side-lobe reduction may be obtained by properly attenuating the frequencies at the edges of the band  $\Delta$ . Such a reduction is accompanied by a slight, but inevitable, increase in the pulse width.

The design of a practical radar system is not complete unless it is accompanied by a set of acceptable equipment tolerances; Section 3.4 discusses this important problem. The basis of the analytical study in this section is the *paired echo* concept introduced by MacColl.<sup>8</sup> Following a review of MacColl's treatment of the problem, there is a discussion of the effect on the collapsed pulse of phase and amplitude distortions. Also in Section 3.4 there appears a detailed discussion of spectrum shaping networks to reduce the side-lobe level based on Taylor's<sup>9</sup> approximation to the "ideal" Dolph-Tchebycheff signal. To present a clear and intuitive picture, Taylor's model is analyzed with the help of paired-echo theory. Effects on the pulse width and side-lobe level are presented, as well as a discussion of the influence of Taylor weighting on the S/N.

The final section of this paper, Section 3.5, is devoted to the unusual effects produced by targets moving in a radial direction with respect to the radar. As is well known, this relative motion gives rise to a small frequency shift of the returning signal; this phenomena is known as the *Doppler effect*. The principle qualitative effect of this frequency shift may be obtained by referring to Fig. 3(a), which shows the delay versus frequency characteristic of the receiver network. One sees from this figure that a uniform shift of the returning spectrum upwards (or downwards) in frequency will produce a collapsed pulse that will lead (or lag) the unaffected signal's output time. These effects will be discussed in terms of *ambiguity diagrams* introduced by Woodward.<sup>10</sup>

### III. DETAILED ANALYSIS

The practical realization of any radar, including the Chirp radar, involves an enormous amount of complex equipment. It is gratifying that analysis of the radar need not include the bulk of these details. Much of the following analysis, therefore, deals with highly simplified ideal transmission and reception processes. However, one must always be sure that the ideal process can be essentially realized, at least in principle. This is not the case for the frequently made replacement of the true transmitted signal, which of course must be real, by a signal that is a complex function of time. The validity of considering complex signals is a simple consequence of the assumed linearity of the system. However, complex signals are useful, not only because the system is linear but also because they permit important simplifications regarding

the assumed receiving network characteristics to be made. In particular, the analysis in Section 3.1 will be concerned only with the positive frequency portion of signals and with networks having desired characteristics in this frequency range. The true signal output is obtained as usual by taking, say, the real part of the complex response.

The initial part of the analysis is devoted to studying the rectangular signal with linear FM. Crudely speaking, this may be regarded as assuming an "active" generation scheme; i.e., the problem of obtaining the signal illustrated in Fig. 2 is left to the engineer. However, this is not an accurate statement because, from an analytical point of view, consideration of the long rectangular signal in no way prejudgets its means of generation. The discussion on the very important "passive" technique to generate the long-duration signal can then draw on the preceding analysis regarding the collapse process of a long FM pulse. Furthermore, there are two related reasons why an intrinsic study of the rectangular signal has special significance: (a) the rectangular envelope represents the most efficient use of transmitting tubes (as remarked in Section I), and (b) even the signals passively generated, which, for economical tube operation are again subjected to amplitude-limiting, seem to approach the characteristics of the ideal rectangular signal.

### 3.1 Analytical Discussion of the Reception and Collapse of the Chirp Radar Signal

Let  $e_1(t)$  denote the analytical waveform of a single pulse received from an isolated, stationary point target. This real signal is chosen for convenience to be the real part of a complex waveform  $\epsilon_1(t)$ , where

$$\epsilon_1(t) = \text{rect}\left(\frac{t}{T}\right)e^{2\pi i(f_0 t + kt^2/2)}. \quad (1)$$

As customary,  $f_0$  denotes some suitable carrier frequency. The function, rect  $z$ , introduced by Woodward, is defined by the following relations:

$$\begin{aligned} \text{rect } z &= 1, & \text{if } |z| < \frac{1}{2} \\ &= 0, & \text{if } |z| > \frac{1}{2}. \end{aligned} \quad (2)$$

Therefore, the received signal (1) is conveniently, but arbitrarily, selected to be of unit amplitude. The particular phase characteristic in this signal is chosen to duplicate the linear FM properties illustrated in Fig. 2. With the phase of (1) represented by  $\varphi = 2\pi(f_0 t + kt^2/2)$ , the instantaneous signal frequency is defined, as usual, by

$$f_i = \frac{1}{2\pi} \frac{d\varphi}{dt} = f_0 + kt. \quad (3)$$

Thus, during the  $T$ -second interval of the pulse, the instantaneous frequency changes in a linear fashion from  $f_0 - kT/2$  to  $f_0 + kT/2$  [see Fig. 2(b)]. The net frequency sweep,  $\Delta$ , is then the difference of these two values, or  $kT$ . This frequency interval  $\Delta$  provides a convenient means to introduce natural units into the Chirp radar problem. The natural variables in which to measure time and frequency are expressed as follows:

$$y = t\Delta, \quad \text{a "time" variable,} \quad (4a)$$

$$x = f/\Delta, \quad \text{a "frequency" variable.} \quad (4b)$$

In conjunction with these natural variables the dimensionless product  $T\Delta$  frequently appears. This product is called the *dispersion factor* and is denoted by  $D$ :

$$D \equiv T\Delta. \quad (5)$$

The complex received waveform (1) takes the following form when expressed in terms of the natural time and frequency variables:

$$\epsilon_1(y) = \text{rect}\left(\frac{y}{D}\right) e^{2\pi i(x_0 y + y^2/2D)}, \quad (6)$$

where  $x_0 \equiv f_0/\Delta$  and  $k = \Delta/T$  have been used. This signal is now  $D$  units of "time" in duration.

The signal illustrated in (1) or (6) possesses, by construction, the characteristics of Fig. 2. However, the qualitative argument regarding the instantaneous frequency does not necessarily provide an accurate description of the signal's frequency content. Such an accurate picture is obtained by studying the signal's Fourier transform. Let  $\tilde{A}(f)$  denote the Fourier transform of an arbitrary function of time,  $A(t)$ .

The transform of the signal in (1) becomes

$$\begin{aligned} \tilde{\epsilon}_1(f) &= \int_{-\infty}^{\infty} \epsilon_1(t) e^{-2\pi ift} dt \\ &= \int_{-T/2}^{T/2} e^{2\pi i[(f_0-f)t + kt^2/2]} dt. \end{aligned} \quad (7a)$$

Following some algebraic manipulations, (7a) becomes

$$\tilde{\epsilon}_1(f) = \sqrt{\frac{T}{2\Delta}} e^{-i\pi(f-f_0)^2/k} [Z(u_2) - Z(u_1)], \quad (7b)$$

where  $Z(u)$  is the complex Fresnel integral:

$$Z(u) = C(u) + iS(u) = \int_0^u e^{i\pi\alpha^2/2} d\alpha. \quad (8)$$

The arguments  $u_2$  and  $u_1$  are defined by

$$u_2 = -2(f - f_0) \sqrt{\frac{T}{2\Delta}} + \sqrt{\frac{T\Delta}{2}}, \quad (9a)$$

$$u_1 = -2(f - f_0) \sqrt{\frac{T}{2\Delta}} - \sqrt{\frac{T\Delta}{2}}. \quad (9b)$$

The shape of the frequency spectrum, as would be determined, for example, by a spectrum analyser, contains only the amplitude information. The amplitude of the signal spectrum in (7) is obtained simply by taking the absolute value:

$$|\tilde{e}_1(f)| = \sqrt{\frac{T}{2\Delta}} |Z(u_2) - Z(u_1)| \quad (10a)$$

$$= \sqrt{\frac{T}{2\Delta}} \{[C(u_2) - C(u_1)]^2 + [S(u_2) - S(u_1)]^2\}^{\frac{1}{2}},$$

where  $C(u)$  and  $S(u)$  are defined in (8) as the real and imaginary part of  $Z(u)$ . In establishing the relative frequency content, a normalized form of (10a) is used. Figs. 4, 5 and 6 illustrate various spectra obtained by plotting

$$\frac{1}{\sqrt{2}} \{[C(u_2) - C(u_1)]^2 + [S(u_2) - S(u_1)]^2\}^{\frac{1}{2}}, \quad (10b)$$

where  $u_2$  and  $u_1$  appear in (9a) and (9b). Inspection of (9a) and (9b)

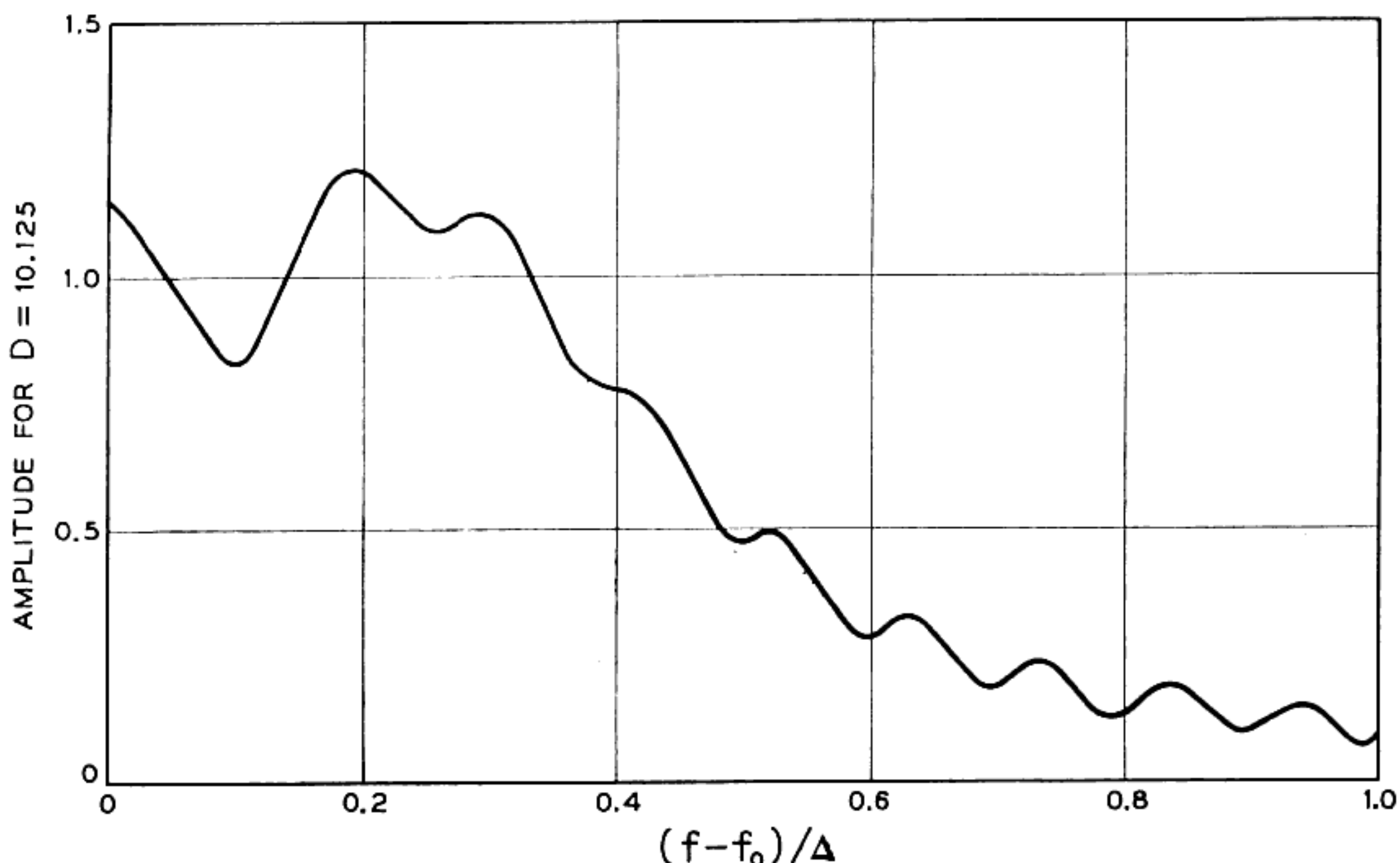


Fig. 4 — Spectral amplitude of a rectangular Chirp signal for  $D = 10.125$ . The shape is symmetric about the point  $(f - f_0)/\Delta = 0$ .

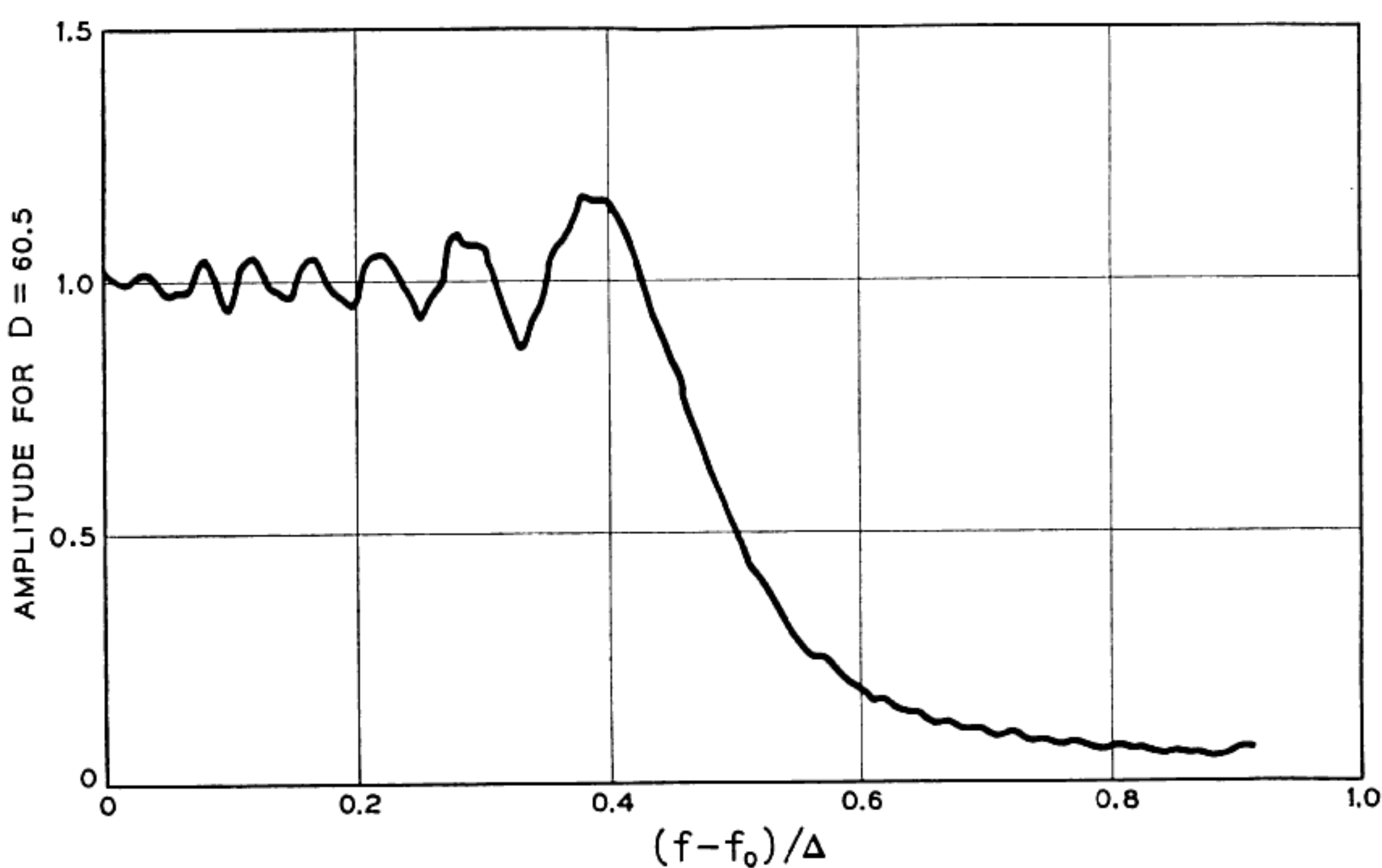


Fig. 5 — Spectral amplitude of a rectangular Chirp signal for  $D = 60.5$ .

shows that the dispersion factor,  $D$ , is the only auxiliary variable present besides the "frequency"  $x - x_0$ , i.e.  $(f - f_0)/\Delta$ . The values of  $D$  chosen for the curves in Figs. 4, 5 and 6 were selected so that  $\sqrt{2D}$  would be rational. In this manner full use (no interpolation) was made of the ex-

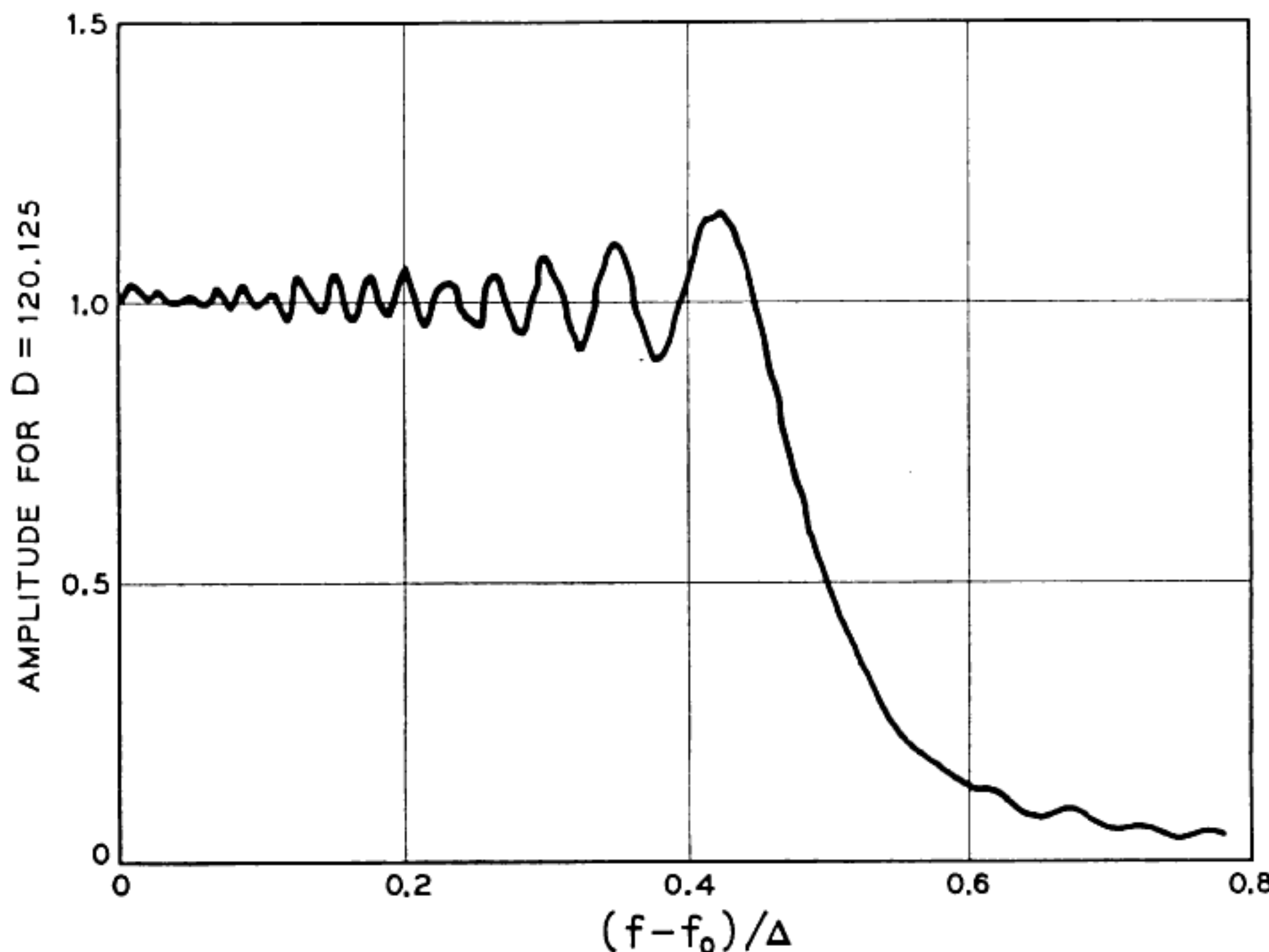


Fig. 6 — Spectral amplitude of a rectangular Chirp signal for  $D = 120.125$ .

cellent Fresnel integral tables compiled by Van Wijngaarden and Scheen.<sup>11</sup> Since  $Z(-u) = -Z(u)$ , it is easily established that the spectrum amplitude function in (10b) is an even function of the frequency variable  $x - x_0$ . Thus, in Figs. 4, 5 and 6 the spectrum shape is illustrated only for frequencies greater than the carrier  $f_0$ ; a symmetric reflection provides the spectrum for frequencies  $f$  below  $f_0$ . Qualitatively, these curves show that, as the dispersion factor  $D$  is increased, the spectrum shape becomes more nearly rectangular, with a total bandwidth approaching  $\Delta$ . For smaller  $D$  values, there appears, from Fig. 4, to be considerable frequency content outside a band  $\Delta$  wide centered at  $f_0$ . However, a numerical integration has shown that almost 95 per cent of the spectral energy is contained in the band  $\Delta$  for  $D$ 's as low as 10; when  $D$  becomes 100, approximately 98 to 99 per cent of the energy is confined between  $f_0 - \Delta/2$  and  $f_0 + \Delta/2$ . Only for extremely large  $D$  values will the intuitive instantaneous frequency picture yield results for the frequency spectrum with any quantitative accuracy. In practice, the value of  $f_0$ , whether at radio frequency (RF) or some intermediate frequency (IF), will always be at least several times the approximate bandwidth  $\Delta$ . So long as  $f_0$  continues to be several times  $\Delta$ , Fourier analysis shows that the complex radar signal in (1) contains only positive frequencies to a very high degree of accuracy. As stated previously, simplified receiver network characteristics may be assumed when the ideal received waveform contains only positive frequencies.

The function of the receiving network may be conveniently divided into two parts. First, there is a phase-equalizing network whose function is to cancel the phase distortion intentionally introduced in the Chirp signal illustrated in Fig. 2 and described analytically above. The characteristics of the phase-equalizing network are shown in Fig. 3(a). For an input given by (1), the response of this network will have a form, illustrated in Fig. 3(b), that possesses a multiple-side-lobe (in time) structure. The second function of the receiving network, then, will be to reduce the relative amplitudes of these side lobes. This important second network function will be discussed in detail in Section 3.4.2. It will be found that the necessary corrective networks need affect only the amplitude and not the phase characteristic of the signal spectrum. Thus, there is also a natural splitting of the network characteristics from an analytical viewpoint.

The following expression is chosen for the analytical specification of a network admittance function possessing a linear delay characteristic:

$$\tilde{Y}(f) = e^{i\pi p(f-f_0)^2}. \quad (11)$$

This network is given a uniform amplitude characteristic with the particular amplitude value of unity. To see that the chosen phase characteristic represents the linear delay property, it is necessary to investigate the instantaneous delay of  $\tilde{Y}(f)$ . The instantaneous delay is proportional to the phase  $\psi = \pi p(f - f_0)^2$  differentiated with respect to frequency. Let  $t_d$  denote the instantaneous delay; then

$$t_d \equiv -\frac{1}{2\pi} \frac{d\psi}{df} = -p(f - f_0). \quad (12)$$

It should be noted that this linear delay characteristic has been chosen so as to give zero delay to a frequency  $f$  equal to the carrier  $f_0$ . This choice is made for analytical convenience only, and a linear phase is frequently ignored, since it gives rise only to a uniform, distortionless signal delay. When  $p = k^{-1}$ , the differential delay over the band  $\Delta$  is given by  $p\Delta = \Delta/k = T$ . It is this particular case that is illustrated in Fig. 3(a). Throughout this paper only this optimum case is considered:

$$\tilde{Y}(f) = e^{i\pi(f-f_0)^2/k}. \quad (13)$$

The detailed response of the lossless phase equalizer to the input Chirp signal, (1), will now be investigated. The complex response function will be denoted by  $\epsilon(t)$  and its Fourier transform by  $\tilde{\epsilon}(f)$ . The true, real response  $e(t)$  is obtained, as usual, by taking the real part of  $\epsilon(t)$ :  $e(t) = \text{Re } \epsilon(t)$ . From the definition of the network admittance function, the output spectrum is given by

$$\tilde{\epsilon}(f) = \tilde{Y}(f)\tilde{\epsilon}_1(f). \quad (14)$$

A well-known result of Fourier analysis permits the response  $\epsilon(t)$  to be defined according to

$$\epsilon(t) = Y(t)*\epsilon_1(t). \quad (15)$$

Here  $Y(t)$ , the network impulse response, is simply the Fourier transform of the network function in (13). The star (\*) denotes the convolution operation, which is defined for two arbitrary functions as follows:

$$f(z)*g(z) = \int_{-\infty}^{\infty} f(z-w)g(w) dw, \quad (16a)$$

or equivalently

$$f(z)*g(z) = \int_{-\infty}^{\infty} f(v)g(z-v) dv. \quad (16b)$$

It is somewhat easier to calculate the response  $\epsilon(t)$  by using (15). First, the impulse response,  $Y(t)$ , must be computed:

$$\begin{aligned} Y(t) &= \int_{-\infty}^{\infty} \tilde{Y}(f) e^{2\pi i f t} df \\ &= \int_{-\infty}^{\infty} e^{2\pi i [ft + (f-f_0)^2/2k]} df. \end{aligned} \quad (17)$$

This is a well-known integral,<sup>†</sup> and (17) is evaluated as

$$Y(t) = \sqrt{\frac{i\Delta}{T}} e^{2\pi i (f_0 t - kt^2/2)}. \quad (18)$$

The complex output,  $\epsilon(t)$ , is obtained by forming the convolution product of  $Y(t)$  and  $\epsilon_1(t)$  given, respectively, in (18) and (1). Thus,

$$\epsilon(t) = \sqrt{\frac{i\Delta}{T}} \int_{-T/2}^{T/2} e^{2\pi i [f_0 t + k\tau^2/2 - k(t-\tau)^2/2]} d\tau,$$

which simplifies considerably, due to cancellations in the exponent, to

$$\epsilon(t) = \sqrt{\frac{i\Delta}{T}} e^{2\pi i (f_0 t - kt^2/2)} \int_{-T/2}^{T/2} e^{2\pi i k t \tau} d\tau.$$

Carrying out the elementary integral that remains,

$$\epsilon(t) = \frac{1}{\pi k t} \sqrt{\frac{i\Delta}{T}} \sin(\pi k t T) e^{2\pi i (f_0 t - kt^2/2)},$$

which, when regrouped becomes

$$\epsilon(t) = \sqrt{D i} \frac{\sin \pi \Delta t}{\pi \Delta t} e^{2\pi i (f_0 t - kt^2/2)}. \quad (19)$$

This response assumes the following form when expressed in terms of the natural time variable  $y = \Delta t$ :

$$\epsilon(y) = \sqrt{D} \frac{\sin \pi y}{\pi y} e^{2\pi i (x_0 y - y^2/2D) + i\pi/4}. \quad (20)$$

Following Woodward's nomenclature<sup>10</sup> it is useful to introduce

$$\text{sinc } y \equiv \frac{\sin \pi y}{\pi y} \quad (21)$$

as a convenient shorthand. The functions  $\text{sinc } y$  and  $\text{rect } x$  are Fourier transforms of one another. The envelope of the complex response is given by the absolute value of (19) and takes the form

---

<sup>†</sup> This transform is number 708.0 in Campbell and Foster.<sup>12</sup>

$$\sqrt{D} \left| \frac{\sin \pi \Delta t}{\pi \Delta t} \right| = \sqrt{D} |\operatorname{sinc} \Delta t|. \quad (22)$$

It is this envelope that is shown in Fig. 3(b): this collapsed pulse has an amplitude increase of  $\sqrt{D}$  over the input pulse and a new pulse width  $\tau \sim 1/\Delta$ , measured at the half-power points (3-db points).

There are two important facts to be noted regarding the complex response signal given in (19) and (20). First, there exists a residual FM after phase equalization. By comparing (19) with the input signal  $\epsilon_1(t)$  in (1) one easily sees that the residual FM occurs at the same rate, but is reversed in sense. Otherwise stated, if  $k > 0$ , then the frequency of the transmitted pulse *rises* during the pulse period, while the instantaneous frequency of the collapsed signal (19) *falls*, but at the same absolute rate. This effect has been observed in a laboratory model for a low dispersion factor ( $D \approx 10$ ). One would expect to observe this effect principally for low  $D$ 's, as may be seen from the following qualitative argument. Using (20), the instantaneous "frequency" is given by  $x_0 - y/D$ . Now, about 90 per cent of the signal energy is confined in the "time" interval  $|y| < 1$  by the envelope  $\operatorname{sinc} y$ . If attention is confined to this region of pronounced signal amplitude, the frequency will vary only between  $x_0 + 1/D$  and  $x_0 - 1/D$ . From the discussion following (10b), the value of  $x_0 = f_0/\Delta$  will be seen to lie generally in the range  $x_0 > 2$ . For large  $D$ , the frequency in the significant region of the output signal remains constant to an accuracy of about  $1/Dx_0$ . As  $D$  becomes larger, deviations from a constant frequency are therefore nearly undetectable. A slight reservation to this point will be noted in Section 3.3 but, for the most part (especially in studying the side-lobe reduction in Section 3.4.2), the residual FM in the response will be ignored.

The second important point to be noted regarding the output signal (19) pertains to the envelope,  $\operatorname{sinc} \Delta t$ . Although the initial envelope,  $\operatorname{rect}(t/T)$ , and the final one,  $\operatorname{sinc} \Delta t$ , are both functions of time, there does appear to be a Fourier transform relation between the *functional* form of these envelopes. The two points just stressed above will now be shown to be consequences of an important result of greater generality.

Assume for the moment that, instead of (1), the following complex signal is transmitted:

$$\epsilon'(t) = E(t)e^{2\pi i(f_0 t + kt^2/2)}. \quad (23)$$

This signal differs from (1) insofar as the envelope  $\operatorname{rect}(t/T)$  has been replaced by an *arbitrary* envelope denoted by  $E(t)$ . The linear FM characteristic remains unchanged. Attention is now turned to finding the

response of the same lossless network given before in (13) to the modified input,  $\epsilon'(t)$ . The spectrum of the new output signal is given by

$$\begin{aligned}\tilde{\epsilon}''(f) &= \tilde{Y}(f)\tilde{\epsilon}'(f) \\ &= \int_{-\infty}^{\infty} E(\tau) e^{2\pi i [(f_0-f)\tau + k\tau^2/2 + (f-f_0)^2/2k]} d\tau.\end{aligned}\quad (24a)$$

The terms in the brackets constitute a perfect square, so that

$$\tilde{\epsilon}''(f) = \int_{-\infty}^{\infty} E(\tau) e^{(\pi i/k)[(f-f_0)-k\tau]^2} d\tau. \quad (24b)$$

By applying another Fourier transform, the output signal  $\epsilon''(t)$  is generated:

$$\epsilon''(t) = \int_{-\infty}^{\infty} \int_{-\infty}^{\infty} E(\tau) e^{2\pi ift + \pi i/k[(f-f_0)-k\tau]^2} df d\tau. \quad (25)$$

The integration over  $f$  is similar to one carried out previously, and (25) becomes

$$\tilde{\epsilon}''(t) = \sqrt{ki} e^{2\pi i(f_0 t - kt^2/2)} \int_{-\infty}^{\infty} E(\tau) e^{2\pi ik\tau t} d\tau. \quad (26)$$

The remaining integral in (26) essentially defines the Fourier transform of  $E(t)$ , so that our final expression for  $\epsilon''(t)$  becomes

$$\epsilon''(t) = \sqrt{ki} \tilde{E}(-kt) e^{2\pi i(f_0 t - kt^2/2)}. \quad (27)$$

This result shows that the two points stressed above are special cases of an exceedingly general result. That is, the output response in (27) possesses the same linear FM property as the input signal but with the reversed sense, and the Fourier-transform functional relation between input and output envelopes is established as a general rule.

The preceding general analysis for the arbitrary envelope  $E(t)$  provides an excellent intuitive picture for the next topic to be discussed: the *generation* of the long transmitted pulse by passive means.

### 3.2 Passive Generation of the Long FM Transmitter Signal

In any scheme of generating the long-duration FM signal, the foremost objective is to secure a signal whose properties are similar to those illustrated in Fig. 2. The passive generation means described in this section can be no exception to this rule.

The previous section concluded with a general theorem relating the input and output envelopes of a signal with linear FM when passed

through a lossless, linear delay equalizer. This theorem illustrates how an input signal with a long-duration envelope becomes transformed by the equalizer to a signal whose new envelope is much shorter in duration. In addition, implicitly contained in this theorem is the effect produced by an input signal that possesses a very *short*-duration envelope. Since the output and input envelopes are functionally connected through the Fourier transform, the response envelope will be one of long-duration when a narrow input signal is used. Inspection of (23) and (27) shows that, if the initial envelope  $E(t)$  is chosen as  $\text{sinc } \Delta t$ , then the envelope of the equalizer output is given by  $\sqrt{k} \tilde{E}(-kt) = \sqrt{k} \Delta^{-1} \text{rect}(kt/\Delta) = D^{-\frac{1}{2}} \text{rect}(t/T)$ . The full signal, with its linear FM characteristic, may then be amplified to achieve the proper transmission level.

There are two points that arise in connection with the passive generation scheme described above. The first deals with the particular characteristics of the narrow-input signal whose envelope  $E(t) = \text{sinc } \Delta t$ . One of the additional requirements for this signal, according to (23), is a linear FM characteristic. In the discussion following (22) it was shown, for all cases of practical instance, that the linear FM characteristic would cause only a very slight deviation from a constant frequency. Qualitatively, it appears that the properties of the output signal (27) will remain essentially unchanged if the input signal contains *no* FM; i.e., if (23) is replaced by  $\epsilon'(t) = (\text{sinc } \Delta t)e^{2\pi i f_0 t}$ . Practically, it is of course much easier to generate simply the required short envelope than a signal with such delicate FM properties. It is the neglect of the linear FM characteristic that is responsible for what analytical distinctions there are in studying the passive generation scheme.

The second issue to be discussed relates to the particular sign of the linear FM slope in the network output signal in (27). By comparing (27) and (1) it is clear that the response signal's FM is directed oppositely to the FM of the desired input in (1). This means that the same network *characteristics* cannot be used both to generate the long FM signal in the transmitter *and* to collapse that signal in the receiver. What is clearly needed, then, is two distinct network characteristics, one with  $k > 0$  and the other with  $k < 0$ , so that the sum of the delays in these two characteristics is a constant, independent of frequency. If one of these characteristics is used in generating the long FM signal, then the remaining one represents the appropriate collapsing characteristic. The reciprocal relation existing between these two network characteristics is illustrated in Fig. 7.

In discussing the generation of the long FM signal by passive means it was stated that, for practical reasons, a short, constant-frequency

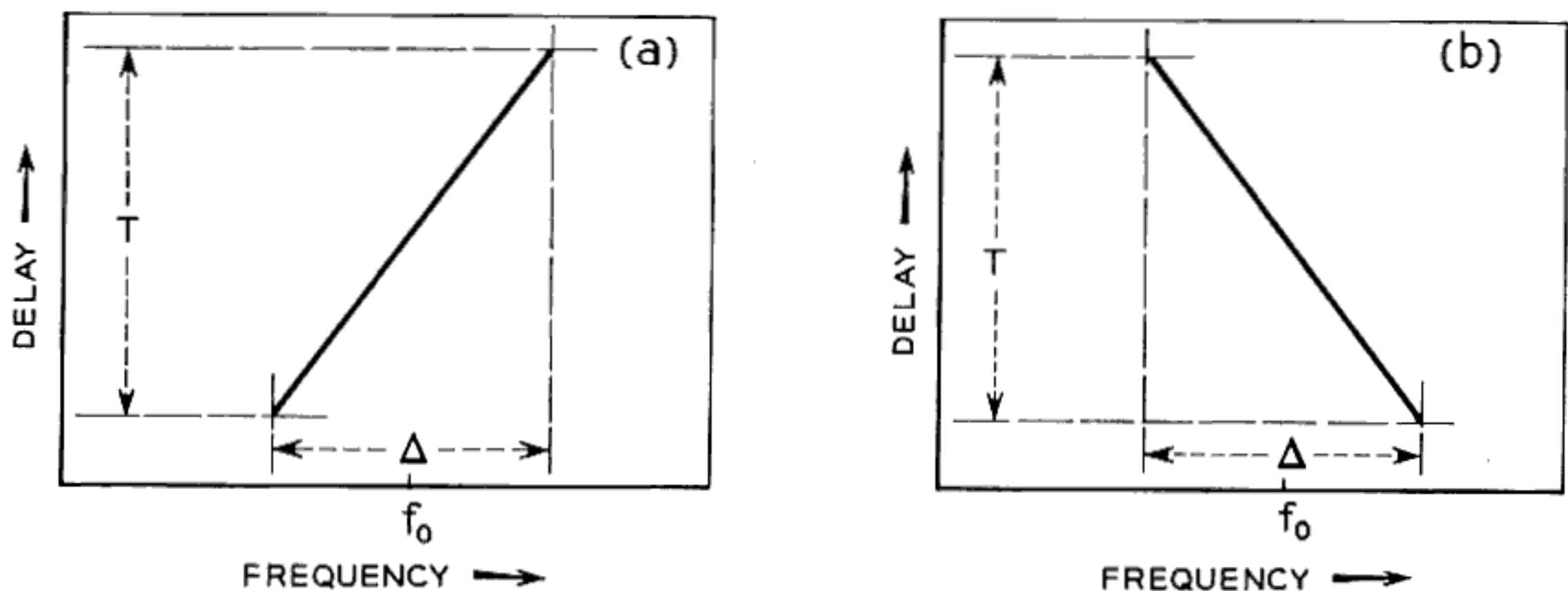


Fig. 7 — (a) Equivalent network characteristics for the transmitter in the passive generation scheme; a uniform amplitude characteristic is assumed along with the phase characteristic illustrated. (b) Appropriate receiver network characteristic to be used with the passive transmitter network in (a); note that the sum of the delay introduced by the transmitter and receiver networks is a constant.

input signal is used whose envelope is given by  $\text{sinc } \Delta t$ . The network output envelope will no longer match that shown in Fig. 2, due to the neglect of a small-input FM characteristic. It is important to determine the quantitative effect that this approximation has on the network output, since this is the characteristic signal transmitted by the radar. The equivalent transmitter network characteristics are chosen in accord with Fig. 7(a):

$$\tilde{Y}'(f) = e^{-i\pi(f-f_0)^2/k}. \quad (28)$$

The complex input to this network is denoted by  $\epsilon_2(t)$ , where

$$\epsilon_2(t) = (\text{sinc } \Delta t)e^{2\pi i f_0 t}, \quad (29)$$

and again the shorthand  $\text{sinc } y$  has been used. The response of the transmitter network is given by

$$\begin{aligned} \epsilon'_2(t) &= \int_{-\infty}^{\infty} e^{2\pi i f t} \tilde{\epsilon}_2(f) \tilde{Y}'(f) df \\ &= \frac{1}{\Delta} \int_{f_0-\Delta/2}^{f_0+\Delta/2} e^{2\pi i [ft - (f-f_0)^2/2k]} df. \end{aligned} \quad (30)$$

This result, like (7), may be expressed in terms of the complex Fresnel integral  $Z(u)$  defined in (8):

$$\epsilon'_2(t) = \frac{1}{\sqrt{2\Delta T}} e^{2\pi i (f_0 t + k t^2/2)} [Z^*(v_2) - Z^*(v_1)], \quad (31)$$

where the superscript star (\*) denotes complex conjugate. The arguments  $v_2$  and  $v_1$  are given by

$$v_2 = \sqrt{2} \left( \sqrt{\frac{\Delta}{T}} t + \frac{1}{2} \sqrt{\Delta T} \right), \quad (32a)$$

$$v_1 = \sqrt{2} \left( \sqrt{\frac{\Delta}{T}} t - \frac{1}{2} \sqrt{\Delta T} \right). \quad (32b)$$

What is the relation between the desired rectangular envelope and the true one given in (31)? Apart from a scale factor, this envelope is given by

$$\frac{1}{\sqrt{2}} \{ [C(v_2) - C(v_1)]^2 + [S(v_2) - S(v_1)]^2 \}^{\frac{1}{2}}. \quad (33)$$

Notice that this envelope is of precisely the same functional form as (10b), which describes the amplitude of the frequency spectrum for the rectangular Chirp signal in (1). Consequently, by merely reinterpreting Figs. 4, 5 and 6, curves representing the transmitted signal envelope may be obtained. To facilitate the reinterpretation the definitions of the arguments used in calculating (10b) are repeated here [see (9a) and (9b)]:

$$u_2 = \sqrt{\frac{2}{D}} \left[ -D(x - x_0) + \frac{D}{2} \right],$$

$$u_1 = \sqrt{\frac{2}{D}} \left[ -D(x - x_0) - \frac{D}{2} \right].$$

A comparison with the new arguments in (32) for the transmitted envelope shows that the appropriate reinterpretation of the abscissa is given by the transformation:  $(x - x_0) \rightarrow y/D = t/T$ . Thus, Fig. 4, for example, shows one-half of the symmetric envelope for the case  $D = 10.125$ ; the abscissa value of 0.5 is to be understood as the value of the parameter  $t/T$ . This value of  $t/T$  marks the boundary in time of the desired rectangular envelope. The value 1.0 on the ordinate represents the corresponding amplitude of the ideal rectangular envelope. A similar abscissa relabeling and reinterpretation applies to Figs. 5 and 6. These latter two figures illustrate that, as  $D$  becomes larger, the transmitted signal envelope approaches the rectangular envelope more closely. The deviation from a rectangular shape is entirely due to the neglect of the small linear FM in the input.

After the transmitted signal is reflected from, say, a point target, the return signal undergoes phase equalization in the receiver. Although Section 3.1 was devoted to the properties of a collapsed pulse, it is instructive to see what new shape is obtained when the transmitted envelope is no longer exactly rectangular. The calculation of the final

response signal is almost immediate. The short signal in the transmitter is given in (29):  $\epsilon_2(t) = (\text{sinc } \Delta t)e^{2\pi i f_0 t}$ . The transmitter network that spreads out this short pulse has a characteristic given in (28):  $\tilde{Y}'(f) = e^{-i\pi(f-f_0)^2/k}$ . The receiver network characteristic to collapse the transmitted signal appears in (13):  $\tilde{Y}(f) = e^{i\pi(f-f_0)^2/k}$ . The ideal receiver output, then, is simply

$$\begin{aligned}\epsilon_2''(t) &= \int_{-\infty}^{\infty} \tilde{Y}(f) \tilde{Y}'(f) \tilde{\epsilon}_2(f) e^{2\pi i f t} df \\ &= \int_{-\infty}^{\infty} \tilde{\epsilon}_2(f) e^{2\pi i f t} df \\ &= \epsilon_2(t).\end{aligned}\tag{34}$$

That is, the receiver equalizer output equals the short generating signal employed in the transmitter:  $\epsilon_2''(t) = (\text{sinc } \Delta t)e^{2\pi i f_0 t}$ . It is to be noted that the *envelope* of the response,  $\text{sinc } \Delta t$ , achieved by passive generation is equivalent to the *envelope* obtained from an “active” generation given in (19) and (22). The only distinction in the two modes of generation rests in the presence or absence of a small, residual linear FM. One possible consequence of this small distinction will be discussed in the next section.

### 3.3 Some Signal-to-Noise Considerations in the Study of Chirp Radars

Up to this point the analysis has been confined only to uniformly lossless delay-equalizing networks. In practice, of course, this idealization cannot hold true, nor would one even want it to hold true. For a study of the S/N properties of Chirp radars, additional networks must be used which shape the spectrum by introducing some loss. Spectrum shaping will be discussed again in Section 3.4.2 from a different point of view.

#### 3.3.1 Maximum Signal-to-Noise and the Matched Filter

Since the presence of noise represents a degradation of signal information, it is important that the ratio of signal to noise be made as large as practical. Woodward<sup>10</sup> discusses several different criteria for just which quantity should be maximized. For this paper, the peak signal power to mean noise power ratio is selected as the definition of S/N. The noise perturbing the ideal Chirp system is assumed to be additive and to have the properties of so-called white gaussian noise. Such noise is (a) statistically independent at each frequency, (b) of uniform mean power density independent of frequency and (c) gaussian in its amplitude dis-

tribution at each frequency. With no loss of generality, the mean noise power can be normalized to take the value one. Therefore, the total noise output is given by the noise energy in a "typical" output noise signal whose Fourier transform is denoted by  $\tilde{Y}(f)\tilde{n}(f)$ , where  $\tilde{Y}(f)$  denotes an arbitrary network characteristic. Using the criteria for mean noise level, the noise power output becomes

$$N \equiv \int |\tilde{Y}(f)|^2 |\tilde{n}(f)|^2 df = \int |\tilde{Y}(f)|^2 df, \quad (35)$$

when expressed in terms of the arbitrary filter  $\tilde{Y}(f)$ . It is clear that additional spectrum shaping of the linear delay network is necessary to give meaning to the noise defined by (35).

In order to make signal-to-noise comparisons meaningful, both the signals and the noise must be normalized. The common practice is to normalize the signal power by dividing it by the total energy content in the signal:  $\int |\epsilon(t)|^2 dt = \int |\tilde{\epsilon}(f)|^2 df$ , where  $\epsilon(t)$  now denotes an arbitrary signal chosen, for convenience, to have only positive frequencies. The normalized peak signal power,  $S$ , is then defined by

$$S = (\text{maximum over } t) \frac{\left| \int \tilde{Y}(f)\tilde{\epsilon}(f)e^{2\pi ift} df \right|^2}{\int |\tilde{\epsilon}(f)|^2 df}. \quad (36)$$

Finally, the S/N is given by

$$S/N = \frac{\left| \int \tilde{Y}(f)\tilde{\epsilon}(f)e^{2\pi ift_M} df \right|^2}{\int |\tilde{\epsilon}(f)|^2 df \int |\tilde{Y}(f)|^2 df}, \quad (37)$$

where the maximum of the right-hand side occurs at  $t = t_M$ ;  $t_M$  will in general be a function of both  $\tilde{\epsilon}(f)$  and  $\tilde{Y}(f)$ . Suppose now that  $\tilde{\epsilon}(f)$  is fixed. For which filter  $\tilde{Y}(f)$  will the value of S/N achieve its maximum value? This is a problem in the calculus of variations whose solution, for present purposes, is summarized in the well-known Schwarz inequality, which states, for two arbitrary functions  $f(z)$  and  $g(z)$ , that

$$\frac{\left| \int f(z)g(z) dz \right|^2}{\int |f(v)|^2 dv \int |g(w)|^2 dw} \leq 1. \quad (38)$$

The equality holds only when  $f(z)$  is proportional to  $g^*(z)$ . Upon applying this theorem to (37), the maximum S/N is achieved when  $\tilde{Y}(f)$  is proportional to  $\tilde{\epsilon}^*(f) e^{-2\pi i f t_M}$ . The exponential factor merely represents a gross delay without distortion, which will be ignored. Consequently, the *matched filter*,  $\tilde{Y}_m(f)$ , for the signal  $\epsilon(t)$  is defined as

$$\tilde{Y}_m(f) \equiv \tilde{\epsilon}^*(f). \quad (39)$$

It should be noticed that the particular value of the maximum S/N is in no way related to which specific signal and matched filter are used; any signal coupled with its matched filter attains the same maximum value of "one".

It is important to find the specification of the output response when a matched filter is used. According to (39), the complex response  $\epsilon_m(t)$  is determined by

$$\epsilon_m(t) = \int_{-\infty}^{\infty} |\epsilon(f)|^2 e^{2\pi i f t} df, \quad (40a)$$

which may be re-expressed with the aid of the convolution operator defined in (16):

$$\begin{aligned} \epsilon_m(t) &= \epsilon^*(-t) * \epsilon(t) \\ &= \int_{-\infty}^{\infty} \epsilon^*(\tau - t) \epsilon(\tau) d\tau. \end{aligned} \quad (40b)$$

It follows from (40b) that the complex response from a matched filter is determined by a correlation process. As usual, the true, real response is obtained by taking the real part of  $\epsilon_m(t)$  in (40a) or (40b). The matched filter for Chirp radars can now be studied with the aid of the general theory just presented.

### 3.3.2 Matched Filter for Chirp

3.3.2.1 *Matched Filter for the Active Generation Case.* For the case of active generation, the initial signal is  $\epsilon_1(t)$  in (1), namely,

$$\epsilon_1(t) = \text{rect}\left(\frac{t}{T}\right) e^{2\pi i (f_0 t + k t^2/2)},$$

where  $\text{rect } z$  is defined by (2). The matched filter for this signal,  $\tilde{Y}_{m_1}(f)$ , may be readily obtained from the analysis of the spectrum of  $\epsilon_1(t)$  in (7):

$$\begin{aligned} \tilde{Y}_{m_1}(f) &= \tilde{\epsilon}_1^*(f) \\ &= \sqrt{\frac{T}{2\Delta}} e^{+i\pi(f-f_0)^2/k} [Z^*(u_2) - Z^*(u_1)], \end{aligned} \quad (41)$$

where  $u_2$  and  $u_1$  are given in (9). The matched filter impulse response is also readily obtained by using the general relation:  $Y_m(t) = \epsilon^*(-t)$ . Therefore,

$$\begin{aligned} Y_{m_1}(t) &= \epsilon_1^*(-t) \\ &= \text{rect}\left(\frac{t}{T}\right) e^{2\pi i(f_0 t - kt^2/2)}. \end{aligned} \quad (42)$$

The output response when the rectangular Chirp signal is passed through its own matched filter may be computed with the aid of (40b):

$$\epsilon_{m_1}(t) = \int_{-\infty}^{\infty} \text{rect}\left(\frac{\tau - t}{T}\right) \text{rect}\left(\frac{\tau}{T}\right) e^{2\pi i[f_0 t + (k/2)\tau^2 - (k/2)(\tau-t)^2]} d\tau.$$

When  $0 \leq t \leq T$ ,

$$\epsilon_{m_1}(t) = e^{2\pi i(f_0 t - kt^2/2)} \int_{t-T/2}^{T/2} e^{2\pi i k \tau t} d\tau.$$

Finally, after the remaining integration is performed,

$$\epsilon_{m_1}(t) = \frac{1}{\pi k t} e^{2\pi i f_0 t} \sin \pi (ktT - kt^2). \quad (43)$$

It is readily determined that the envelope of  $\epsilon_{m_1}(t)$  is an even function of time. Therefore,

$$T \frac{\sin \pi(\Delta |t| - kt^2)}{\pi \Delta |t|} \quad (44a)$$

represents the envelope of the matched filter response for times  $|t| \leq T$ . For times  $|t| > T$  the envelope vanishes. When (44a) is expressed in terms of the natural time variable,  $y = \Delta t$ , the envelope becomes

$$\sqrt{D} \frac{\sin \pi \left( |y| - \frac{y^2}{D} \right)}{\pi |y|}, \quad (44b)$$

where a normalization has been chosen so as to facilitate a direct comparison with the response envelope in (22) obtained by using the lossless phase equalizer [see (13)]. The output from the simple linear delay equalizer,  $\sqrt{D}(\sin \pi y)/\pi y$ , is a remarkable approximation to the response from the more complicated matched filter,  $\tilde{Y}_{m_1}(f)$ , especially as the dispersion factor increases. The similarity between the two signals does not mean that they possess similar values of S/N, for, as already noted, the noise energy passed by the ideal linear delay equalizer is infinite. The signal similarity does suggest, however, that a large S/N

value may be obtained by combining with the delay equalizer a shaping network that limits the noise but does not seriously attenuate the strong signal frequencies.

As an extreme example of such a shaping network, the S/N properties will be investigated when an ideal filter, which suppresses all frequencies outside the range  $|f - f_0| < \Delta/2$ , is added to the delay equalizer. The combined network is specified by

$$\tilde{Y}_{\text{rect}}(f) = \text{rect}\left(\frac{f - f_0}{\Delta}\right) e^{i\pi(f-f_0)^2/k}. \quad (45)$$

The total noise passed through  $\tilde{Y}_{\text{rect}}$  may be computed from the general definition in (35):

$$N_{\text{rect}} = \int |\tilde{Y}_{\text{rect}}(f)|^2 df = \Delta. \quad (46)$$

From symmetry arguments, the peak output signal value should occur at  $t = 0$ . The response at  $t = 0$  is given by

$$\begin{aligned} \epsilon_{\text{rect}}(0) &= \int \tilde{Y}_{\text{rect}}(f) \tilde{\epsilon}_1(f) df \\ &= \sqrt{\frac{T}{2\Delta}} \int_{f_0-\Delta/2}^{f_0+\Delta/2} [Z(u_2) - Z(u_1)] df, \end{aligned} \quad (47a)$$

where  $u_2$  and  $u_1$  are linear functions of  $f$ . If natural variables are introduced and a shift of the origin is made, (47a) is transformed into

$$\begin{aligned} \epsilon_{\text{rect}}(0) &= \sqrt{\frac{D}{2}} \int_{-\frac{1}{2}}^{\frac{1}{2}} \left\{ Z \left[ \sqrt{\frac{D}{2}} (2x + 1) \right] \right. \\ &\quad \left. - Z \left[ \sqrt{\frac{D}{2}} (2x - 1) \right] \right\} dx, \end{aligned} \quad (47b)$$

where the definition of  $u_2$  and  $u_1$  is equivalent to that given in (9). The integrals appearing in (47b) may be evaluated with the aid of the following general formula:

$$\begin{aligned} \int_a^b Z(\alpha x + \beta) dx &= \frac{1}{\alpha} [(\alpha b + \beta) Z(\alpha b + \beta) - (\alpha a + \beta) Z(\alpha a + \beta)] \\ &\quad + \frac{i}{\pi\alpha} [e^{i\pi(\alpha b + \beta)^2/2} - e^{i\pi(\alpha a + \beta)^2/2}]. \end{aligned}$$

If this general formula is applied to the specific calculation required in (47b), it follows that

$$\epsilon_{\text{rect}}(0) = \sqrt{2D} Z(\sqrt{2D}) - \frac{i}{\pi} (1 - e^{i\pi D}). \quad (48)$$

It is simpler, and sufficient for present purposes, to confine attention to  $D$  values that are even integers. With this restriction, (48) reduces to

$$\epsilon_{\text{rect}}(0) = \sqrt{2D} Z(\sqrt{2D}),$$

and the peak signal power is given by

$$|\epsilon_{\text{rect}}(0)|^2 = 2D |Z(\sqrt{2D})|^2. \quad (49)$$

To complete the calculation for the normalized peak signal power,  $S$ , it is necessary, according to (36), to divide (49) by  $\int |\epsilon_1(t)|^2 dt = \int \text{rect}(t/T) dt = T$ . Finally, the S/N is

$$(S/N)_{\text{rect}} = 2 |Z(\sqrt{2D})|^2, \quad (50)$$

where  $Z(u)$  is the complex Fresnel integral defined in (8). Any decrease of S/N below the matched filter maximum value of "one" represents a S/N degradation. In Fig. 8, the S/N degradation in decibels [i.e. units of  $10 \log_{10} (S/N)$ ] is illustrated for various values of  $D$ , the dispersion factor. Only even integral values of  $D$  were used in calculating this result; a smooth curve was then drawn between the calculated points. Certainly no qualitative error is made in this process. As anticipated, Fig. 8 shows that, as  $D$  becomes larger, the simple filter characteristics specified by  $\tilde{Y}_{\text{rect}}$  approach those of the matched filter. The extremely small S/N degradation, especially for large  $D$ , shows a clear practical preference for characteristics like those of  $\tilde{Y}_{\text{rect}}$  as compared to, say, the complicated amplitude characteristic required in building a matched filter. According to (39), the matched filter amplitude characteristic must match the signal spectrum and, for example, would need to resemble one of the spectra shown in Figs. 4, 5 or 6.

**3.3.2.2 Matched Filter for the Passive Generation Case.** Suppose, instead of the rectangular envelope, that the transmitted waveform had an envelope characteristic of the *passive* generation scheme discussed in Section 3.2. Under ideal circumstances a short signal,  $(\text{sinc } \Delta t)e^{2\pi i f_0 t}$ , is dispersed in the transmitter by a suitable linear delay equalizer. The resulting transmitted signal has a spectrum proportional to

$$\text{rect}\left(\frac{f - f_0}{\Delta}\right) e^{-i\pi(f-f_0)^2/k}.$$

From the definition of a matched filter in (39), the filter  $\tilde{Y}_{\text{rect}}(f)$  in (45)

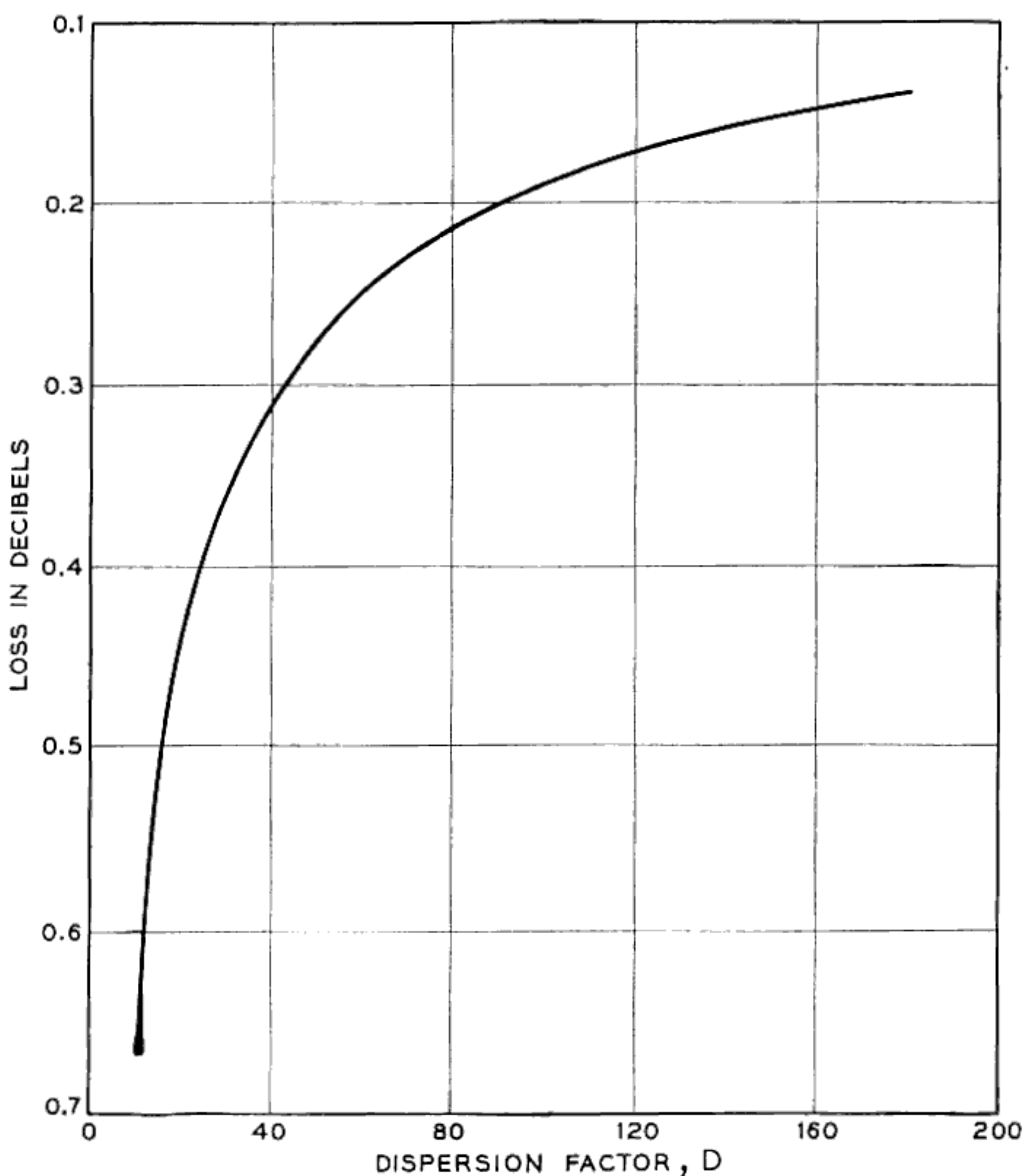


Fig. 8 — Degradation in S/N from ideal maximum when the rectangular Chirp signal passes through a delay equalizer and a sharp cutoff filter of width  $\Delta$ . The loss decreases rapidly as the dispersion factor,  $D$ , increases.

actually represents the matched filter in the case of ideal passive generation. With this filter the response becomes simply  $(\text{sinc } \Delta t)e^{2\pi i f_0 t}$ , as was noted in Section 3.2; now it appears that this particular network also yields the maximum S/N value of "one".

### 3.3.3 Signal-to-Noise for a Shaping Network to Reduce Side Lobes

Frequently there are important advantages to be gained by trading a small amount of S/N for certain desirable signal properties. An important improvement in signal characteristics is obtained when the relative side-lobe strengths are reduced, and it will be found that substantial reduction in side lobes may be obtained at only a very small cost in S/N.

Both the active and passive cases are treated simultaneously by assuming the shaping-network input signal to be specified by

$$(\text{sinc } \Delta t) e^{2\pi i(f_0 t - kt^2/2)}.$$

To obtain results pertaining to the passive generation, it suffices to set  $k = 0$ , which is effectively equivalent to an infinite dispersion factor.

The specific shaping or weighting network to be studied is gaussian in shape and given by

$$\tilde{Y}_{\text{gau}}(f) = e^{-\pi G(f-f_0)^2}. \quad (51)$$

Here,  $G$  is a parameter related to the amount of taper introduced by  $\tilde{Y}_{\text{gau}}(f)$ . It is more convenient to use two other parameters,  $L$  and  $\alpha$ , which are linearly related to  $G$ :

$$\begin{aligned} L &= 20 \log_{10} e^{\pi G \Delta^2 / 4} \\ &= \frac{20\pi}{4} (\log_{10} e) (G \Delta^2) \approx 6.83 \alpha, \end{aligned} \quad (52a)$$

where

$$\alpha \equiv G \Delta^2. \quad (52b)$$

$L$  represents the loss in decibels, imposed by  $\tilde{Y}_{\text{gau}}(f)$ , at the band edges, i.e. when  $f = f_0 \pm \Delta/2$ . Equation (51) may be rewritten in terms of  $x = f/\Delta$  and  $\alpha = G \Delta^2$ :

$$\tilde{Y}_{\text{gau}}(x) = e^{-\pi \alpha (x-x_0)^2}. \quad (53)$$

For convenience, the convolution theorem  $\epsilon_{\text{gau}}(y) = Y_{\text{gau}}(y) * \epsilon(y)$ , will be expressed directly in natural units. For the input  $\epsilon(y)$ , a normalized response of the linear delay equalizer is employed:

$$\epsilon(y) = (\text{sinc } y) e^{2\pi i(x_0 y - y^2/2D)}. \quad (54)$$

The network impulse response,  $Y_{\text{gau}}(y)$ , becomes

$$\begin{aligned} Y_{\text{gau}}(y) &= \int_{-\infty}^{\infty} \tilde{Y}_{\text{gau}}(x) e^{2\pi i x y} dx \\ &= \frac{1}{\sqrt{\alpha}} e^{2\pi i x_0 y - \pi y^2 / \alpha}. \end{aligned} \quad (55)$$

If this result is combined with (54), the modified complex response is given by

$$\epsilon_{\text{gau}}(y) = \frac{1}{\sqrt{\alpha}} e^{2\pi i x_0 y} \int_{-\infty}^{\infty} (\text{sinc } z) e^{-\pi[(y-z)^2/\alpha + iz^2/D]} dz. \quad (56a)$$

The integral in (56a) may be evaluated, and yields the following result for  $\epsilon_{\text{gau}}(y)$ :

$$\epsilon_{\text{gau}}(y) = \frac{1}{2\sqrt{\alpha}} e^{2\pi i x_0 y - \pi y^2/\alpha} \cdot \left\{ \operatorname{erf}\left[\sqrt{\frac{\pi}{c}} \left(\frac{1}{2} - \frac{iy}{\alpha}\right)\right] + \operatorname{erf}\left[\sqrt{\frac{\pi}{c}} \left(\frac{1}{2} + \frac{iy}{\alpha}\right)\right] \right\}, \quad (56b)$$

where  $c$  is a complex constant defined by

$$c = \frac{1}{\alpha} + \frac{i}{D}, \quad (57)$$

and "erf" denotes the usual error function. The peak signal, required for a S/N study, is attained at  $y = 0$ . Since

$$\int_{-\infty}^{\infty} \operatorname{sinc}^2 y dy = 1,$$

the input energy in (54) has the value 1. Therefore, the peak normalized signal power becomes

$$S_{\text{gau}} = |\epsilon_{\text{gau}}(0)|^2 = \frac{1}{\alpha} \left| \operatorname{erf}\left(\frac{1}{2} \sqrt{\frac{\pi}{c}}\right) \right|^2. \quad (58)$$

The noise power may be defined as

$$N_{\text{gau}} = \int |\tilde{Y}_{\text{gau}}(x)|^2 dx, \quad (59)$$

when expressed in terms of the natural frequency variable. If (53) and (59) are combined, one obtains  $N_{\text{gau}} = 1/\sqrt{2\alpha}$ . From (57) and (58), then,

$$(S/N)_{\text{gau}} = \sqrt{\frac{2}{\alpha}} \left| \operatorname{erf}\left(\frac{1}{2} \sqrt{\frac{\alpha D \pi}{D + i\alpha}}\right) \right|^2. \quad (60)$$

In the case of ideal passive generation the *effective* value of  $D$  is infinity in (54) and, therefore, also in (60). Under these circumstances, (60) becomes

$$(S/N)_{\text{gau}} = \sqrt{\frac{2}{\alpha}} \left[ \operatorname{erf}\left(\frac{1}{2} \sqrt{\pi\alpha}\right) \right]^2. \quad (61)$$

Actually this result is also quite accurate in the "active" case when  $D$  remains finite. In practice, a typical value of  $L$ , the loss in decibels introduced at the band edges, is of the order of 15–25 db; it follows from (52a) that  $\alpha \approx 3$ . For high-compression Chirp systems, whose  $D$  values are 100

and greater, the S/N in an active generation is well represented by (61). Fig. 9 shows a plot of the S/N degradation for a range of different gaussian weighting networks. It is noticed that there is a minimum loss of about 0.5 db when  $L \approx 8.6$  db. A detailed study of the full response signal, (56b), has been made for the passive case; the results are approximately correct for actively generated pulses. Two gross signal features have been studied: (a) the output pulse width measured at the 3-db level and (b) the relative level between the main signal peak and the first adjacent side-lobe peak. The results of this study are summarized in Figs. 10(a) and 10(b). Qualitatively, as the loss introduced at the band edges by the gaussian network is increased, there is (a) a corresponding increase in pulse width and (b) an increase in side-lobe discrimination. The marked improvement in side-lobe discrimination is well worth the slight pulse-width increase and the small cost in S/N. This example illustrates that the maximum S/N attained only by a matched filter is, in reality, a very broad maximum. This general principle is exploited in Section 3.4.2, where the primary aim of weighting networks will be to improve signal properties using other networks more efficient than the simple gaussian one studied here.

The gaussian case does provide a qualitative picture of the effect produced by the residual FM in the active generation scheme. Suppose

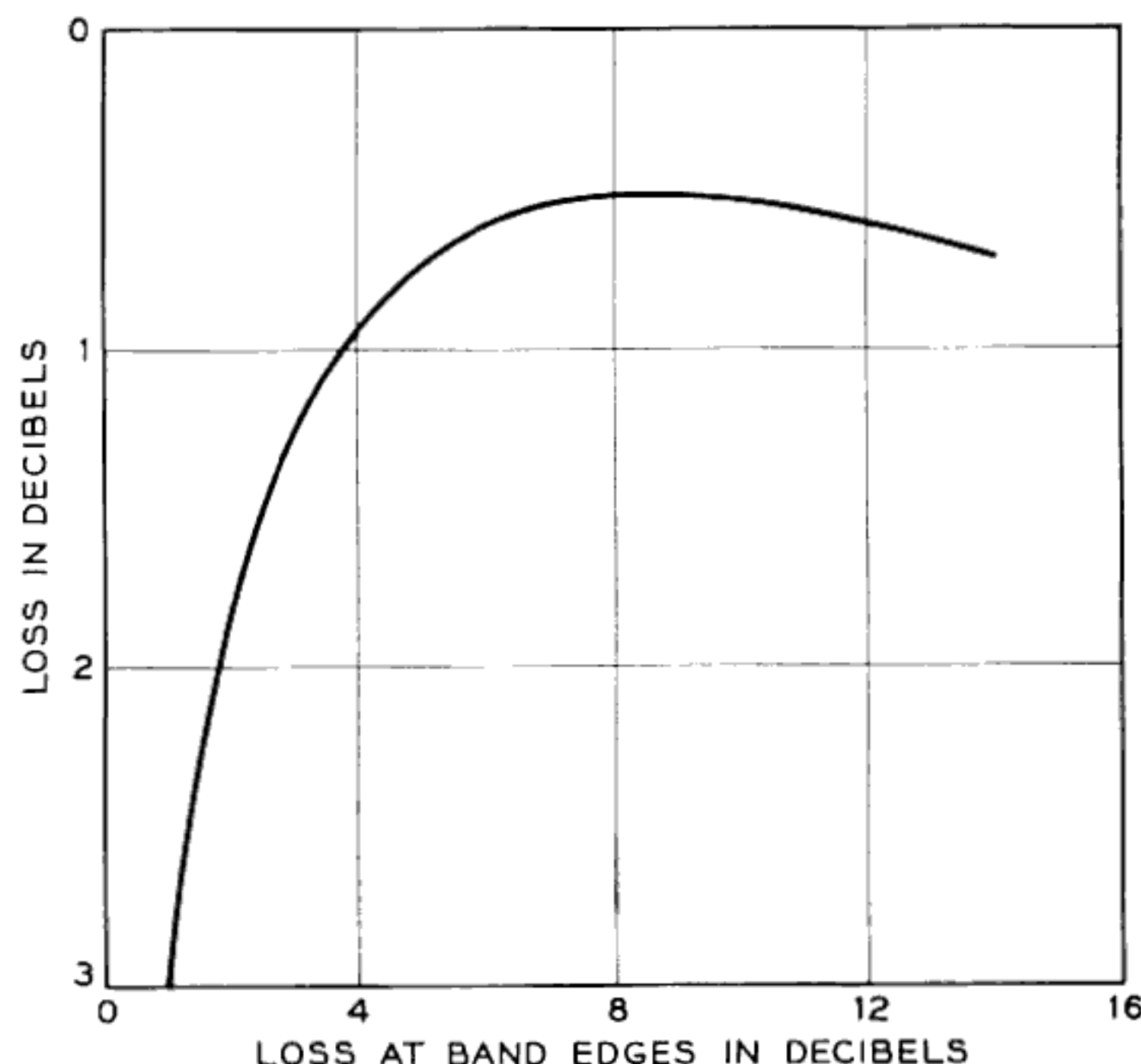


Fig. 9 — Degradation in S/N from ideal maximum when the rectangular Chirp signal passes through the delay equalizer and a smooth, gaussian-taper filter, which introduces a loss of  $L$  db at the band edges.

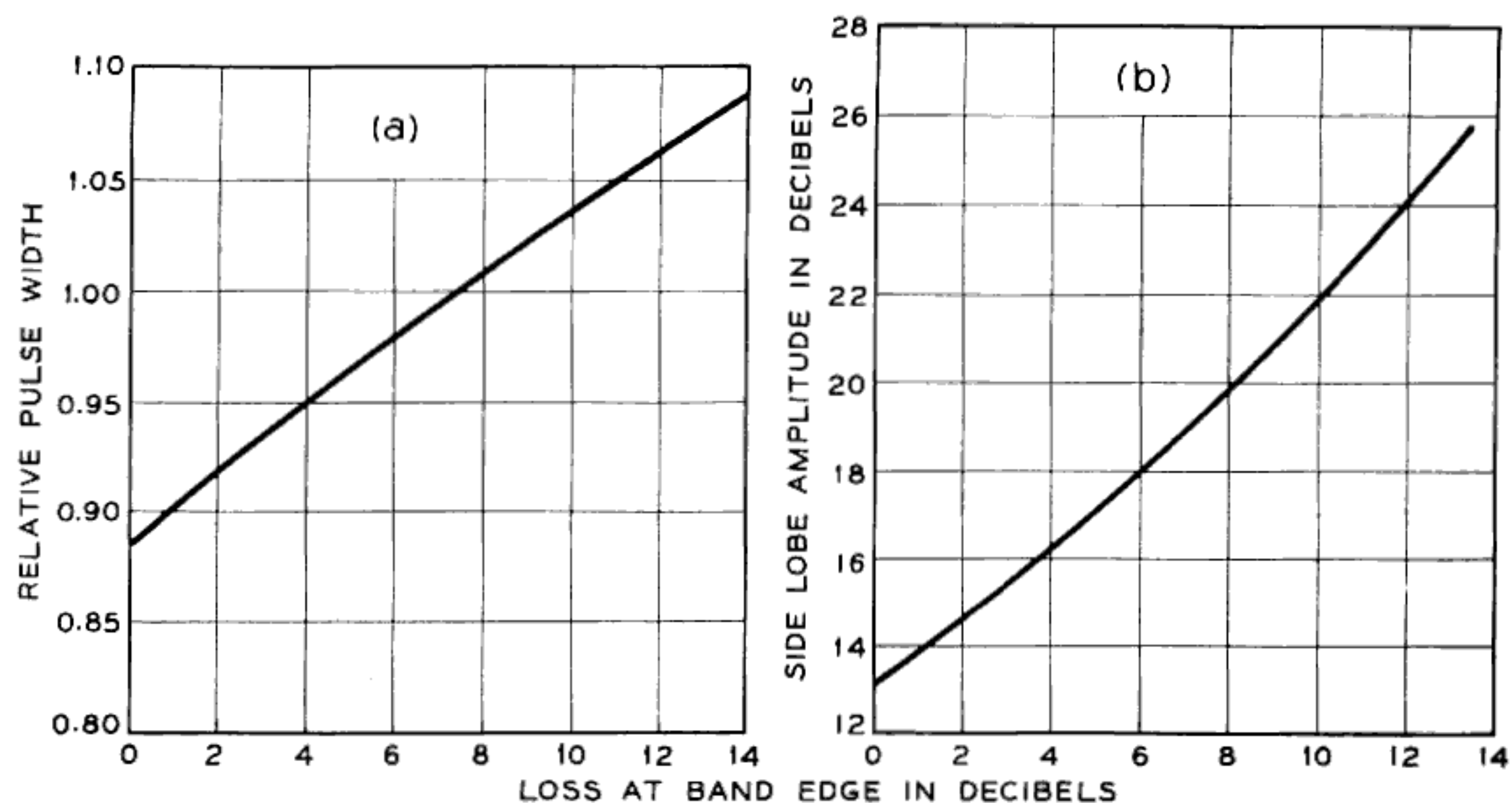


Fig. 10 — (a) Half-power pulse width increase vs.  $L$ , the gaussian filter band edge loss. (b) The relative amplitude between the maximum of the first adjacent side lobe and the central maximum of the output signal following shaping by a gaussian filter.

one was so intent on reducing the side-lobe level that  $L$ , and consequently  $\alpha$ , was increased to a point where (61) no longer approximated (60). In fact, consider the other extreme where  $\alpha \gg D$ , so that (60) becomes essentially

$$\begin{aligned} (\text{S/N})_{\text{gau}} &= \sqrt{\frac{2}{\alpha}} \left| \operatorname{erf}\left(\frac{1}{2} \sqrt{i\pi D}\right) \right|^2 \\ &= 2 \sqrt{\frac{2}{\alpha}} \left| Z\left(\sqrt{\frac{D}{2}}\right) \right|^2. \end{aligned} \quad (62)$$

The relative change, as compared to (61), is given by

$$\frac{2 \left| Z\left(\sqrt{\frac{D}{2}}\right) \right|^2}{\left[ \operatorname{erf}\left(\frac{1}{2} \sqrt{i\pi \alpha}\right) \right]^2},$$

which, for large  $D$  and consequently large  $\alpha$ , is of the order of one. Crudely speaking, therefore, the effect of the residual FM seems to have no significant effect on the S/N. The modification of pulse width and side-lobe level by the residual FM would require a detailed consideration of the exact signal in (56b). This study is not warranted in view of the many advantages inherent in passive generation.

### 3.4 A Study of Departures from Ideal Chirp Systems

In this section, deviations from the ideal system behavior will be analyzed. These deviations will include the planned departures, such as the weighting network to reduce side lobes, and random deviations introduced by imperfect system components. A unified approach has been developed to predict the effects of both types of system irregularities.

The first topic, treated in Section 3.4.1, is the basic analytical tool, "paired-echo theory", which is used in all of the analysis on system distortions. The theory of spectrum weighting, Section 3.4.2, is then presented with the aid of paired-echo theory. The next subject in the sequence, Section 3.4.3, is a consideration of quadratic phase distortion or improper equalization of the FM transmitted pulse in the receiver. The last topic, Section 3.4.4, presents a treatment of the effects of moving targets on the collapsed-signal envelope characteristics. Although the effect of moving targets is not strictly a system distortion, the analytical investigation will also be presented with the aid of the paired-echo theory developed in Section 3.4.1. For this reason, it is natural to include the effects of moving targets in the present section.

#### 3.4.1 Paired-Echo Concept

When an attempt is made to predict the performance of an actual Chirp radar system that includes many elements, a very unwieldy integral is obtained, which can be solved only by numerical methods. This, of course, gives no insight into how various distortional effects perturb the system response. It was hoped that a solution could be obtained that would provide a clear picture of the effects of distortion terms. The characteristics of the Chirp signal permit the use of a previous solution to the problem of amplitude and phase distortion in linear transmission systems. This solution was obtained in 1931 by MacColl<sup>8</sup> of Bell Telephone Laboratories and amplified in 1939 by Wheeler<sup>13</sup> and Burrows.<sup>14</sup> The solution of the distortion problem leads to a result which is interpreted in terms of paired echos. This will be clarified in the next section.

A linear transmission system is to be studied that has a steady-state transfer admittance,  $[\tilde{Y}(\omega)]$ , defined as

$$\tilde{Y}(\omega) = A(\omega)e^{jB(\omega)}, \quad (63)$$

where, as usual  $\omega = 2\pi f$ . The steady-state amplitude response is  $A(\omega)$  and the steady-state phase characteristic is  $B(\omega)$ . In an ideal system,

$A(\omega)$  would be a constant independent of frequency and  $B(\omega)$  would increase linearly with frequency. The physical system will exhibit variations from the ideal behavior that can be described by a Fourier series expansion about the frequency band of interest. This leads to a description of the system by the following equations:

$$A(\omega) = a_0 + \sum_n a_n \cos nc\omega, \quad (64)$$

$$B(\omega) = b_0\omega + \sum_n b_n \sin nc\omega. \quad (65)$$

If all  $a_n$  and  $b_n$  were zero except  $a_0$  and  $b_0$ , the above equations would describe an ideal transmission system. Any distorting influence arising from a passive element can be described by these equations, as can active elements operated in their linear regions. Thus, all of the elements of a linear system can be represented in these terms.

MacColl's analysis<sup>8</sup> considers one term of the Fourier expansion given by (64) and (65). The steady-state amplitude and phase characteristic is given by:

$$A(\omega) = a_0 + a_1 \cos c\omega, \quad (66)$$

$$B(\omega) = b_0\omega + b_1 \sin c\omega. \quad (67)$$

Since a linear system is being considered, superposition will apply; therefore, the resultant output for an input  $E(t)$  can be obtained as the sum of the responses to the various terms of the Fourier series expansion. The analysis obtains an output signal,  $I(t)$ , for an input signal,  $E(t)$ , to a system having the characteristics given in (66) and (67):

$$\begin{aligned} I(t) &= a_0 J_0(b_1) E(t + b_0) + J_1(b_1) \\ &\cdot \left[ \left( a_0 + \frac{a_1}{b_1} \right) E(t + b_0 + c) - \left( a_0 - \frac{a_1}{b_1} \right) E(t + b_0 - c) \right] \\ &+ J_2(b_1) \left[ \left( a_0 + \frac{2a_1}{b_1} \right) E(t + b_0 + 2c) + \left( a_0 - \frac{2a_1}{b_1} \right) \right. \\ &\cdot E(t + b_0 - 2c) \left. \right] + J_3(b_1) \left[ \left( a_0 + \frac{3a_1}{b_1} \right) E(t + b_0 + 3c) \right. \\ &\left. - \left( a_0 - \frac{3a_1}{b_1} \right) E(t + b_0 - 3c) \right] + \dots \end{aligned} \quad (68)$$

The functions  $J_0(b_1)$ ,  $J_1(b_1)$ ,  $J_2(b_1)$ ,  $\dots$  are the usual Bessel functions; the first four are shown graphically in Fig. 11.

The solution given in (68) provides some insight into the perturba-

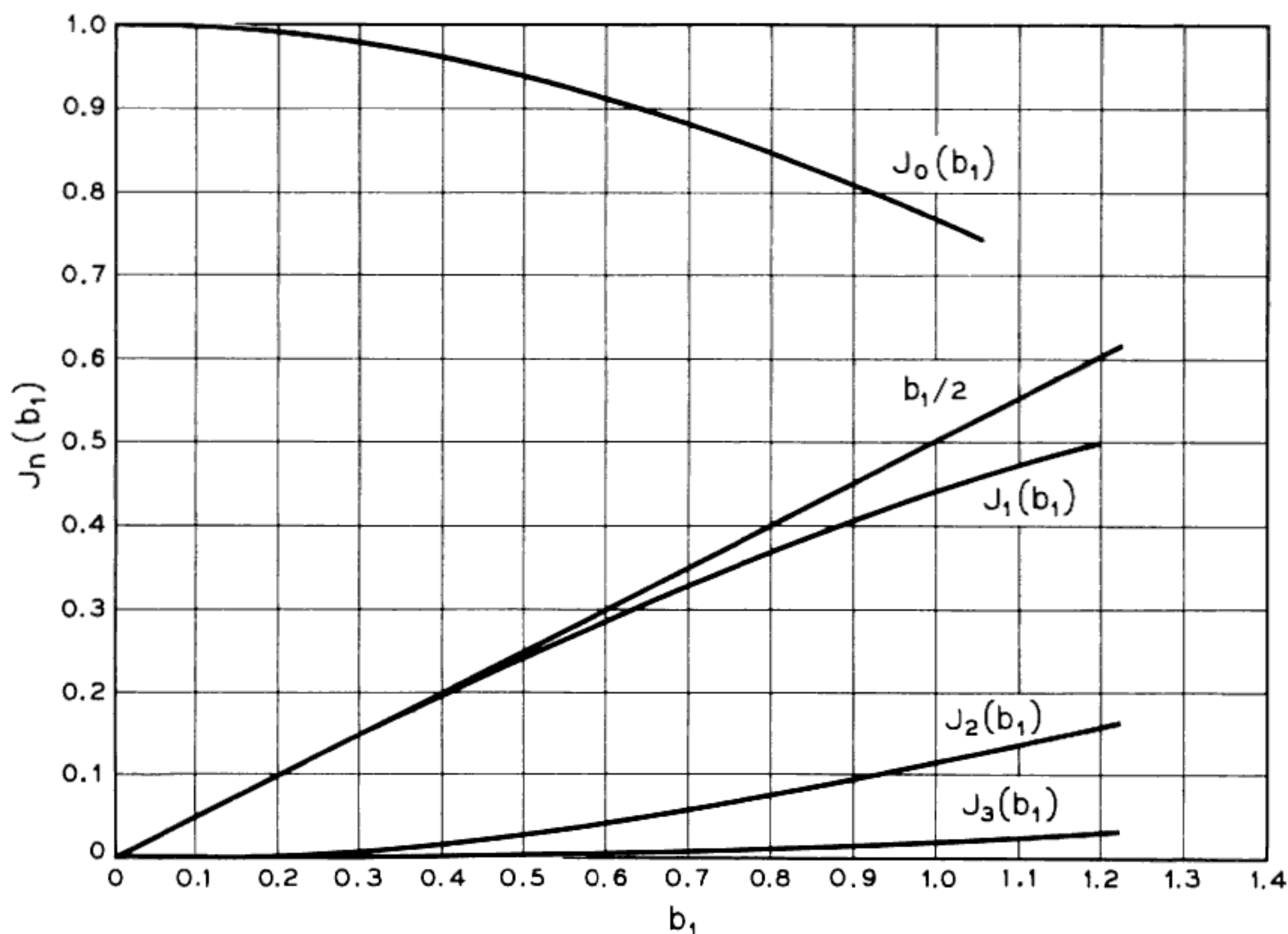


Fig. 11 — Bessel functions.

tions produced by distortion in a physical system. It can be seen that, with only one sinusoidal distortion term, the output is composed of a delayed replica of the input signal,  $E(t + b_0)$ , modified in amplitude by the coefficient,  $a_0 J_0(b_1)$ . The output also has an infinite series of terms — echoes that occur in pairs, one preceding and one lagging the major response — whose amplitude diminishes according to the Bessel function coefficients and whose separation from the major response is proportional to the order of the Bessel function. In a well-designed system, the coefficients  $a_1$  and  $b_1$  would be small. This leads to the following approximation for the Bessel functions:

$$J_0(b_1) = 1, \quad (69)$$

$$J_1(b_1) = \frac{1}{2}b_1, \quad (70)$$

$$J_n(b_1) = 0, \quad \text{for } n > 1. \quad (71)$$

These approximations apply when

$$b_1 < 0.4 \text{ radians.} \quad (72)$$

This leads to a considerably simpler expression for the output,  $I(t)$ :

$$I(t) \cong a_0[E(t + b_0) + \frac{1}{2}(a_1/a_0 + b_1)E(t + b_0 + c) \\ + \frac{1}{2}(a_1/a_0 - b_1)E(t + b_0 - c)]. \quad (73)$$

Thus it can be seen that a *small* sinusoidal distortion term produces a single pair of echoes, one preceding and one lagging the major response of the system. Notice also that an even function in the amplitude  $A(\omega)$ , i.e., a cosine ripple, gives rise to even symmetry in the echoes in the output. This is to say that both amplitude echoes ( $a_1/2a_0$ ) will be of the same polarity, either positive or negative. Similarly, an odd function of phase gives rise to odd symmetry in the output echoes, i.e., echoes of opposite polarity. Thus, a condition can be obtained where  $a_1/2a_0$  is equal to  $\frac{1}{2}b_1$  and there will be no echo preceding the main response. This is a very important case and occurs in a minimum-phase network. The phenomena, often called *ringing*, is familiar to anyone who has observed the response of an unequalized low-pass filter to a very narrow pulse.

The coefficients of (73) have been calculated and are given in graphical form in Figs. 12 and 13. It is apparent from these results that the design of a system with low residual baseline clutter (or coherent noise) is a difficult problem. If a 40-db baseline clutter level is a design objective, each component,  $a_n$  or  $b_n$ , of the Fourier series expansion of (64) and (65) would have to be kept below the following low value for a minimum phase condition:

$$20 \log_{10} \left( 1 + \frac{a_n}{a_0} \right) < 0.085 \text{ db}, \quad (74)$$

$$b_n < 0.57 \text{ degrees}. \quad (75)$$

Thus, it is seen that a 40-db clutter level is indeed extremely difficult to attain.

### 3.4.2 Frequency Weighting to Reduce Side-Lobe Levels

**3.4.2.1 Choice of Weighting Scheme.** Before proceeding into a detailed discussion of the weighting scheme employed in the present Chirp radar system, a simplified qualitative picture of the mechanics of weighting will be presented; this will permit a clearer understanding of the weighting process. The paired-echo theory of the preceding section will be used in the simplified description.

If a network with a raised-cosine amplitude response (as in Fig. 14) and a linear phase characteristic is excited with a sinc  $\Delta t$  input signal, the output signal, shown in Fig. 15, can be derived by paired-echo theory. The resultant output signal is the sum of a main delayed replica of the

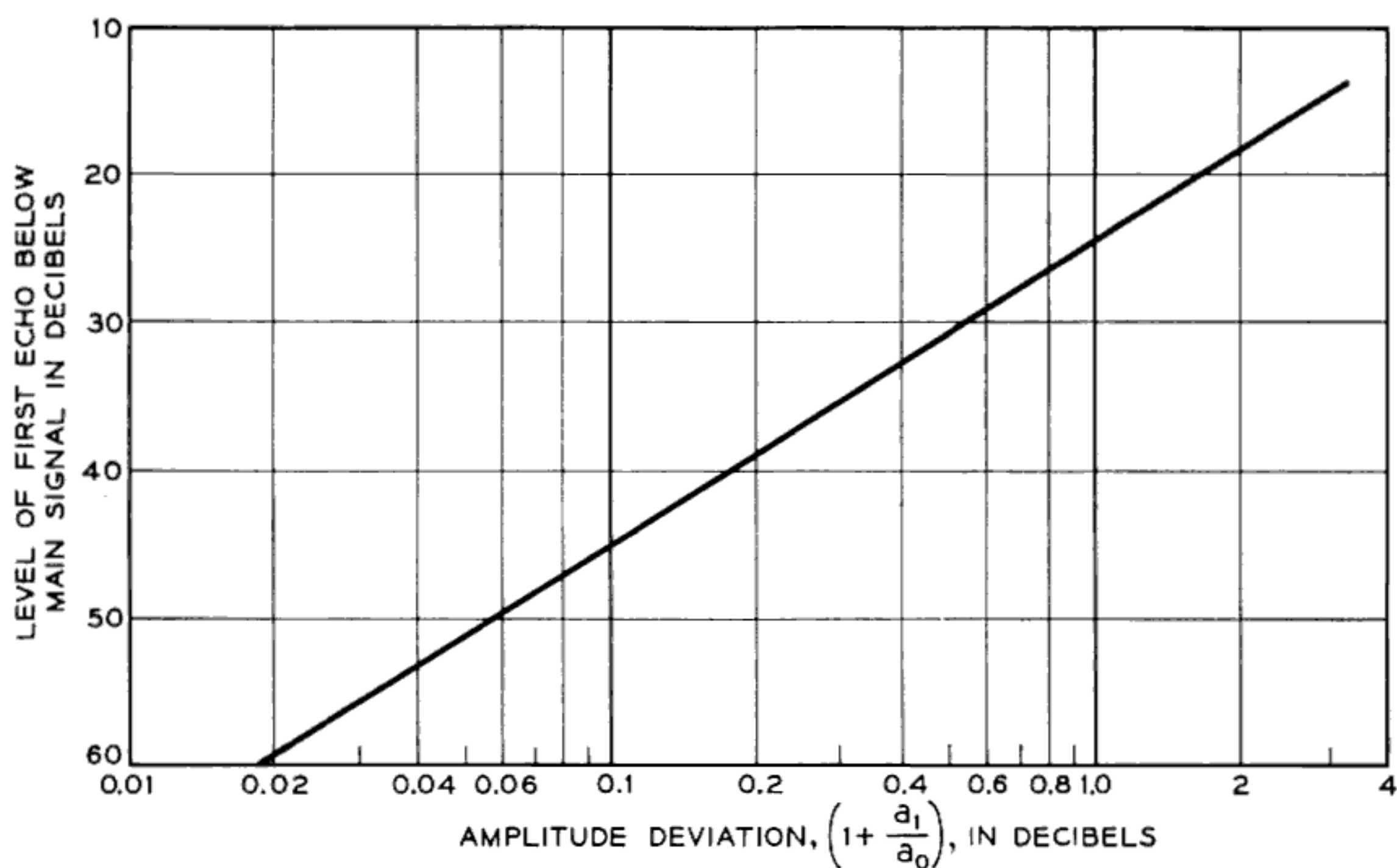


Fig. 12 — Amplitude of echo with amplitude distortion.

input signal (main response) and two echoes, one leading and one lagging the main response. It is seen that the amplitude of the echoes is equal to  $a_1/2a_0$  and the time displacement of the echoes with respect to the main response is equal to the period of the cosine ripple,  $1/\Delta$ . The sum of the main response and the two echoes gives the resultant output signal, which

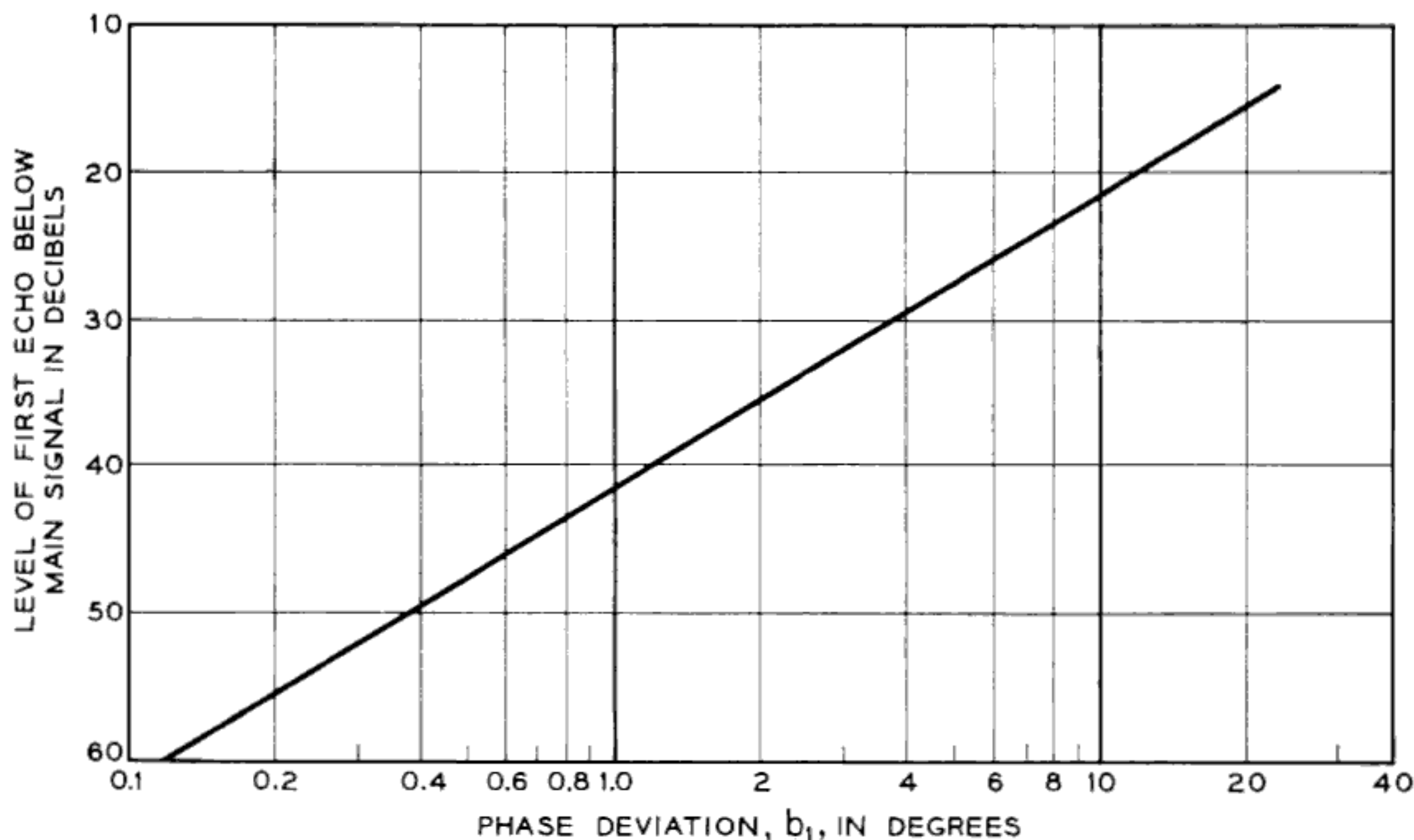


Fig. 13 — Amplitude of echo with phase distortion.

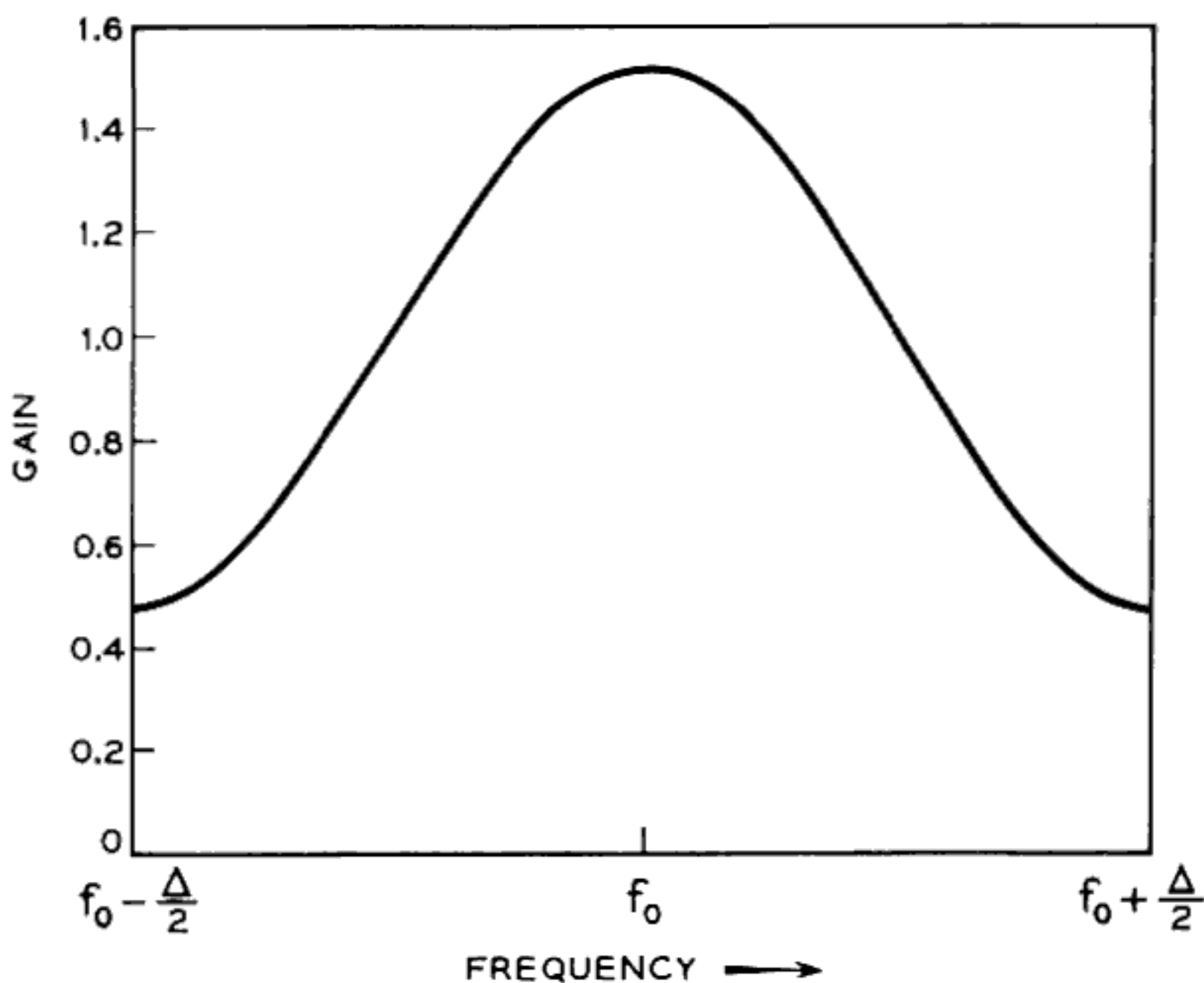


Fig. 14 — Network amplitude response.

has the desired lower side lobes at the expense of a slightly wider main pulse and a small loss in signal-to-noise ratio over the matched filter optimum.

The ideal weighting scheme should provide maximum attenuation of the sidelobes with minimum broadening of the main pulse. An analogous situation occurs in antenna theory with a line source. The antenna designer attempts to minimize the spatial side lobes without broadening the main lobe appreciably. As in the antenna case, Taylor weighting<sup>9</sup> of the Chirp signal spectrum offers a good compromise between side-lobe level and pulse-width increase.

**3.4.2.2 Theory.** The optimum weighting function to achieve low side lobes with the least degradation of the pulse length is a so-called Dolph-Tchebycheff<sup>15</sup> function, which would give an output pulse of the form

$$E_0(t) = \frac{\cos \pi \sqrt{(\Delta t)^2 - A^2}}{\cosh \pi A}. \quad (76)$$

This is a signal of unit peak amplitude which has a uniform side-lobe level,  $\eta = (\cosh \pi A)^{-1}$  (expressed in decibels by means of  $\bar{N} = 20 \log_{10} \eta$ ). This signal possesses infinite energy and is not physically realizable but provides a suitable standard of comparison. The 3-db pulse width of  $E_0(t)$  is given by

$$\beta_0 = \frac{2}{\pi} \left[ (\cosh^{-1} \eta)^2 - \left( \cosh^{-1} \frac{\eta}{\sqrt{2}} \right)^2 \right]^{\frac{1}{2}}. \quad (77)$$

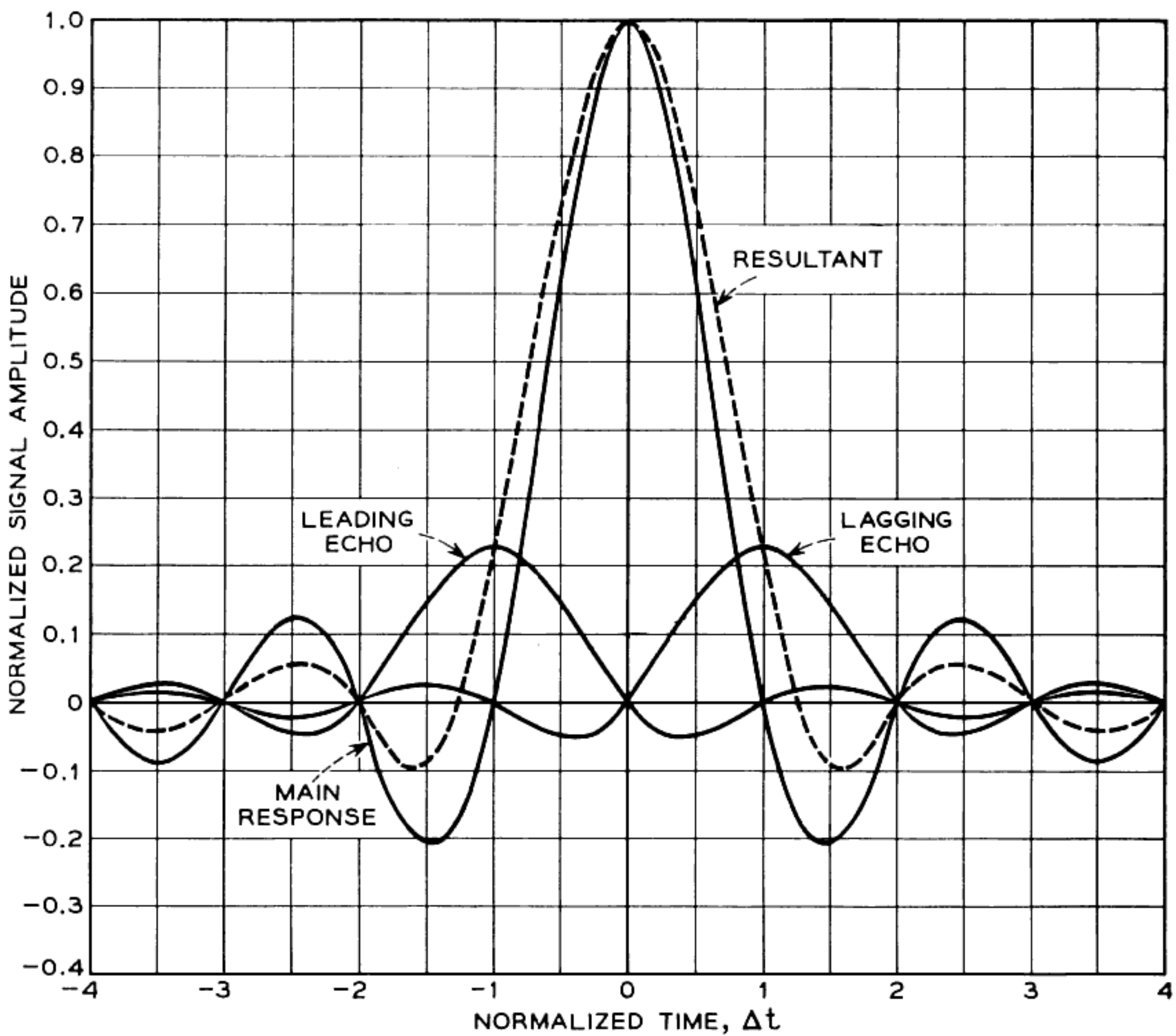


Fig. 15 — Weighting mechanics.

This relationship is plotted in Fig. 16 as normalized pulse length,  $\beta_0$ , versus  $\bar{N}$ .

An approximation of the Dolph-Tchebycheff signal has been derived by Taylor.<sup>9</sup> When Taylor weighting functions are used, the output pulse envelope takes the form

$$E_{\text{tay}}(t) = \text{sinc } \Delta t \left[ \frac{\prod_{n=1}^{\bar{n}-1} \left( 1 - \frac{\sigma^{-2} \Delta t^2}{A^2 + (n - \frac{1}{2})^2} \right)}{\prod_{n=1}^{\bar{n}-1} \left( 1 - \frac{\Delta t^2}{n^2} \right)} \right], \quad (78)$$

where  $A$  is the same parameter that appears in (76), and

$$\sigma^2 \equiv \frac{\bar{n}^2}{A^2 + (\bar{n} - \frac{1}{2})^2}. \quad (79)$$

The parameter,  $\bar{n}$ , will be described presently. The Taylor function,  $E_{\text{tay}}(t)$ , of (78) is a compromise between the unweighted Chirp output

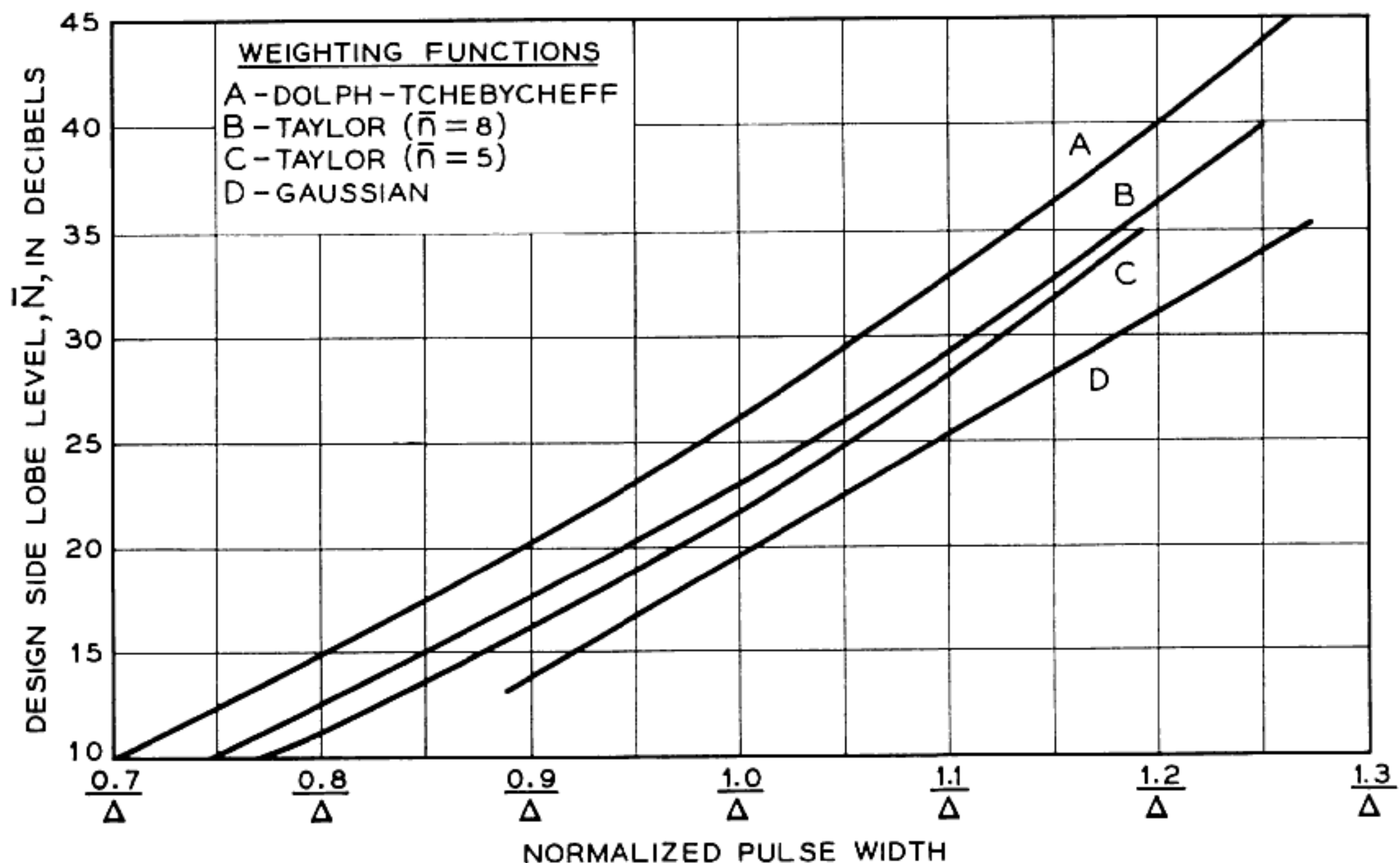


Fig. 16 — Pulse widening due to weighting.

signal envelope, sinc  $\Delta t$ , and the Dolph-Tchebycheff signal envelope of (76).

The spectrum-weighting function [Fourier transform of  $E_{\text{tay}}(t)$ ] is most easily obtained by techniques similar to sampling theory. The Fourier transform of  $E_{\text{tay}}(t)$ ,  $\tilde{Y}_{\text{tay}}(X)$ , is zero for  $|X| > 0.5$ , where  $X = (f - f_0)/\Delta$ :

$$E_{\text{tay}}(t) = \int_{-\frac{1}{2}}^{\frac{1}{2}} \tilde{Y}_{\text{tay}}(X, A, \bar{n}) e^{2\pi i X \Delta t} dX. \quad (80)$$

Sampling theory suggests the following substitution:

$$\tilde{Y}_{\text{tay}}(X, A, \bar{n}) = \sum_{-\infty}^{\infty} F_m e^{-2\pi i m X}. \quad (81)$$

From this, one finds

$$E_{\text{tay}}(t) = \sum_{-\infty}^{\infty} F_m [\text{sinc } (\Delta t - m)]. \quad (82)$$

It also follows that

$$F_m = F(m, A, \bar{n}). \quad (83)$$

The coefficients,  $F_m$ , can be obtained as follows:

$$F_0 = 1, \quad (84)$$

$$F_m = F_{-m} = \frac{0.5(-1)^{m+1}}{\prod_{n=1}^{(\bar{n}-1)'} \left(1 - \frac{m^2}{n^2}\right)} \prod_{n=1}^{\bar{n}-1} \left[1 - \frac{\sigma^{-2} m^2}{A^2 + (n - \frac{1}{2})^2}\right], \quad (85)$$

for  $0 < |m| < \bar{n}$ . The prime in (85) means that  $n \neq m$ ; the symbol  $\prod$  denotes a product of successive terms. Finally,

$$F_m = 0 \quad \text{for } |m| \geq \bar{n}. \quad (86)$$

It follows that

$$\tilde{Y}_{\text{tay}}(X, A, \bar{n}) = 1 + 2 \sum_{m=1}^{\bar{n}-1} F_m \cos 2\pi m X. \quad (87)$$

The weighting network characteristic can be expressed in terms of the parameters of a Chirp system:

$$\tilde{Y}_{\text{tay}}(f, A, \bar{n}) = 1 + 2 \sum_{m=1}^{\bar{n}-1} F_m \cos \frac{2\pi m}{\Delta} (f - f_0), \quad (88)$$

where  $f_0$  is the center frequency of the IF signal if weighting is to be performed at other than video frequencies.

**3.4.2.3 Effect of Weighting on the Pulse Shape.** In the previous section a parameter,  $\bar{n}$ , was used but has not yet been defined; it is appropriate to discuss it at this time. When a comparison is made of the Dolph-Tchebycheff and Taylor pulse envelopes for the same design side-lobe level (see Fig. 17), there are several important differences: The Taylor pulse width, expressed at the 3-db pulse width, is

$$\beta = \sigma \beta_0, \quad (89)$$

where  $\beta_0$  is the Dolph-Tchebycheff 3-db pulse width given in (77) and the quantity  $\sigma$  is defined in (79). An important analytical difference is the location of the zeros of the two functions. The Dolph-Tchebycheff envelope has all of its zeros occurring at nonintegral values of the argument  $\Delta t$ , while the Taylor envelope has two distinct regions: a region of nearly uniform side lobes where the zeros occur at nonintegral values of the argument  $|\Delta t| \leq \bar{n} - 1$ , and a region of decaying side lobes where the zeros always occur at integers  $|\Delta t| \geq \bar{n}$ . The central region of near-uniform side lobes approximates the Dolph-Tchebycheff behavior. It is essential to have the remote side lobes decay to keep their energy content down.

From the previous discussion it is easy to see the significance of the parameter  $\bar{n}$ , since it gives a bound on the region of approximation to Dolph-Tchebycheff behavior. Higher values of  $\bar{n}$  mean a closer approxi-

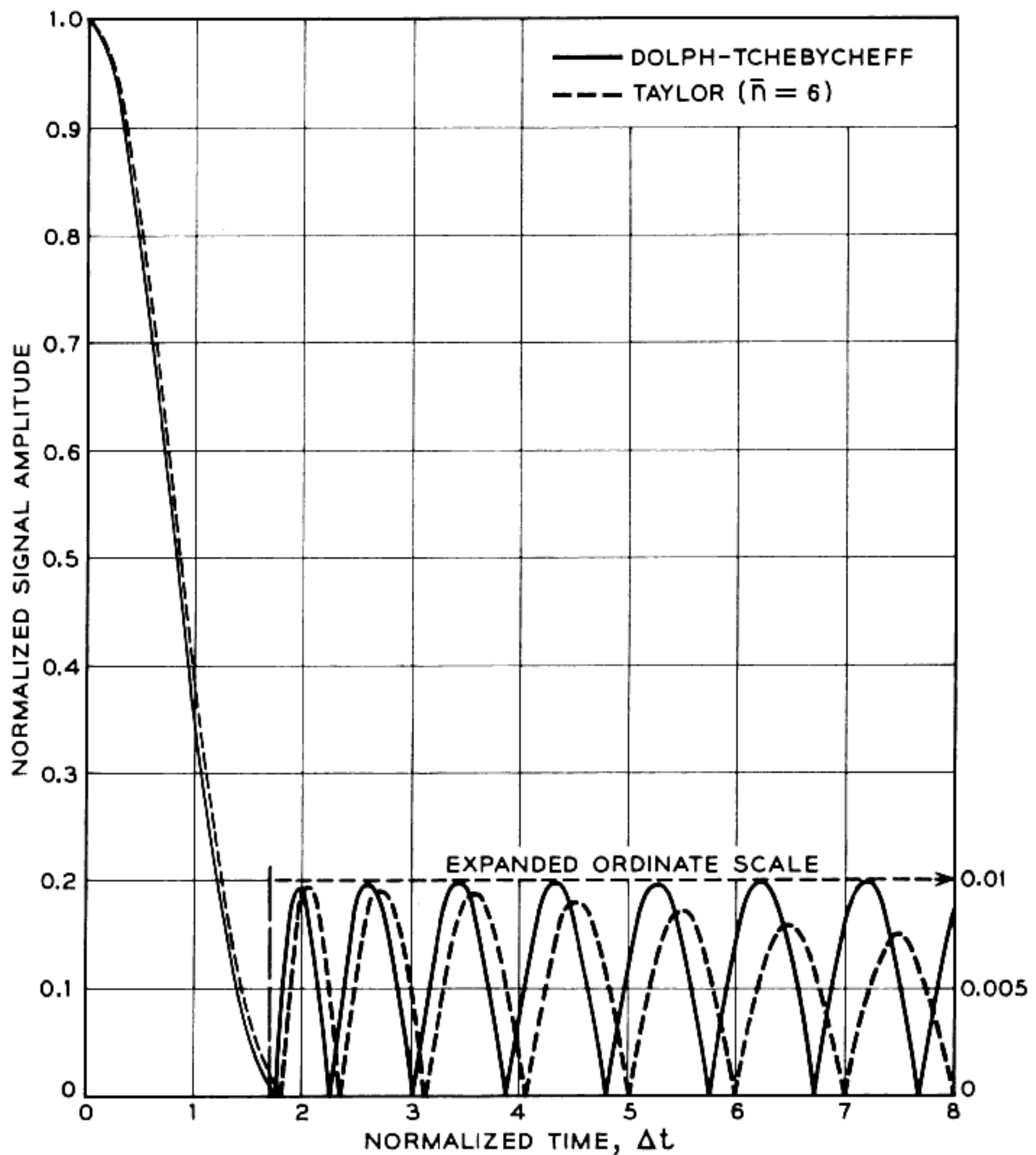


Fig. 17 — Comparison of Taylor and Dolph-Tchebycheff signal envelopes for  $\bar{N} = 40$  db.

mation. The upper bound in the antenna case is determined by super-gaining but, for the Chirp case, it is not desirable to use any larger value of  $\bar{n}$  than the minimum permissible. When the minimum value of  $\bar{n}$  is chosen, the required weighting characteristic is easily obtained with a bandpass filter. This is evident from the results presented in Figs. 18 and 19, which are plots of the required loss functions for design side-lobe levels of 40 and 47.5 db for various values of  $\bar{n}$ , ranging upward from the minimum permissible value in both cases. In order to obtain the minimum permissible value, Taylor employs the rule that, as  $\bar{n}$  is increased by one, the value of  $\sigma$  should not increase.

The required loss functions for side-lobe levels of 34, 37.5, 40 and 47.5 db have been calculated for the minimum value of  $\bar{n}$  in each case and are plotted in Fig. 20. The resultant pulse envelopes are shown in Figs. 21 through 24. The side-lobe levels have been amplified in some of the figures to show the details.

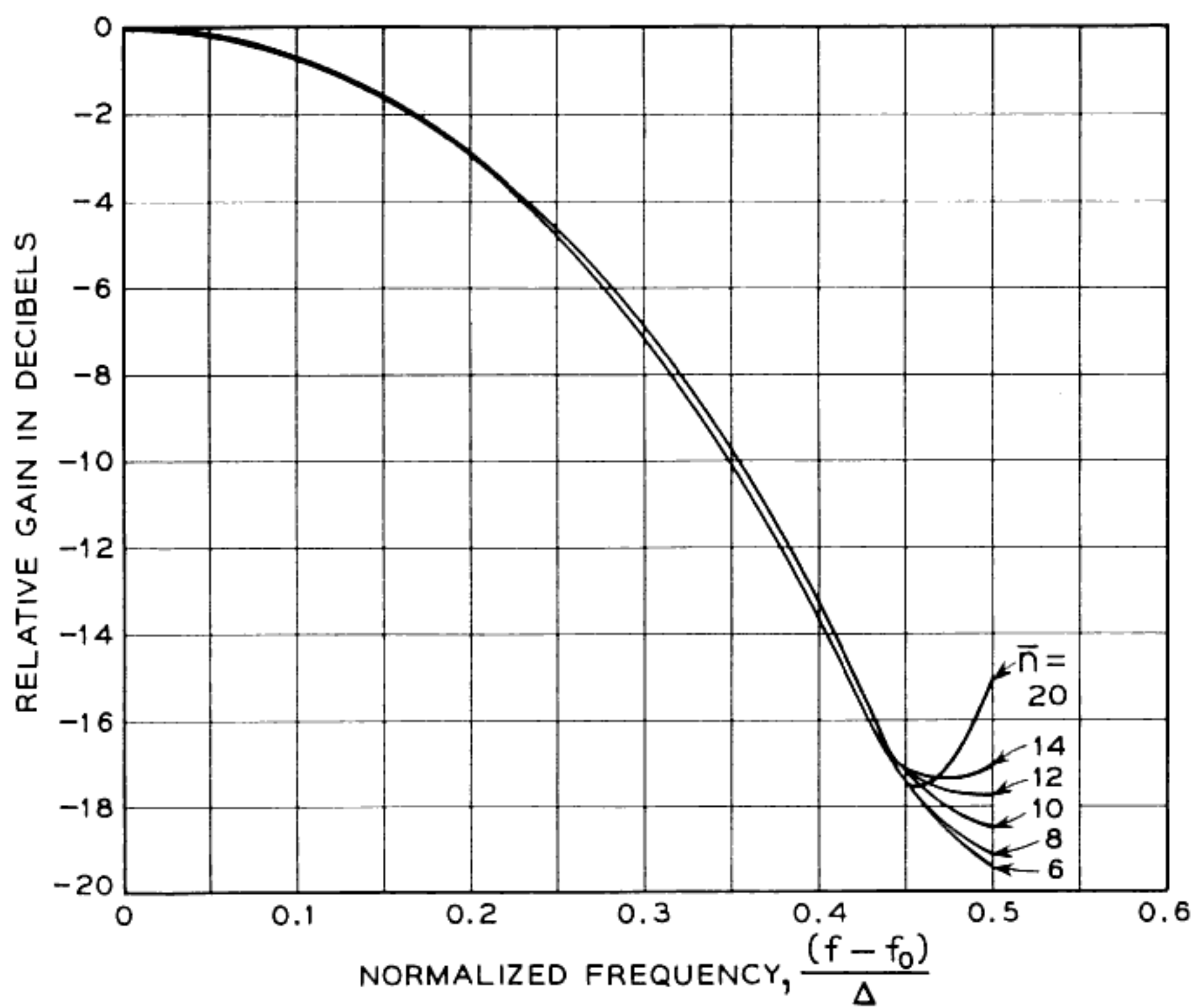


Fig. 18 — Taylor weighting characteristics for  $\bar{N} = 40$  db.

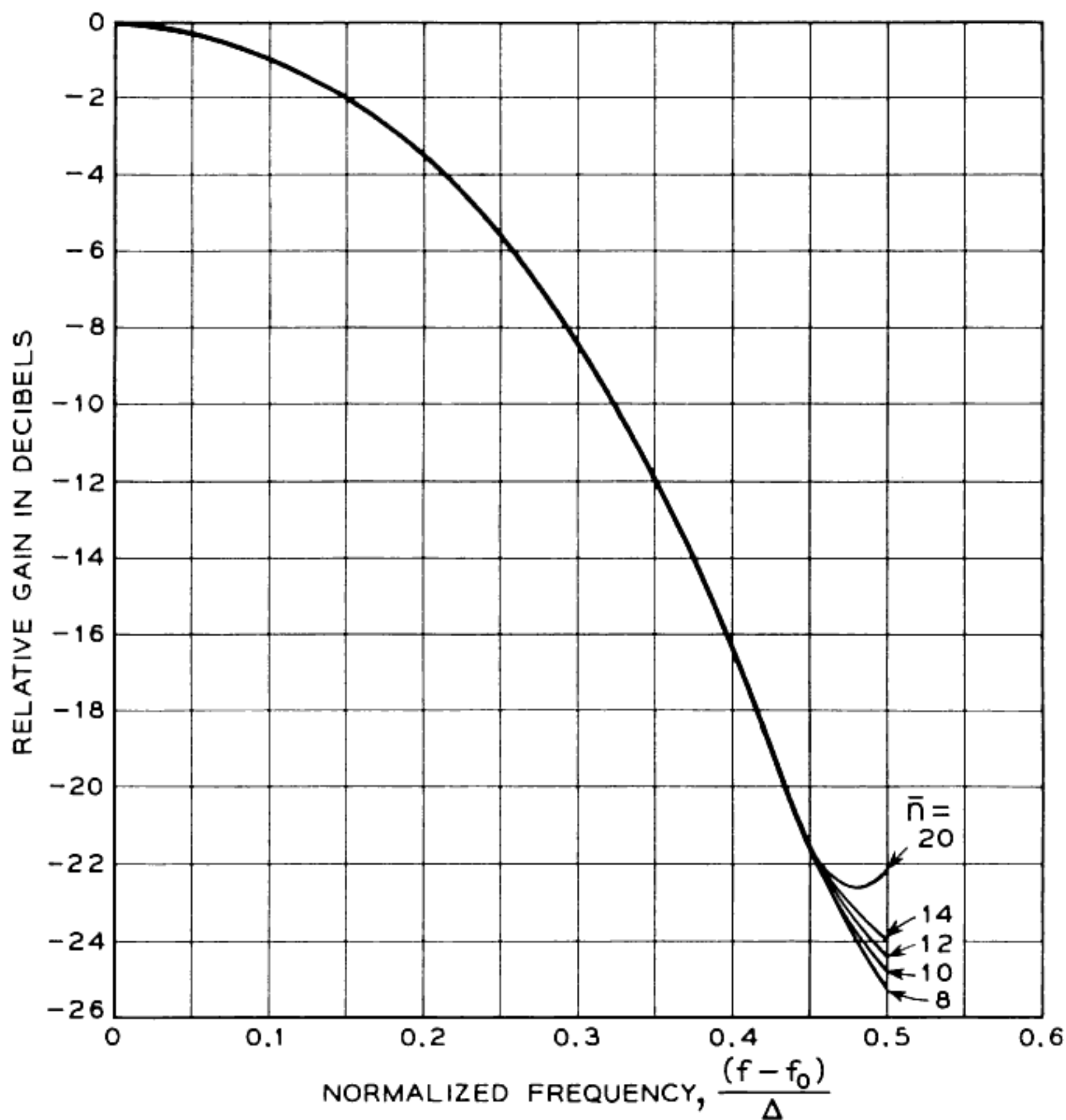


Fig. 19 — Taylor weighting characteristics for  $\bar{N} = 47.5$  db.

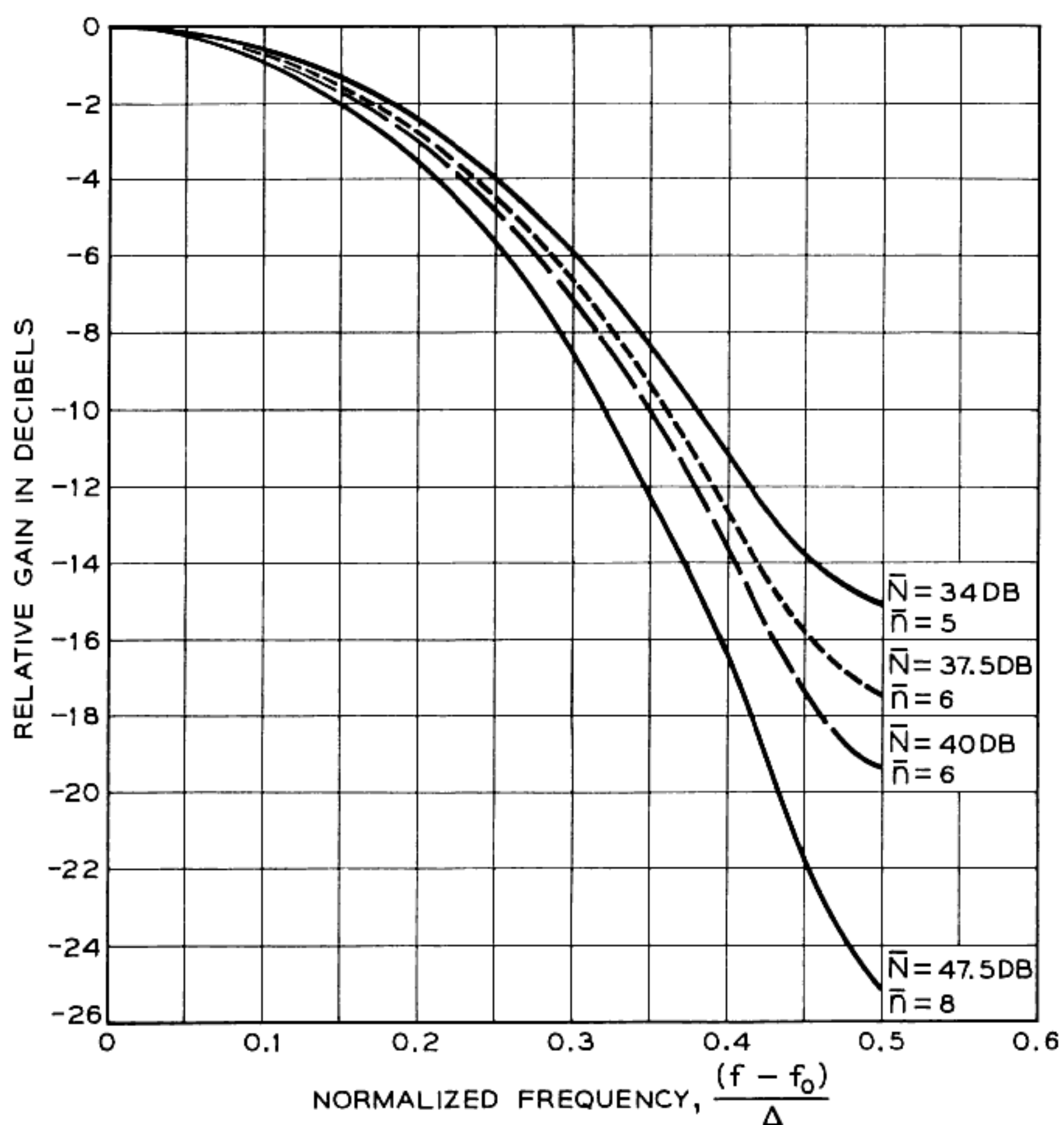


Fig. 20 — Taylor weighting characteristics for various side-lobe levels.

**3.4.2.4 Effect of Weighting on Signal-to-Noise Ratio.** The concept of a matched-filter radar has been explained in Section 3.3. Clearly, this is the goal that one should strive for in the design of a radar system. If a matched-filter receiver were designed using the theory described in earlier parts of this paper, the output pulse would have the side lobes of  $(\sin z)/z$ , which are undesirable in many applications. The use of Taylor weighting does not seriously effect the system detection capability when compared to a matched-filter radar that utilizes the same transmitted energy.

The loss in system performance of the Taylor-weighted Chirp radar compared to a matched-filter radar is expressed most easily in terms of the parameters  $F_m$ . The S/N ratio of a Taylor-weighted signal relative to the S/N ratio of the matched filter optimum is given by

$$\frac{(S/N)_{\text{matched}}}{(S/N)_{\text{taylor}}} = 1 + 2 \sum_{m=1}^{\bar{n}-1} F_m^2. \quad (90)$$

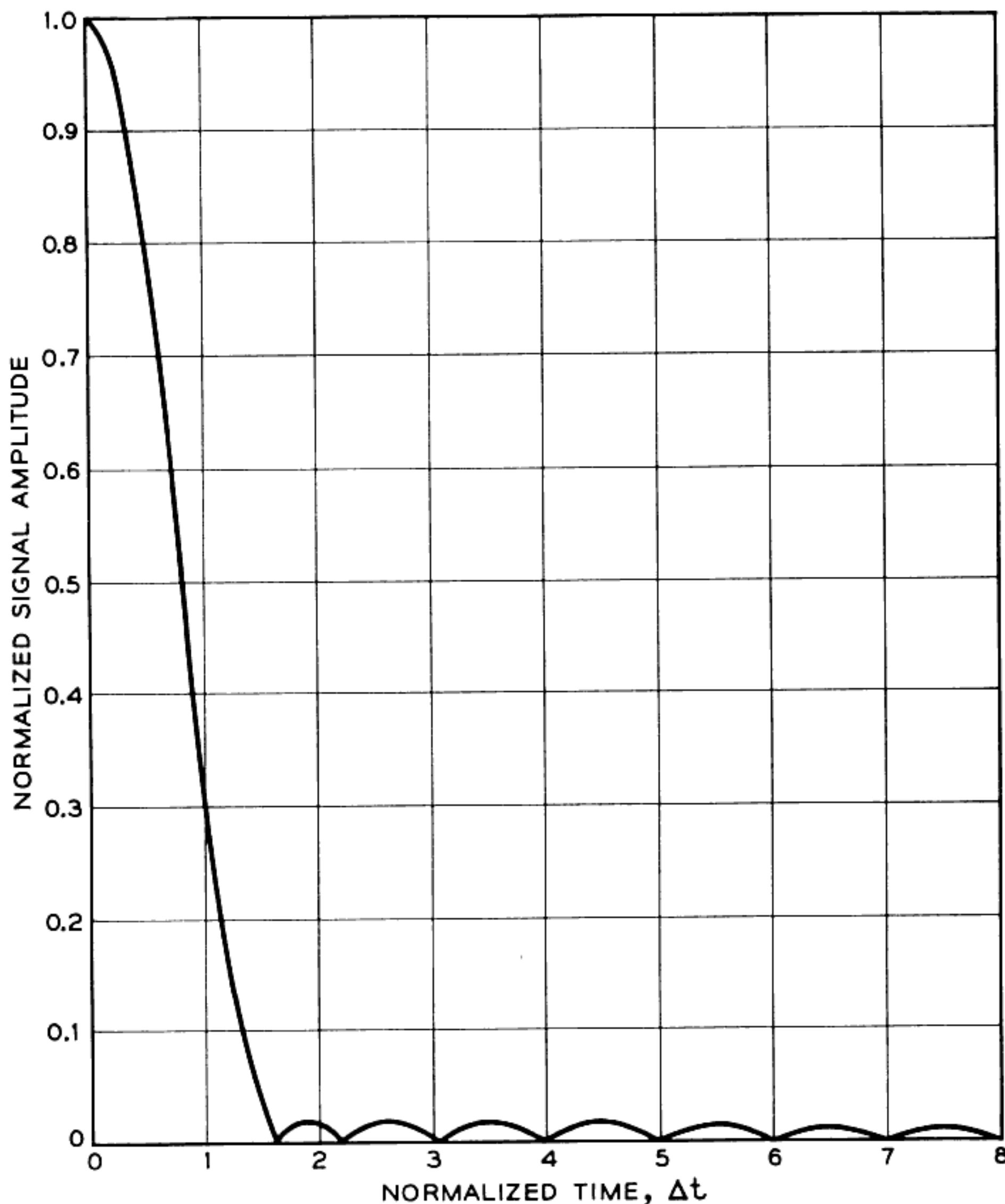


Fig. 21 — Taylor weighting pulse envelope for  $\bar{N} = 34$  db,  $\bar{n} = 5$ .

This expression has been evaluated (see Fig. 25) for a number of side-lobe levels and values of the parameter  $\bar{N}$ . A loss in S/N ratio of only 1.455 db is obtained when the design side-lobe level,  $\bar{n}$ , is 47.5 db below the peak signal.

### 3.4.3 Tolerance of Chirp Pulses to Quadratic Phase Distortion

This section is concerned with the unwanted degradation of collapsed Chirp pulses as a result of quadratic phase distortion, which could be the result of an imperfect match of the transmitter and receiver delay-equalizer slopes. Some experimental evidence exists that heavily weighted pulses possessing very low side lobes can tolerate more of this type of distortion than their unweighted counterparts  $(\sin z)/z$ . This section

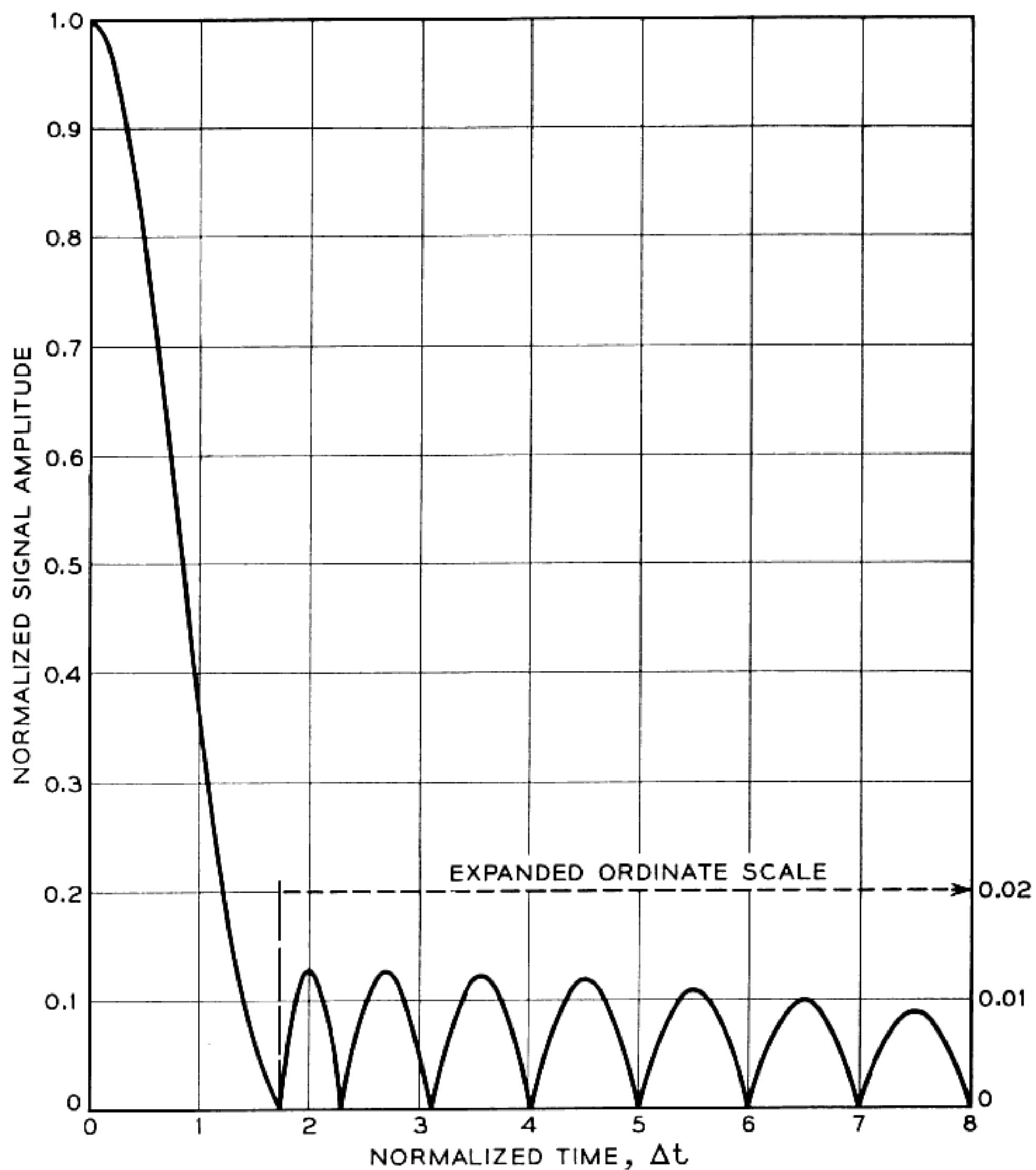


Fig. 22 — Taylor weighting pulse envelope for  $\bar{N} = 37.5$  db,  $\bar{n} = 6$ .

shows analytically that unweighted pulses are degraded more than heavily weighted pulses. The particular weighting function chosen for this analysis is slightly less efficient than those previously described (Section 3.4.2) but represents the Taylor-weighted optimum to a reasonable approximation. It is believed that the general results of this section are appropriate for any *heavily* weighted pulse.

**3.4.3.1 Analysis of Quadratic Phase Distortion.** The weighting scheme described in Section 3.4.2 used a network having a transfer admittance given by

$$\tilde{Y}_{\text{tay}}(f, A, \bar{n}) = 1 + 2 \sum_{m=1}^{\bar{n}-1} F_m \cos \frac{2\pi m}{\Delta} (f - f_0). \quad (91)$$

This network, when excited by the collapsed signal,

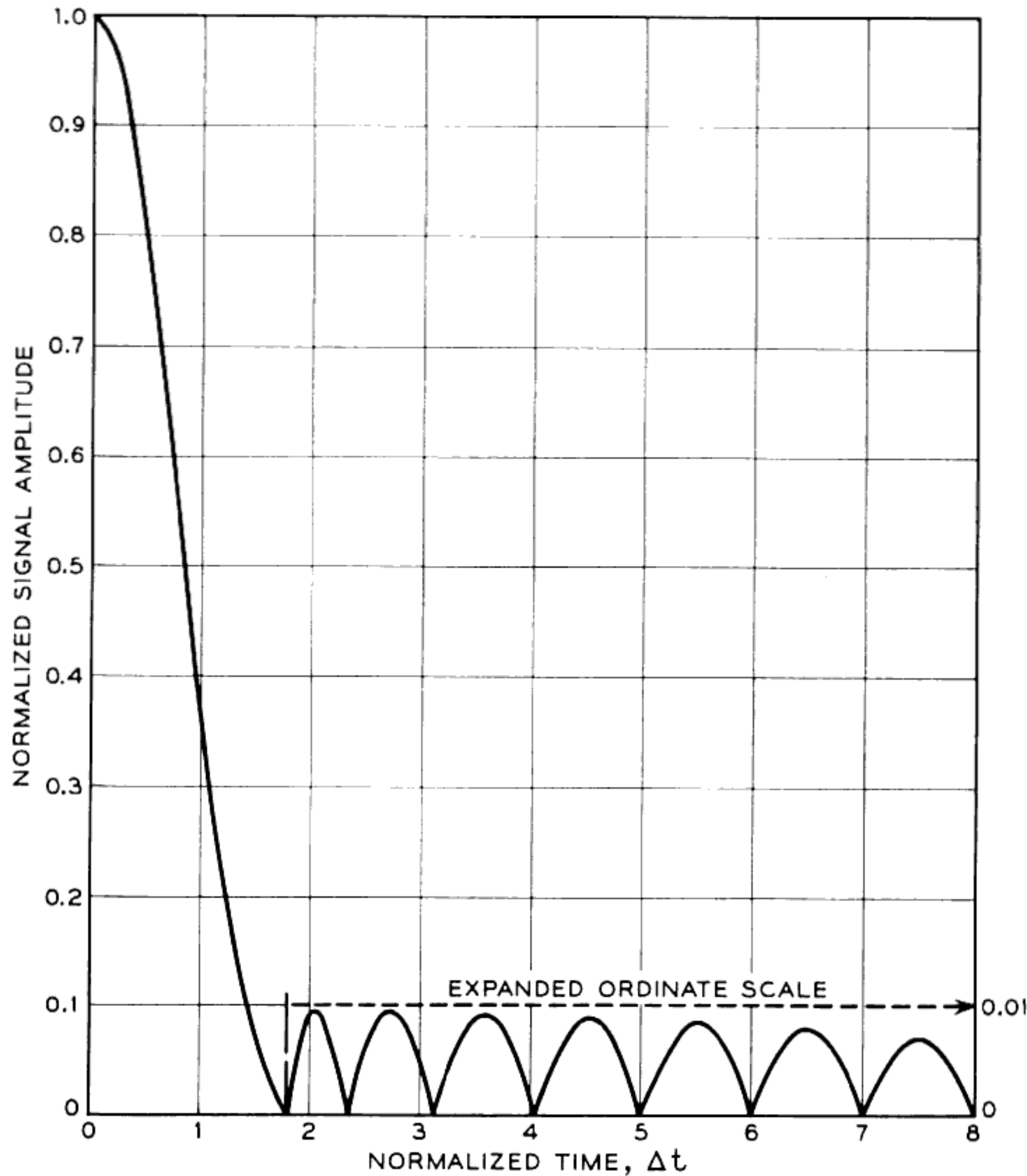


Fig. 23 — Taylor weighting pulse envelope for  $\bar{N} = 40$  db,  $\bar{n} = 6$ .

$$e(t) = \cos 2\pi f_0 t \operatorname{sinc} \Delta t, \quad (92)$$

gives rise to an output signal envelope,  $E_{\text{tay}}(t)$ , where

$$E_{\text{tay}}(t) = \sum_{m=-(\bar{n}-1)}^{(\bar{n}-1)} F_m \operatorname{sinc} (\Delta t - m). \quad (93)$$

The desired weighting-network characteristic is described by (91), but the coefficients  $F_m$  decrease rapidly as  $m$  increases. In the particular case considered in this section,  $\bar{N} = 40$  db and  $\bar{n} = 6$  (the minimum permissible value), the following ratios exist:

$$\left| \frac{F_5}{F_1} \right| < \left| \frac{F_4}{F_1} \right| < \left| \frac{F_3}{F_1} \right| < \left| \frac{F_2}{F_1} \right| < 0.025. \quad (94)$$

Thus, it can be seen that the echoes introduced in  $E_{\text{tay}}(t)$  by the second through fifth terms in the expansion in (91) are at least an order of mag-

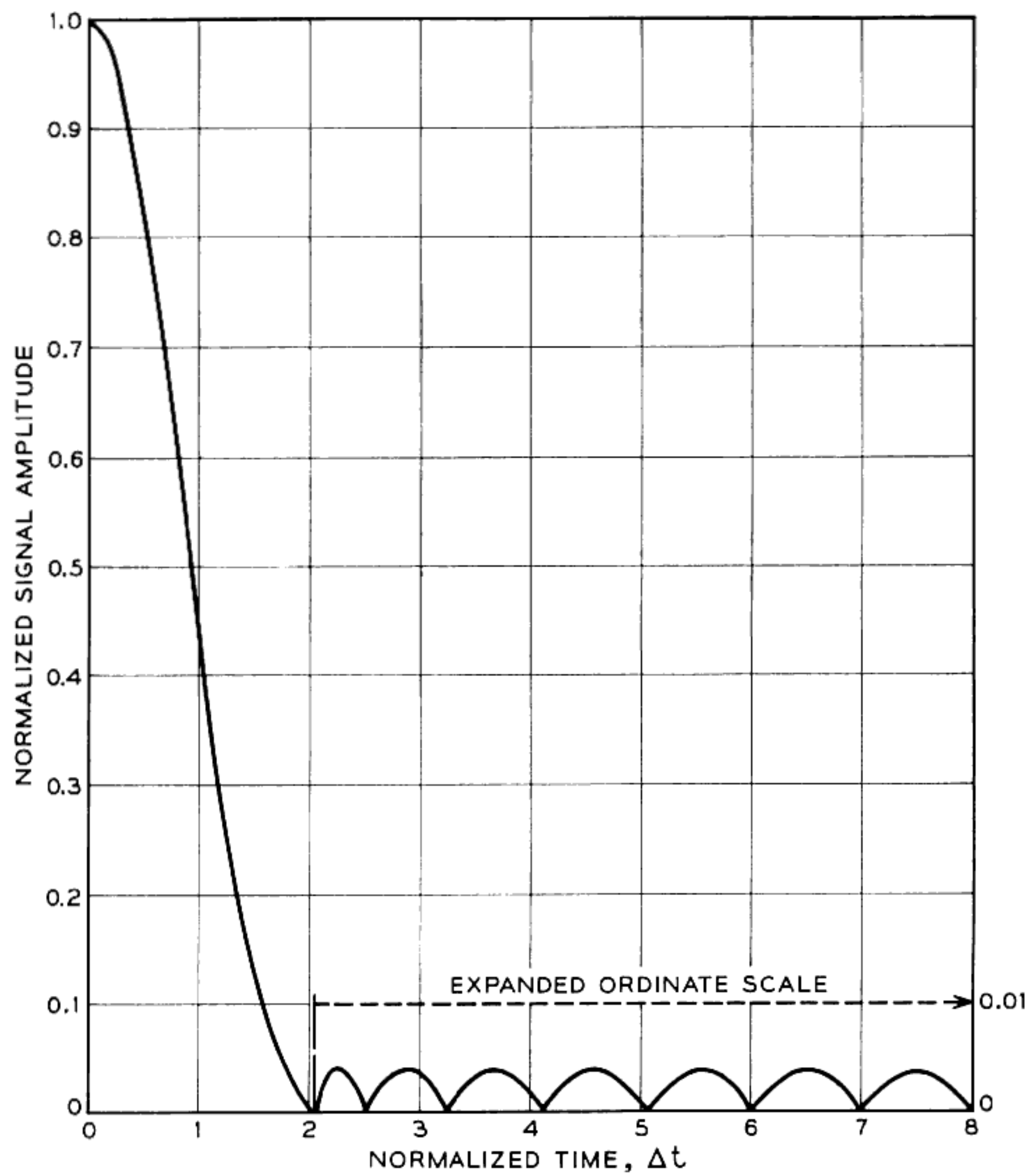


Fig. 24 — Taylor weighting pulse envelope for  $\bar{N} = 47.5$  db,  $\bar{n} = 8$ .

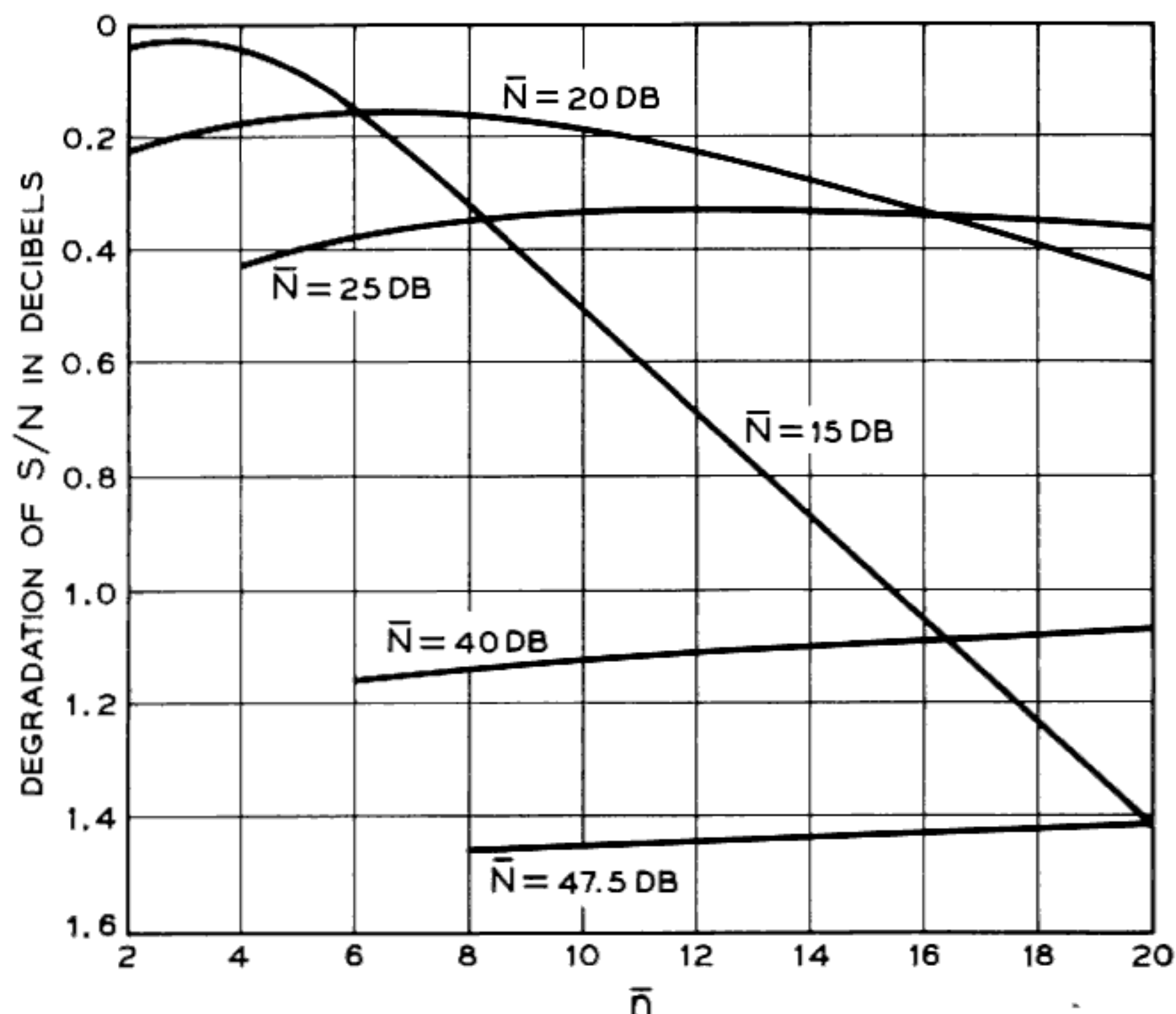


Fig. 25 — Signal-to-noise effects.

nitude smaller than the echo introduced by the first term. For this reason and also to simplify the analysis, only the first term of the expansion of (91) will be considered. Specifically, the following weighting-network characteristic will be considered:

$$\tilde{Y}'_{\text{tay}}(f) = 1 + 2F_1 \cos \frac{2\pi}{\Delta} (f - f_0). \quad (95)$$

This network, when excited with an input pulse of the form of (92), has the output envelope

$$E'_{\text{tay}}(t) = \text{sinc } (\Delta t) + F_1 \text{sinc } (\Delta t - 1) + F_1 \text{sinc } (\Delta t + 1). \quad (96)$$

A value of  $F_1 = 0.42$  gives an output pulse in which all side lobes are 40 db or more below the peak signal. This output signal is shown in Fig. 26.

Let this pulse be subject to a quadratic phase distortion,  $\Phi_d$ , where

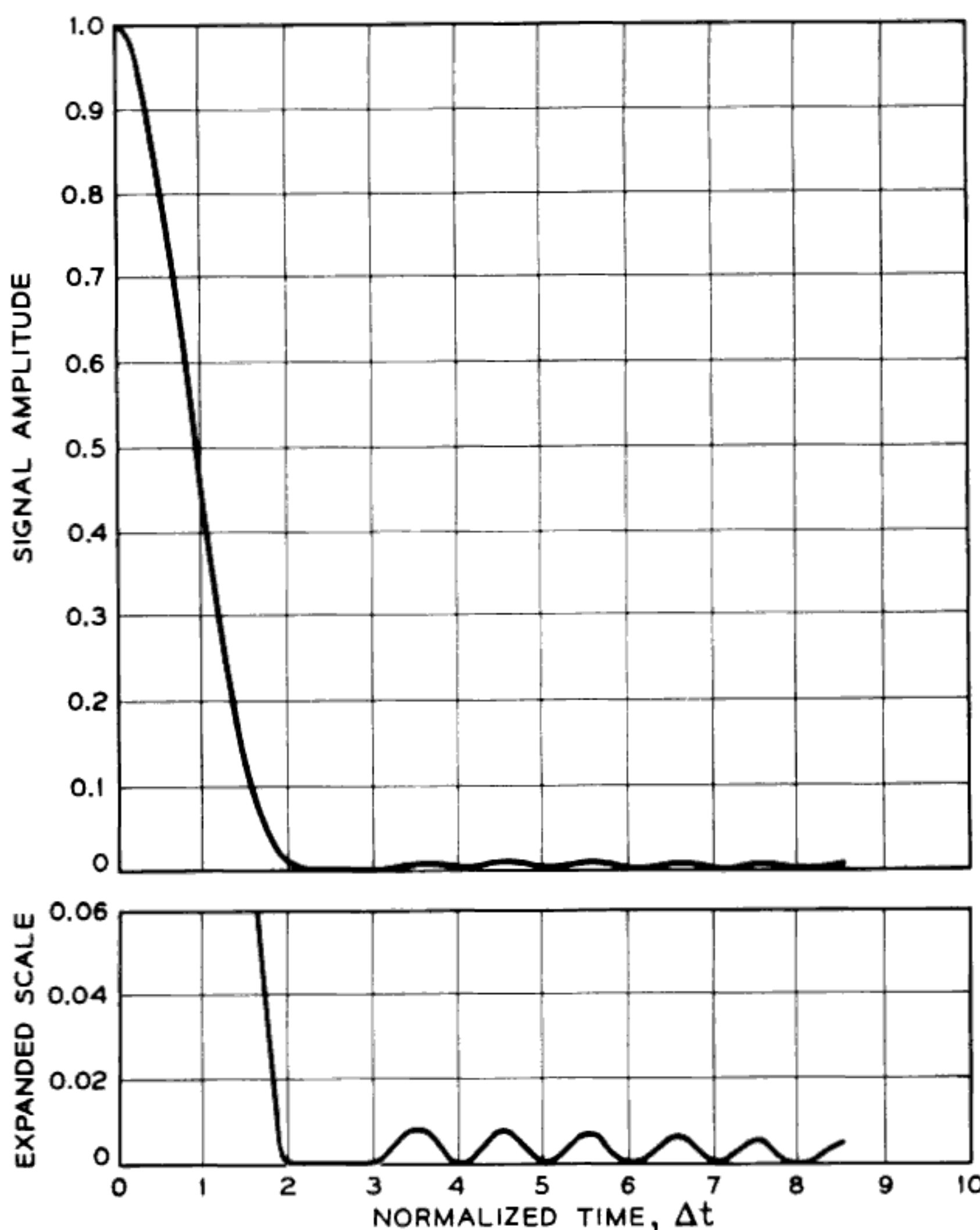


Fig. 26 — Quadratic phase distortion effects, weighted pulse,  $\varphi = 0$ .

$$\Phi_d \equiv -\frac{1}{2}T_0^2(\omega - \omega_0)^2. \quad (97)$$

This can be expressed as a linear delay distortion

$$t_d = -\frac{d\Phi}{d\omega} = T_0^2(\omega - \omega_0). \quad (98)$$

It should be emphasized that the linear delay in (98) represents a *distortion* over and above the *planned* linear delay introduced by the Chirp receiving network in (13).

The distorted output-pulse envelope is found by use of the inverse Fourier transform. Omitting constant values,

$$E_{\text{dis}}(t) = \int_{-\pi\Delta}^{\pi\Delta} \tilde{Y}'_{\text{tay}}(\omega') e^{i\omega' t} e^{-i[T_0^2(\omega')^2]/2} d\omega', \quad (99)$$

where

$$\tilde{Y}'_{\text{tay}}(\omega') = 1 + 2F_1 \cos \frac{\omega'}{\Delta}, \quad (100)$$

and

$$(\omega')^2 = (\omega - \omega_0)^2. \quad (101)$$

It is more convenient to express the distortion in terms of the phase shift at the edge of the band,  $\Phi$ , where

$$\Phi = \pi^2 \frac{T_0^2(\Delta)^2}{2}. \quad (102)$$

This transforms (99) into

$$E_{\text{dis}}(t) = \int_{-\pi\Delta}^{\pi\Delta} \tilde{Y}'(\omega') e^{i\omega' t} e^{-i\Phi\omega'^2/\pi^2\Delta^2} d\omega'. \quad (103)$$

The general result of (103), apart from a constant, is expressed as

$$\begin{aligned} |E_{\text{dis}}(t)| &= |C(P) - C(Q) + iS(P) - iS(Q) \\ &\quad + F_1[C(P + \pi) + C(P - \pi) - C(Q + \pi) - C(Q - \pi)] \\ &\quad + jF_1[S(P + \pi) + S(P - \pi) - S(Q + \pi) - S(Q - \pi)]|, \end{aligned} \quad (104)$$

where  $C$  and  $S$  are the Fresnel integrals defined in (8) and the arguments are given by

$$P = \frac{1}{\sqrt{\pi}} \left( \frac{\Delta t}{2n} + n \right), \quad (105)$$

$$Q = \frac{1}{\sqrt{\pi}} \left( \frac{\Delta t}{2n} - n \right), \quad (106)$$

$$n = \sqrt{2\Phi}. \quad (107)$$

Notice that the echo structure of the signal is unchanged by the distortion process. The unweighted signal response is found very simply by setting  $F_1$  equal to zero.

**3.4.3.2 Discussion of Results of Quadratic Phase Distortion Analysis.** The effect of quadratic phase distortion on weighted and unweighted pulses has been calculated according to (104), and the results are shown in Figs. 26 through 36. With no weighting, the side-lobe structure is appreciably distorted with a quadratic phase distortion as small as  $\Phi = \pi/8 = 45^\circ$  (see Fig. 34). Moreover, when  $\Phi = 2\pi$  (Fig. 36), the peak signal is attenuated by more than 7 db, the pulse breaks up into two peaks, and the 3-db pulse length increases tenfold. This result agrees with the rule of thumb, long applied by antenna designers to uniformly illuminated apertures, that near field distortion starts at about  $\pi/8 < \Phi < \pi/4$ .

On the other hand, the results for quadratic distortion of a heavily weighted pulse (Figs. 26 through 32) bear out the previous observation: heavily weighted pulses can tolerate much more quadratic phase distortion than can unweighted pulses. At  $\Phi = \pi$ , the peak attenuation is only 1.5 db, the pulse broadening 40 per cent, and the side-lobe level remains less than 38 db (Fig. 31). Even at  $\Phi = 2\pi$ , the pulse shape exhibits no breakup. The pulse remains smooth with the peak signal attenuated 4 db and the 3-db pulse width increased 2.3-fold; the peak side-lobe level remains more than 36 db down.

In present-day radar systems such as Chirp, the design side-lobe level is less than 40 db. In view of the results of this section, it is believed that a quadratic phase distortion of  $\Phi = \pi = 180^\circ$  can be tolerated at the edges of the frequency band.

#### 3.4.4 Problem of Fixed Weighting in the Reception of Doppler-Shifted Signals

**3.4.4.1 Introduction.** The analysis thus far has assumed that there is no relative motion between the radar and the target. If the target is moving relative to the radar, the returned signal experiences a slight shift in frequency (known as the Doppler shift) given by

$$\nu = \frac{2v}{c} f_{RF}, \quad (108)$$

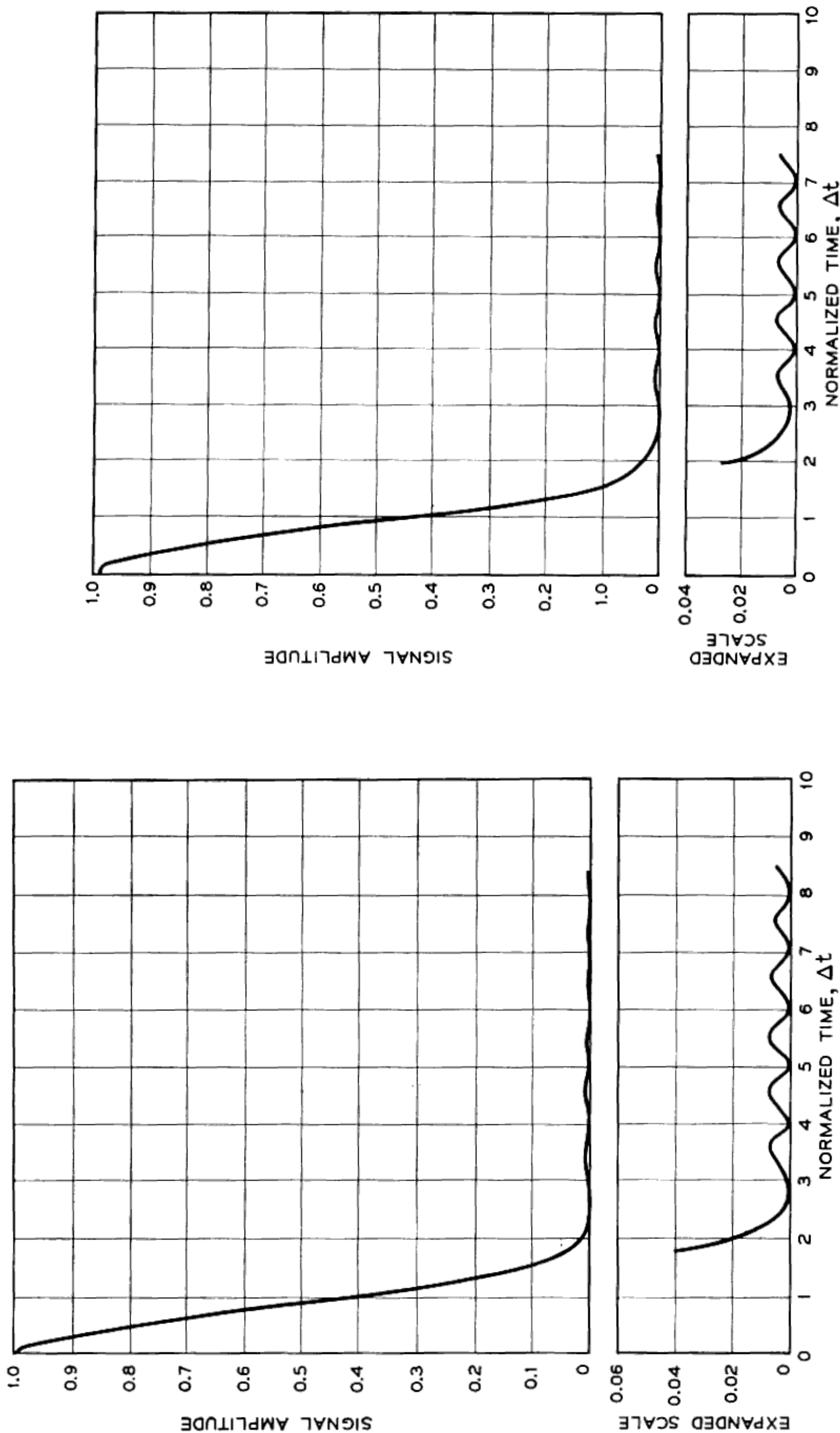


Fig. 27 — Quadratic phase distortion effects, weighted pulse,  $\varphi = \pi/8$ .

Fig. 28 — Quadratic phase distortion effects, weighted pulse,  $\varphi = \pi/6$ .

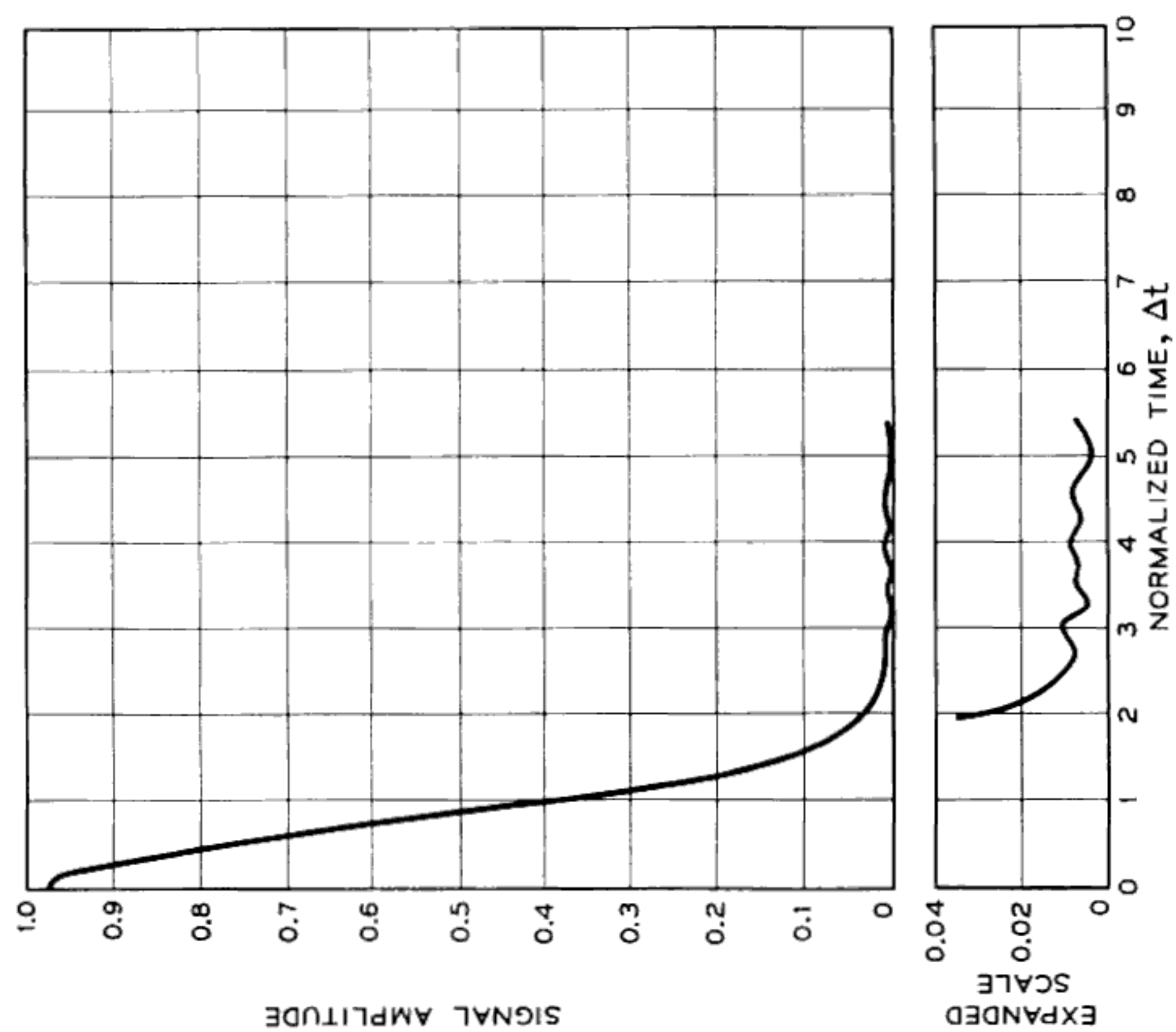


Fig. 29 — Quadratic phase distortion effects, weighted pulse,  $\varphi = \pi/4$ .

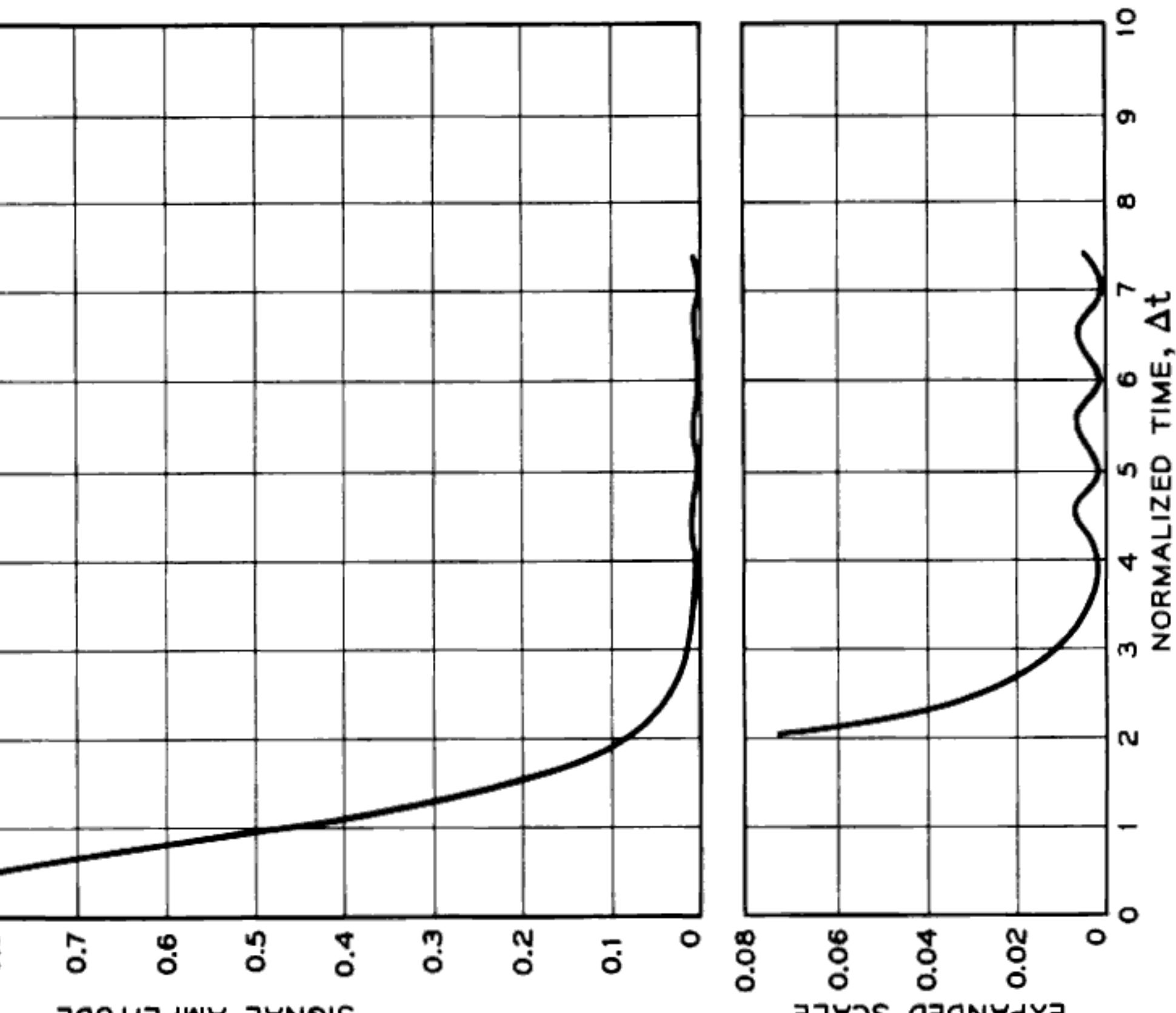


Fig. 30 — Quadratic phase distortion effects, weighted pulse,  $\varphi = \pi/2$ .

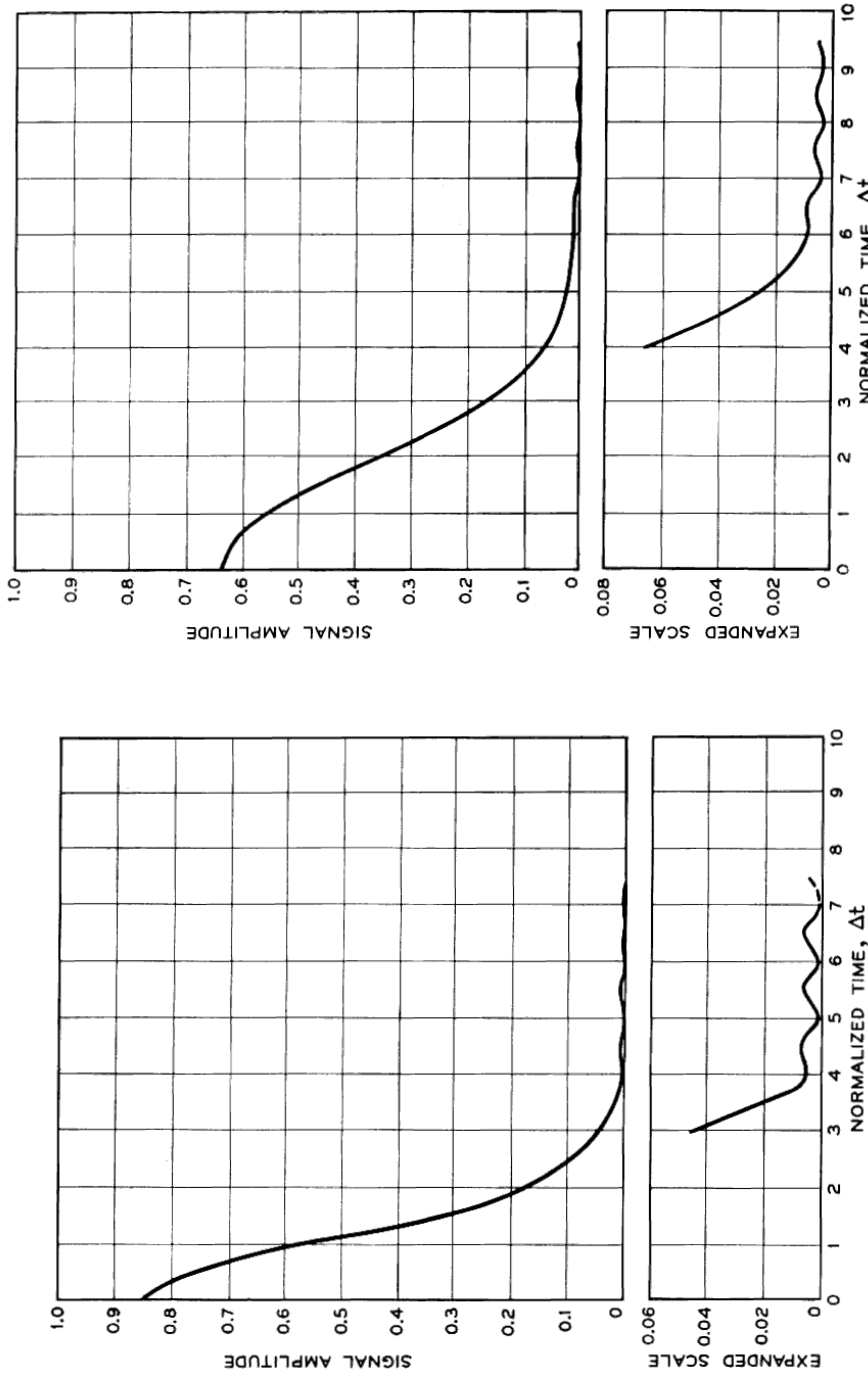


Fig. 31 — Quadratic phase distortion effects, weighted pulse,  $\varphi = \pi$ .

Fig. 32 — Quadratic phase distortion effects, weighted pulse,  $\varphi = 2\pi$ .

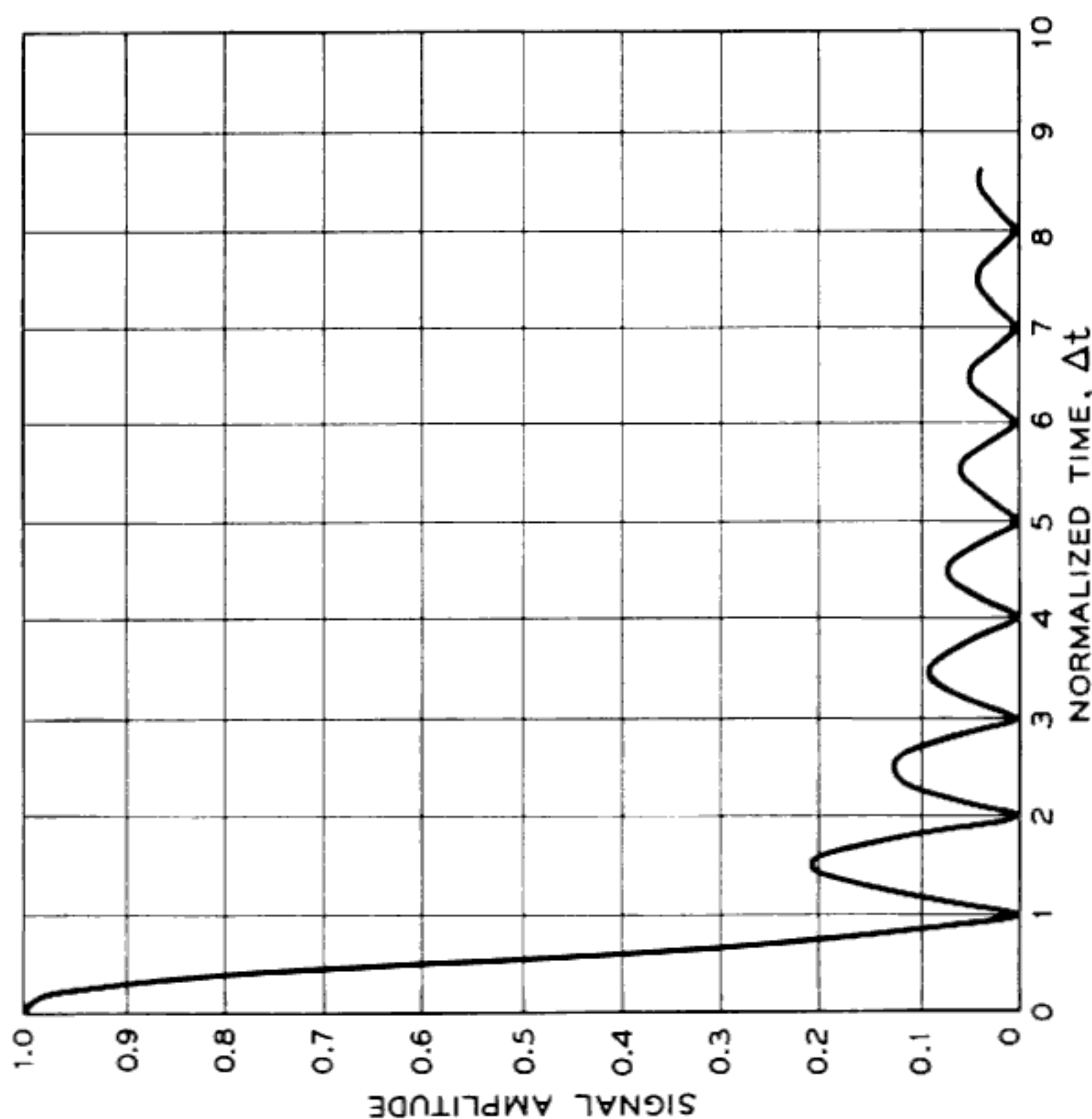
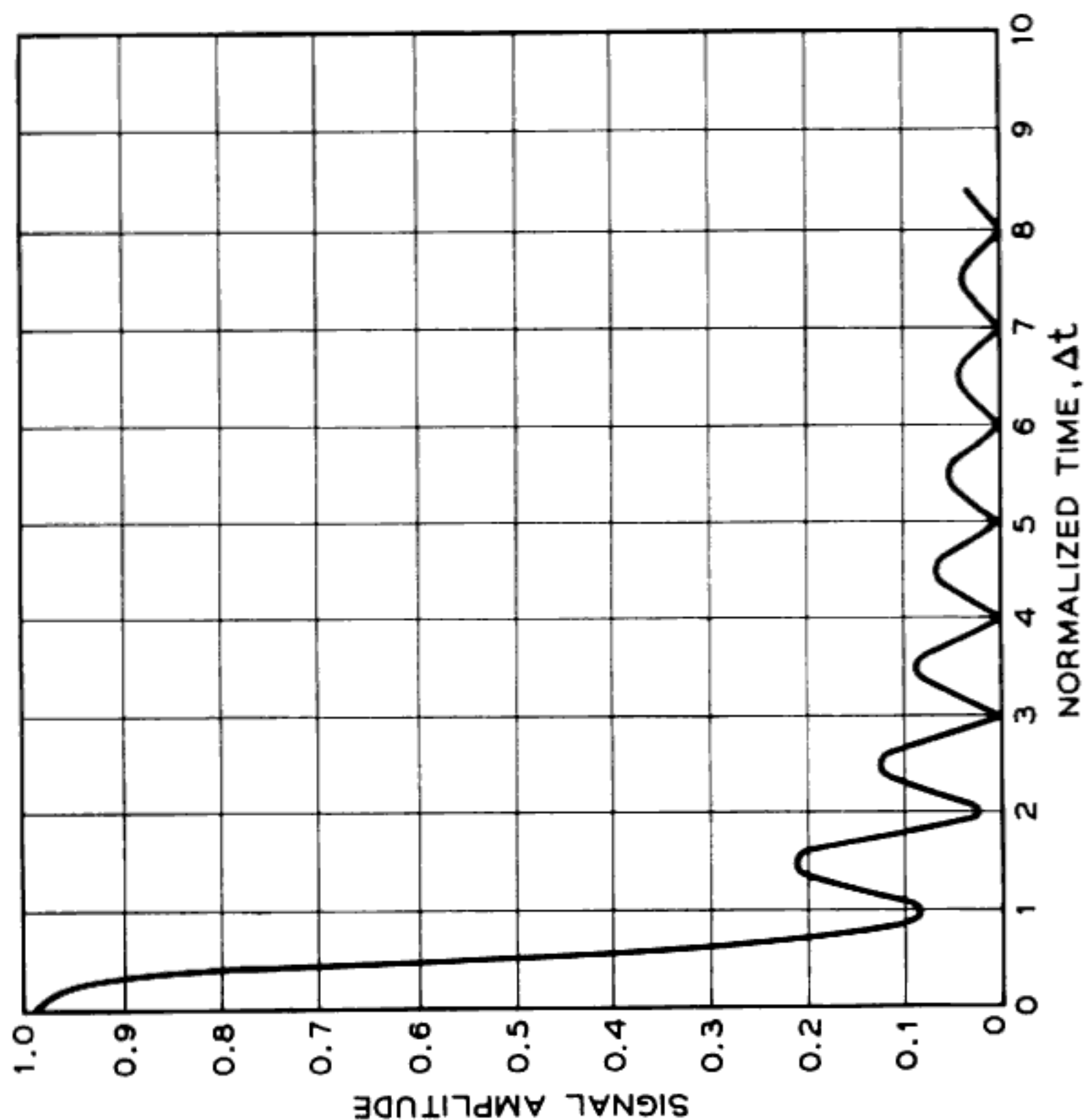


Fig. 33—Quadratic phase distortion effects, unweighted pulse,  $\varphi = 0$ .

Fig. 34—Quadratic phase distortion effects, unweighted pulse,  $\varphi = \pi/8$ .

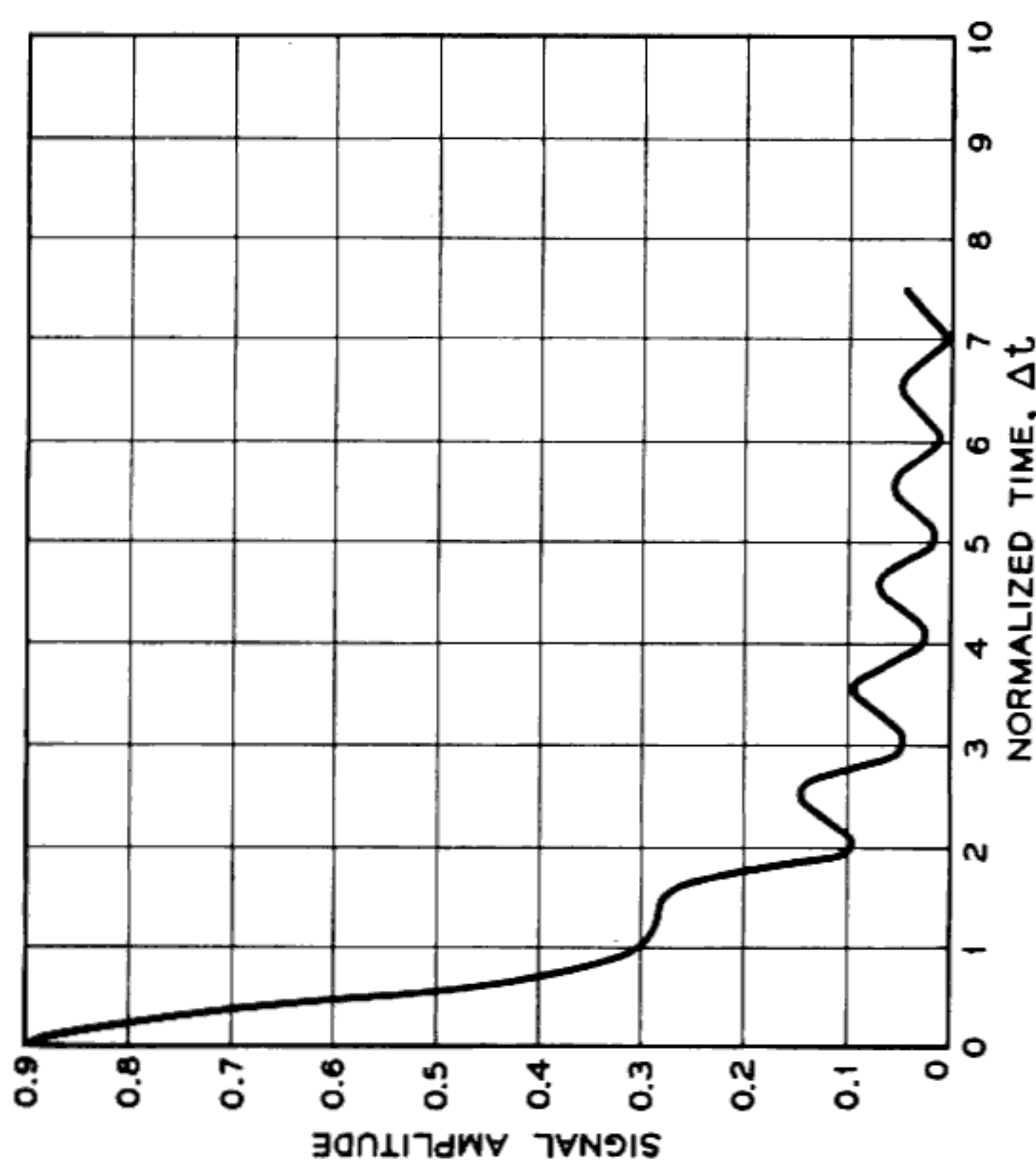


Fig. 35—Quadratic phase distortion effects, unweighted pulse,  $\varphi = \pi/2$ .

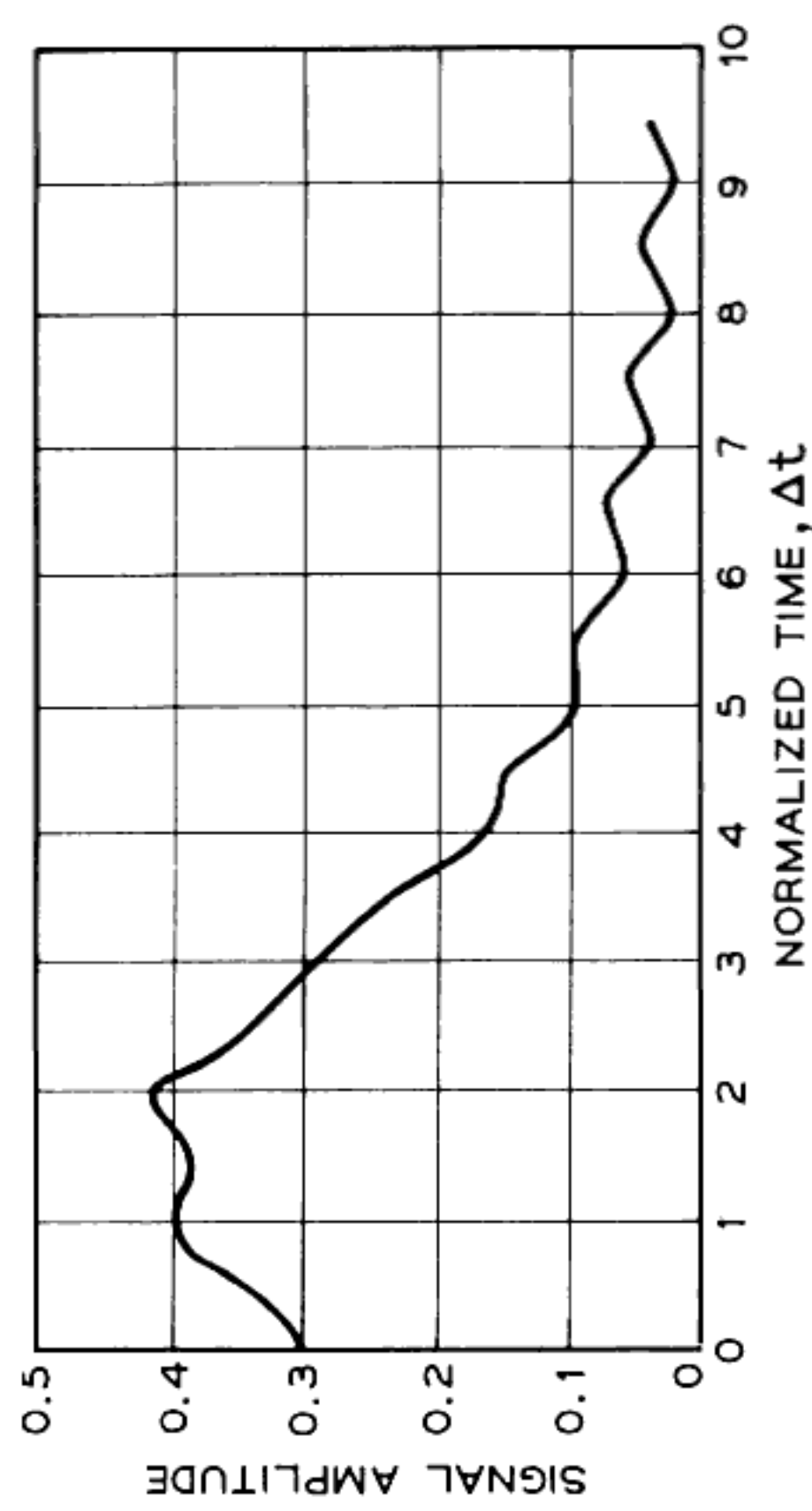


Fig. 36—Quadratic phase distortion effects, unweighted pulse,  $\varphi = 2\pi$ .

where  $v$  is the relative radial velocity between the target and the radar,  $c$  is the velocity of light, and  $f_{RF}$  is the radio-frequency carrier of the transmitted signal. Actually, each frequency in the transmitted spectrum will be shifted an amount proportional to that frequency; in practice, the spectrum width is usually such a very small percentage of the RF carrier that it is assumed the entire spectrum is bodily translated an amount  $v$ . Negligible error results from this assumption.

The radar return signal, shifted an amount  $v$ , is modulated down to the IF range of the collapsing and weighting networks. The IF signal resulting from a moving target has a different center frequency than does the signal from a stationary target. Since the collapsing and weighting networks were optimized for stationary targets, the effect of these collapsing and weighting networks on the Doppler-shifted signals must be calculated. The effect of the linear delay equalizer on Doppler-shifted signals is discussed in Section 3.5. A principal result of that analysis shows that collapsing networks may be constructed that will not modify the collapsed pulse envelope. The present section considers only the effect of the weighting process on Doppler-shifted signals when the Doppler frequency shift,  $v$ , is a small fractional part of the system bandwidth,  $\Delta$ .

**3.4.4.2 Analysis.** The paired-echo explanation of the weighting process (Section 3.4.2) suggests another method of realizing the necessary weighting characteristic, in addition to a loss equalizer. The output of the weighting network can be viewed as the superposition of a large major response [delayed replica of the  $(\sin z)/z$  input] pulse and a series of  $\bar{n} - 1$  leading echoes and  $\bar{n} - 1$  lagging echoes. An equivalent realization of the weighting network would be a delay line with  $[2(\bar{n} - 1) + 1]$  taps, each with adjustable amplitude and 0 or  $180^\circ$  phase shift, brought together in a central summing network. If the tap spacing is equal to the reciprocal of the signal bandwidth,  $\Delta$ , and the amplitude setting of the  $m$ th tap is proportional to  $F_m$  in the weighting network expansion [see (91)], then the performance of the tapped delay line is identical to the weighting network previously described. The tapped delay line method of synthesizing a loss characteristic has been used in the past,<sup>16,17</sup> and the resultant network is known as a transversal filter. The analysis and results of this section are not essentially different from the work of Bellows and Graham<sup>18</sup> on transversal filters.

As in Section 3.4.3, the weighting characteristic will be considered as

$$\tilde{Y}'_{\text{tay}}(f) = 1 + 2F_1 \cos \frac{2\pi}{\Delta} (f - f_0). \quad (109)$$

For a moving target the mean echo frequency is

$$f_m = f_0 + \nu, \quad (110)$$

where  $\nu$  has been defined in (108). The spectrum of the received signal is translated and will be constant in the range

$$f_m - \Delta/2 < f < f_m + \Delta/2, \quad (111)$$

and equal to zero elsewhere. With this fact, the output of the weighting network is proportional to

$$E'_{\text{tay}}(t) = \int_{f_m-\Delta/2}^{f_m+\Delta/2} \left[ 1 + 2F_1 \cos \frac{2\pi}{\Delta} (f - f_0) \right] e^{i2\pi f t} df. \quad (112)$$

An equivalent result is obtained by the passage of a signal with no Doppler shift through a weighting network with a slightly shifted center frequency. With this interpretation, (112) becomes

$$E'_{\text{tay}}(t) = \int_{f_0-\Delta/2}^{f_0+\Delta/2} \left[ 1 + 2F_1 \cos \frac{2\pi}{\Delta} (f - f_0 - \nu) \right] e^{i2\pi f t} df. \quad (113)$$

The envelope of this function is given by

$$\begin{aligned} |E'_{\text{tay}}(t)| = & |\operatorname{sinc} \Delta t + F_{11} \operatorname{sinc}(\Delta t + 1) + F_{11} \operatorname{sinc}(\Delta t - 1) \\ & + iF_{12}[-\operatorname{sinc}(\Delta t + 1) + \operatorname{sinc}(\Delta t - 1)]|, \end{aligned} \quad (114)$$

where

$$F_{11} = F_1 \cos(2\pi\nu/\Delta), \quad (115)$$

and

$$F_{12} = F_1 \sin(2\pi\nu/\Delta). \quad (116)$$

For small values of  $\nu/\Delta$ ,

$$\begin{aligned} F_{11} &\cong F_1, \\ F_{12} &\cong 2\pi\nu/\Delta. \end{aligned} \quad (117)$$

Therefore, the real component of the side lobes remains unchanged. The quadrature echoes become increasingly important as the percentage Doppler shift,  $\nu/\Delta$ , increases.

From the results of (114), it can be shown that Doppler shifts of less than 5 per cent of the system bandwidth,  $\Delta$ , will cause very little degradation of the weighted output pulse. The breakover point for serious effects occurs for values of  $\nu/\Delta$  somewhat greater than 10 per cent. This result has been verified by an independent calculation of the output

pulse shape from a 47.5-db weighting network for a 10 per cent Doppler shift. This calculation (Fig. 37) shows a 0.2-db degradation of the peak pulse amplitude and a 13-db increase in the side-lobe level to 34.5 db.

### 3.5 The Influence of Moving Targets on Chirp Systems

This section continues the study of the effect of moving targets initiated in Section 3.4.4. Here attention is concentrated on the influence of moving targets on the process of *compression* as opposed to the study in 3.4.4 which was confined to the influence of moving targets on the process of *weighting*. In the study in this section of the effect of moving targets on a Chirp system it is initially assumed that only the linear-delay phase equalizer is present. With this simplified receiver characteristic, the quantitative effect of the Doppler shift may be readily found. Inspection of the receiver network characteristics in Fig. 7(b) reveals that the distortionless frequency translation caused by the Doppler shift results in a corresponding time translation of the network output

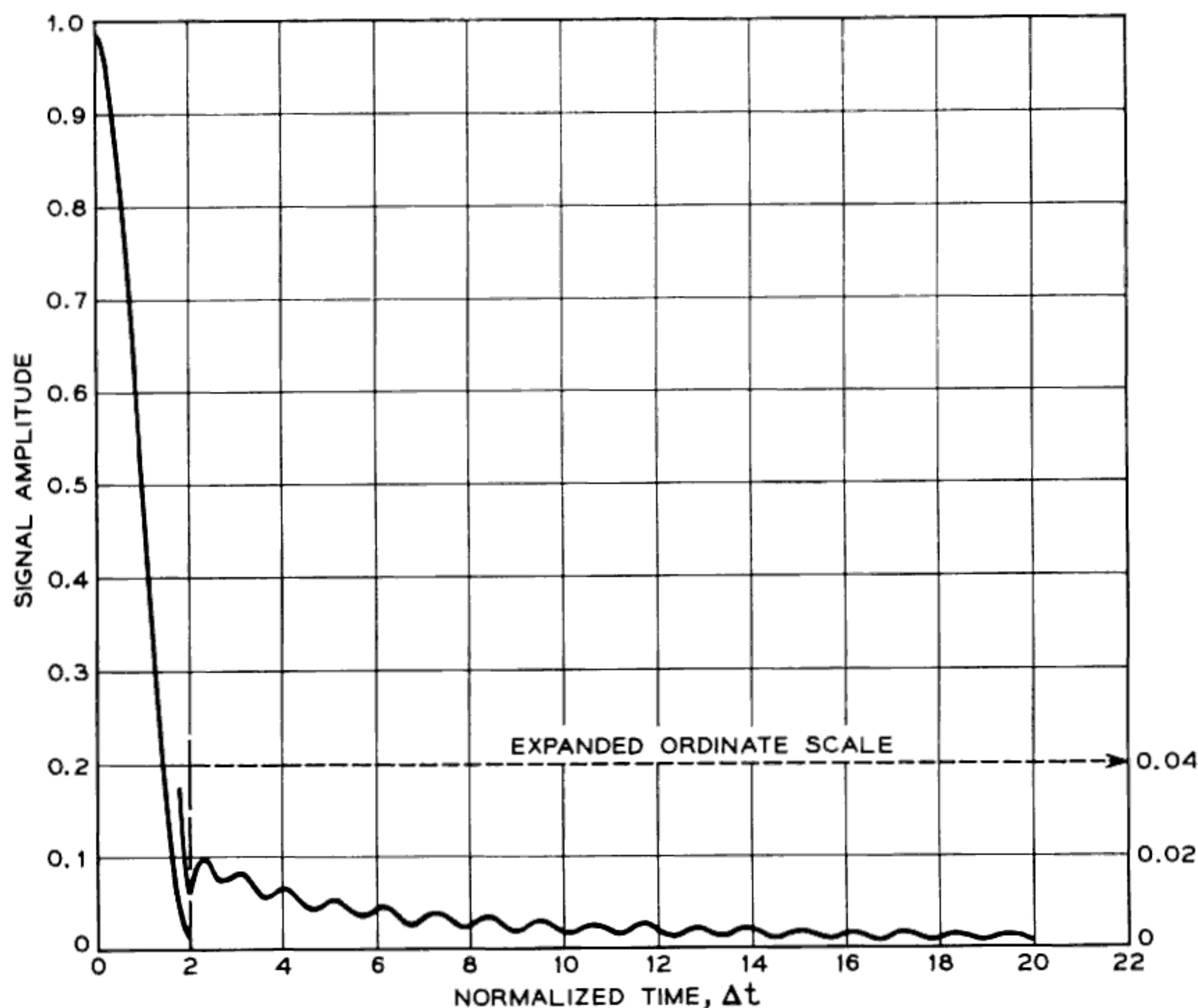


Fig. 37 — Weighting effects on Doppler-shifted signals.

signal. According to the particular network slope illustrated in Fig. 7(b), the response of an approaching target, with positive Doppler shift, will emerge *before* the response of a hypothetical stationary target at the same range. Likewise, the response of a receding target will lag the hypothetical stationary target response. The amount of time lead or lag may be determined from the following relation:

$$\frac{t_l}{v} = -\frac{T}{\Delta}, \quad (118)$$

where  $t_l > 0$  denotes a time lag and  $t_l < 0$  denotes a time lead. If (108) for  $v$  is combined with (118), it follows that

$$t_l = -\frac{2vTf_{RF}}{c\Delta}. \quad (119)$$

It is important to point out that  $t_l$  is simply proportional to the relative velocity of the moving target. The time shift given by (119) will give rise to an error in the indicated range for every moving target. This range error is determined by

$$R_e = \frac{ct_l}{2} = -\frac{vTf_{RF}}{\Delta}, \quad (120)$$

and it has a different value depending on the particular velocity of each individual target. Suppose, for a time interval of the order of  $t_l$ , that the velocity of each target remains essentially fixed. Because the targets are moving, each one will traverse a range increment of  $\delta R$  in a time  $\delta t$ , where  $\delta R = -v\delta t$ , with the minus sign signifying that approaching targets correspond to negative values of  $\delta R$ . If  $\delta t$  is chosen equal to  $Tf_{RF}/\Delta$ , then the range error in the signal at one time equals the range increment incurred in a time  $\delta t = Tf_{RF}/\Delta$ . Therefore, although the complete output signal at any one time does not represent a true distribution of the target positions corresponding to *that time*, that same signal does represent a true distribution of what the target positions *will be*  $Tf_{RF}/\Delta$  seconds later. Thus, what might seem to be a complicated mixture of positive and negative range errors can be viewed simply as an "error of interpretation of the range data." (This time error is a constant of the radar system and can easily be handled by a computer.) One can hardly over-emphasize the importance of such an extremely simple interpretation to unscramble the Doppler effect on the linear-FM Chirp signal!

The addition of shaping networks to reduce the side-lobe levels will not modify the above interpretation in any qualitative manner. The returning signal that has experienced a Doppler shift no longer passes through

the central symmetric region of the weighting network. By forcing the signal to pass through the filter away from the center, an over-all attenuation is introduced accompanied by some modification of the signal details (see Section 3.4.4). The principal feature of concern here is the inevitable signal attenuation and the time lead or lag caused by the receiver delay equalizer.

A useful pictorial representation of this state of affairs is afforded by the ambiguity diagrams of Woodward<sup>10</sup> (p. 118). Similar pictorial representations have been discussed earlier by Gabor<sup>19</sup> and Ville,<sup>20</sup> but the interpretation that will be stressed here was first emphasized by Woodward. Ambiguity diagrams are *joint*-response diagrams in both Doppler frequency and response time. They are most commonly calculated for the case of matched filters but need not be restricted to this ideal situation. Figs. 38(a), 38(b) and 38(c) illustrate, in a qualitative manner, ambiguity diagrams for (a) a long constant-frequency signal, (b) a short constant-frequency signal, and (c) a linear-FM Chirp signal. In each, the matched-filter characteristics, or nearly so, are assumed. The region of heavy shading schematically illustrates the region of strong signal response. The long constant-frequency signal, Fig. 38(a), possesses a good velocity resolution capability but a correspondingly poor range resolution capability. The pattern generated by the short signal shown in Fig. 38(b) has the opposite characteristics: good range resolution and poor velocity resolution. The interpretation to be placed on these ambiguity diagrams may now be readily understood. The shaded region — that is, the region of strong response — represents the “distribution of ambiguity” in interpreting the response of a single point target or in the ability to distinguish and identify several point targets separated either in range or velocity or both. Fig. 38(c) shows a qualitative ambiguity diagram for a linear-FM Chirp system. The Chirp scheme possesses resolution ambiguities situated along an *inclined* axis. The information contained in a *single* returning Chirp signal does not provide an unambiguous determination of both range and velocity, but represents only one quantity, which is a linear combination of these two variables. Unless the target velocity is known *a priori*, it is necessary to obtain several return signals so that a separate velocity determination is possible. For a large class of applications, this method represents an adequate solution to the ambiguity presented either by a Chirp signal or by a short constant-frequency signal.

The question naturally arises as to why one should be confined to ambiguity diagrams with the properties illustrated in Fig. 38. Why not use a signal leading to a small, concentrated shaded region that possesses

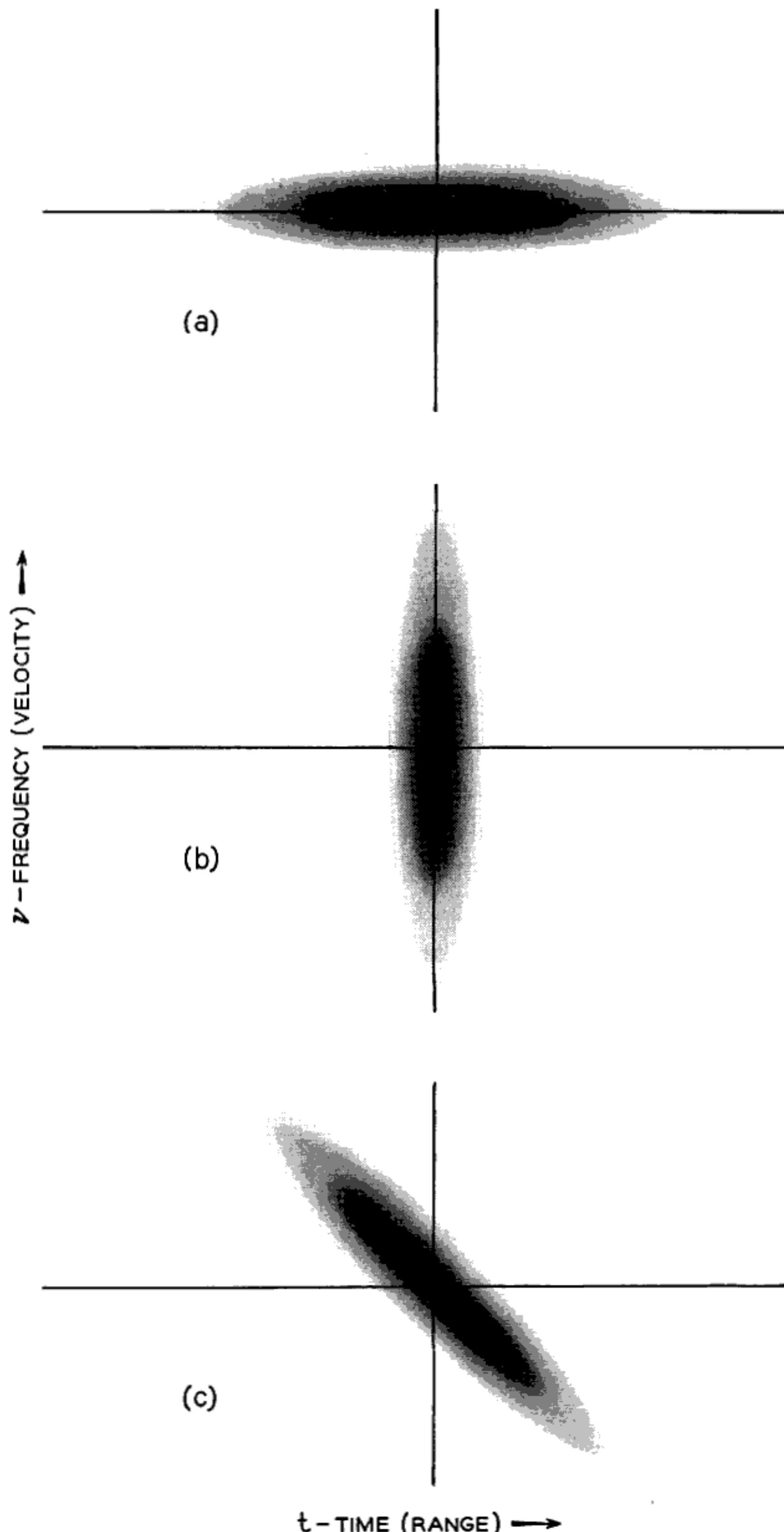


Fig. 38 — (a) Schematic ambiguity diagram for a long constant-frequency radar signal; the more shaded portions denote regions of greater signal response with the time,  $t$ , and for variously moving targets with Doppler frequency  $v$ . (b) Schematic ambiguity diagram for a short constant-frequency radar signal; improved time resolution is secured at the expense of some discrimination against moving targets. (c) Schematic ambiguity diagram for a typical chirp signal; an approaching target with a positive Doppler shift has a response attenuated in amplitude and shifted to an earlier time.

*simultaneous* range and velocity resolution? Although this question is not directly related to the study of Chirp systems, it is a fascinating issue clearly encompassed by the *spirit* of the Chirp scheme. A companion paper<sup>7</sup> considers this question in more detail and investigates an important class of ambiguity diagrams.

#### IV. CONCLUSION

This paper has presented in detail the theory and design of Chirp radars. Throughout the paper the FM characteristic intentionally imposed on the transmitted signal took but one form: a uniform linear FM. Needless to say, such a simple specification as linear FM represents just one of numerous, more complex FM schemes that might be used. However, the simplicity of the Chirp radar would perhaps make it easier to construct than any of the hierarchy of alternative methods. This important feature of ease of construction increases in importance when it is realized that it is theoretically possible to design a high-performance linear-FM Chirp radar whose efficiency is only slightly below the ideal maximum; such is the result of the analysis presented in this paper.

In summarizing the contents of this paper the following remarks can be made:

- i. Passive generation of the transmitted signal appears to be nearly as efficient as an ideal active generation process. In addition, passive generation is very desirable from a practical standpoint.
- ii. The combination of receiver collapsing and weighting networks provides a good approximation to a matched filter. Moreover, the desirable signal property of very low side lobes is obtained by sacrificing only a few decibels in the signal-to-noise ratio.
- iii. Even in the presence of substantial Doppler shifts the output signal maintains low side lobes. The most significant effect on the return signal is a time translation proportional to the velocity of the moving target. But by a simple data "reinterpretation" it is possible to nullify the effect of this time translation. This significant property follows only in the case of linear FM such as in Chirp.
- iv. The design of Chirp radars with dispersion factors of 100 is quite reasonable; such radars are presently in the experimental stages of development. With a dispersion factor of 100, a threefold increase in range is to be expected.

#### V. ACKNOWLEDGMENTS

The authors are indebted to C. N. Nebel for his advice and sugges-

tions during the course of this work. They also take pleasure in acknowledging the assistance of the computing personnel and facilities of Bell Telephone Laboratories at both Whippany and Murray Hill, N. J.

## REFERENCES

1. Darlington, S., U. S. Patent No. 2,678,997, May 18, 1954.
2. Hüttman, E., German Patent No. 768,068, March 22, 1940.
3. Sproule, D. O. and Hughes, A. J., British Patent No. 604,429, July 5, 1948.
4. Cauer, W., German Patent No. 892,772, December 19, 1950.
5. Dieke, R. H., U. S. Patent No. 2,624,876, January 6, 1953.
6. Cook, C. E., Proc. I.R.E., **48**, 1960, p. 310.
7. Klauder, J., this issue, p. 809.
8. MacColl, L. A., unpublished manuscript.
9. Taylor, T. T., I.R.E. Trans., **AP-3**, 1955, p. 316.
10. Woodward, P. M., *Probability and Information Theory, with Applications to Radar*, McGraw-Hill, New York, 1953.
11. Van Wijngaarden, A. and Scheen, W. L., *Tables of Fresnel Integrals*, N. V. Noord-Hollandsche Uitgevers Maatschappij, Amsterdam, 1949.
12. Campbell, G. A. and Foster, R. M., *Fourier Integrals for Practical Applications*, D. Van Nostrand Co., New York, 1942.
13. Wheeler, H. A., Proc. I.R.E., **27**, 1939, p. 359.
14. Burrows, C. R., Proc. I.R.E., **27**, 1939, p. 384.
15. Dolph, C. L., Proc. I.R.E., **34**, 1946, p. 335.
16. Kallman, H. E., Proc. I.R.E., **28**, 1940, p. 302.
17. Graham, R. S. and Sperry, R. V., U. S. Patent No. 2,760,164.
18. Bellows, B. C. and Graham, R. S., B.S.T.J., **36**, 1957, p. 1429.
19. Gabor, D., J.I.E.E., **93**, Pt. III, 1946, p. 429.
20. Ville, J., Cables & Trans., **2**, 1948, p. 61.